

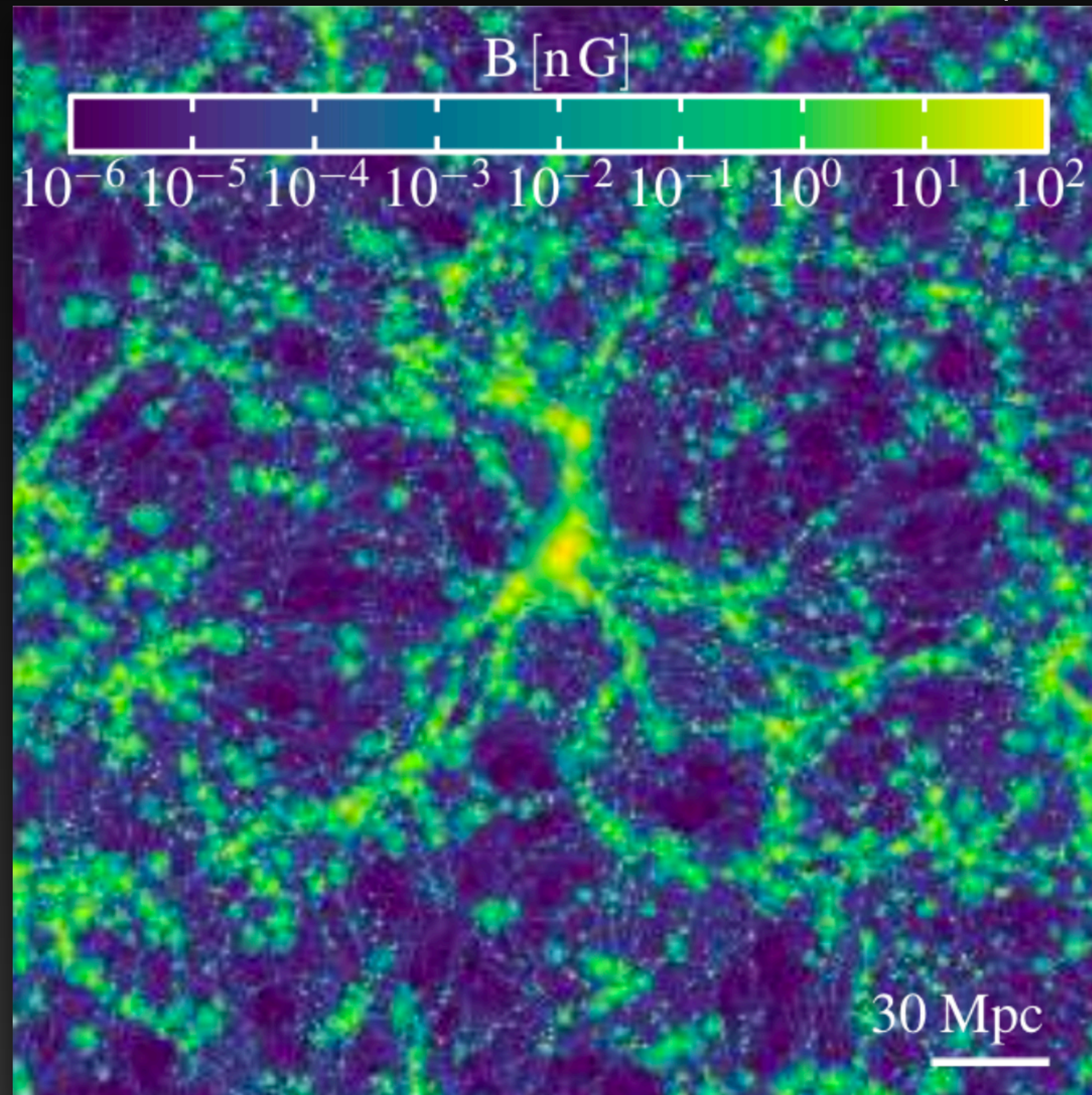
Probing the intergalactic magnetic field through gamma-ray observations with the Fermi LAT and H.E.S.S.

Manuel Meyer for the H.E.S.S. and Fermi LAT collaborations
manuel.meyer@uni-hamburg.de

The Variable Multi-Messenger Sky — WE Heraeus Seminar, Cracow, November 8, 2022

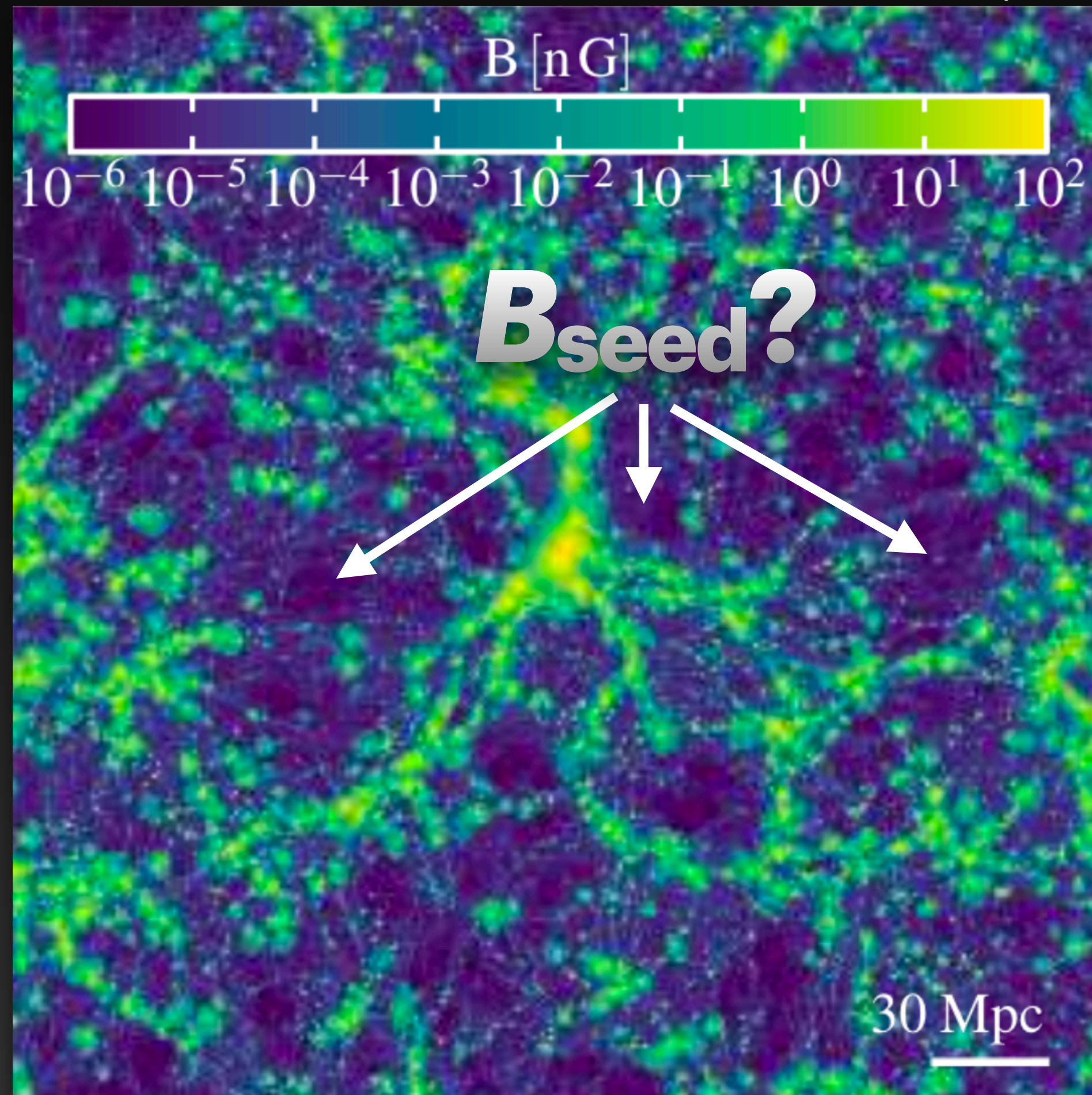
The Intergalactic magnetic field

IllustrisTNG simulation — Marinacci et al. (2018)



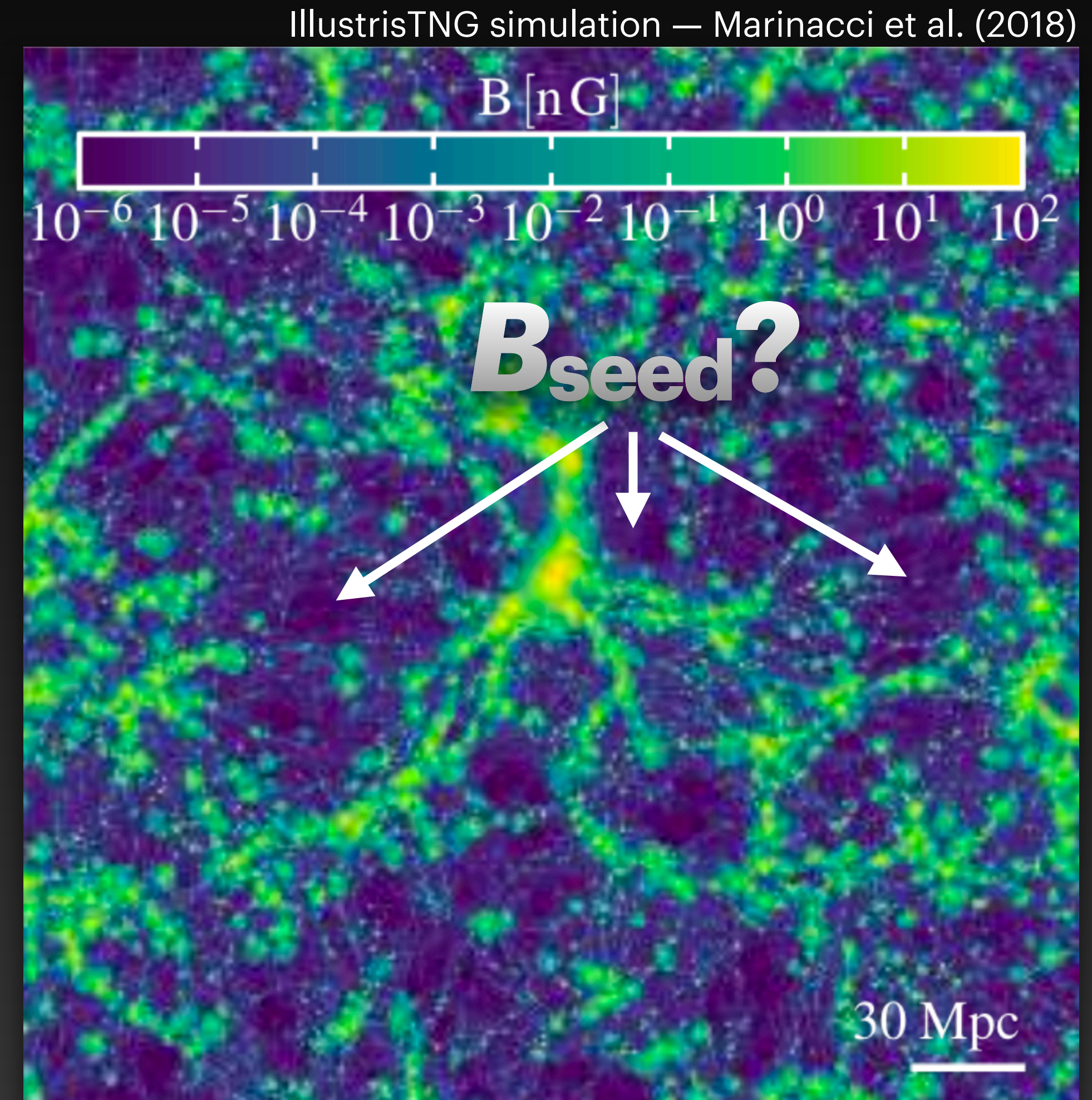
The Intergalactic magnetic field

IllustrisTNG simulation — Marinacci et al. (2018)



The Intergalactic magnetic field

- B-fields in galaxies and galaxy clusters originate from amplified seed field
- Origin, strength, orientation of seed fields unknown
- Extremely difficult to measure directly



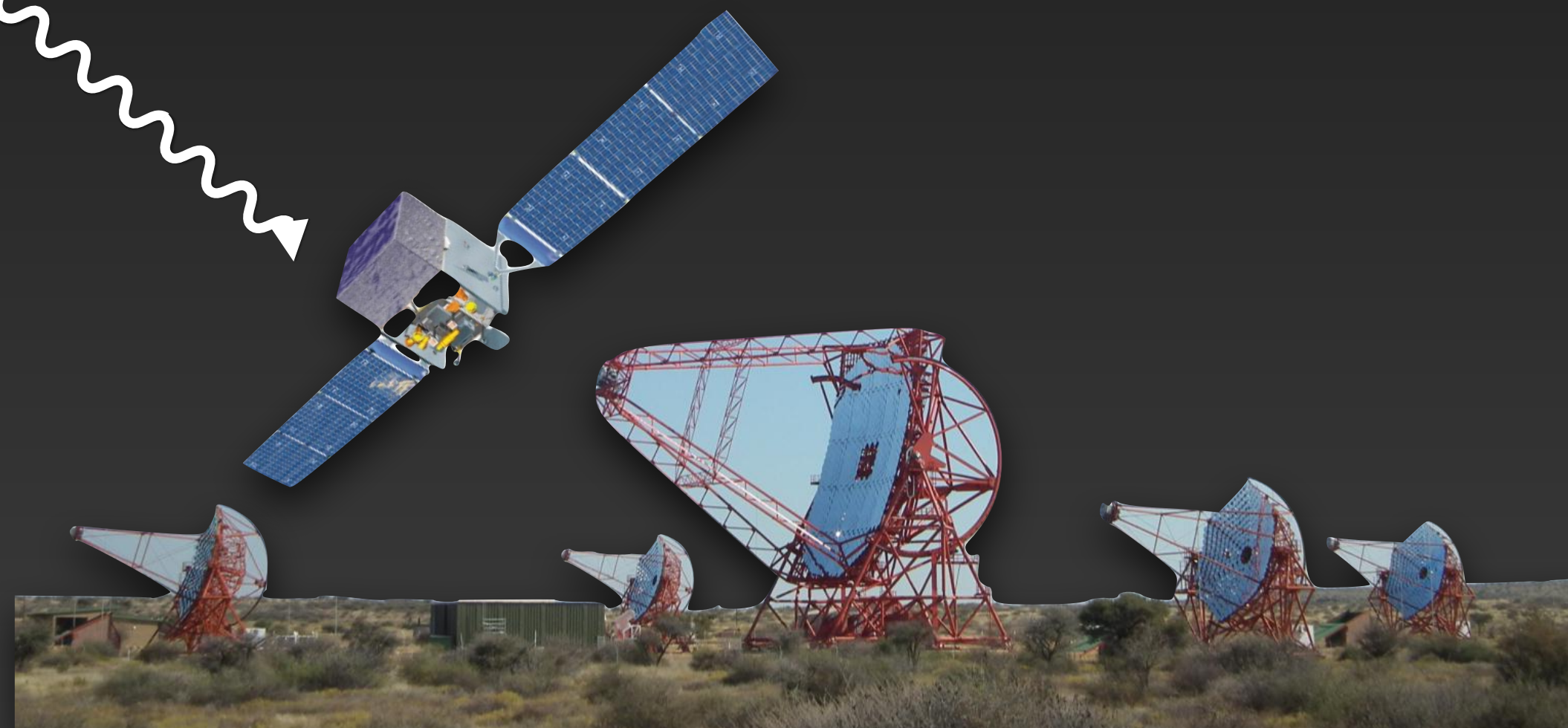
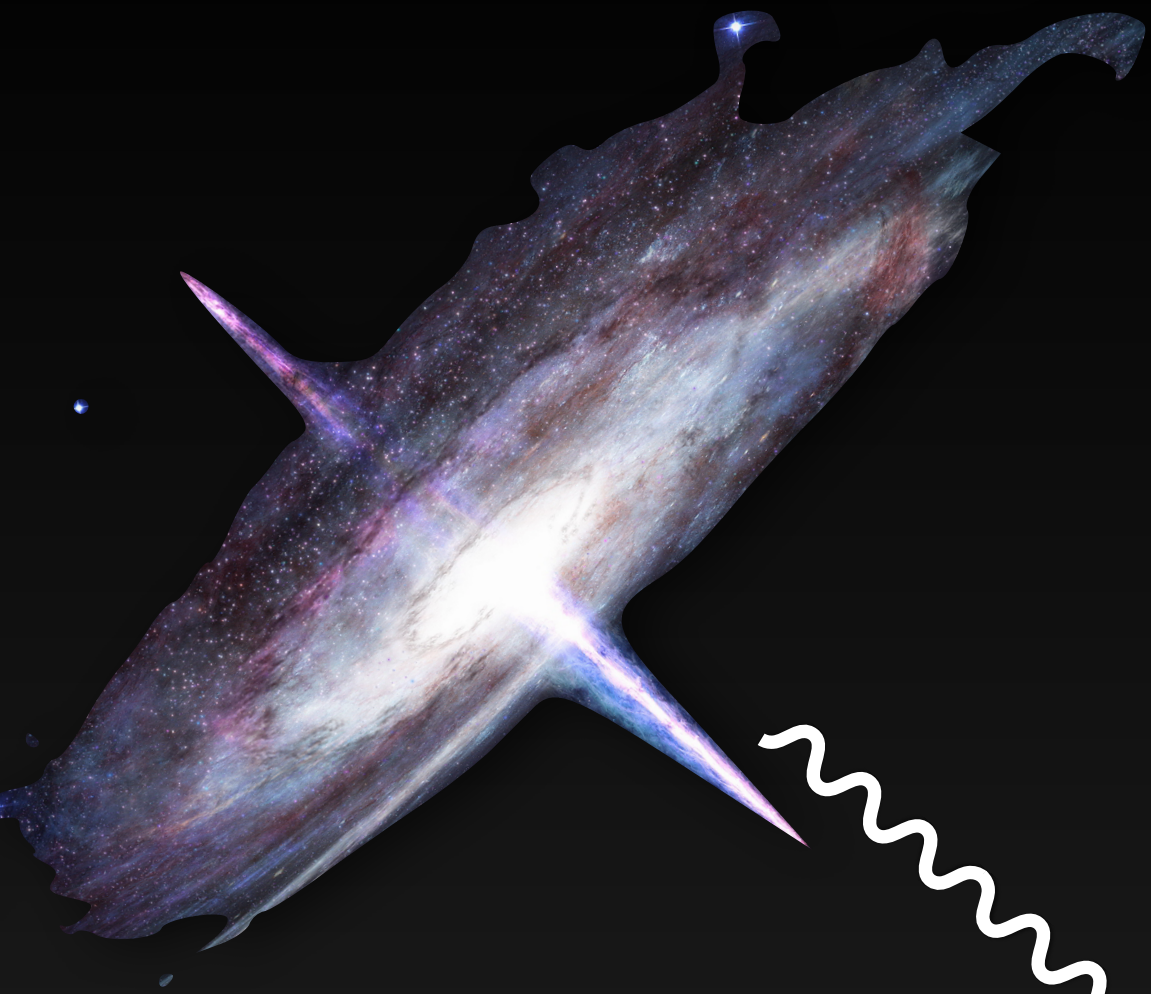


Indirect detection of the IGMF

Using gamma-ray observations of blazars

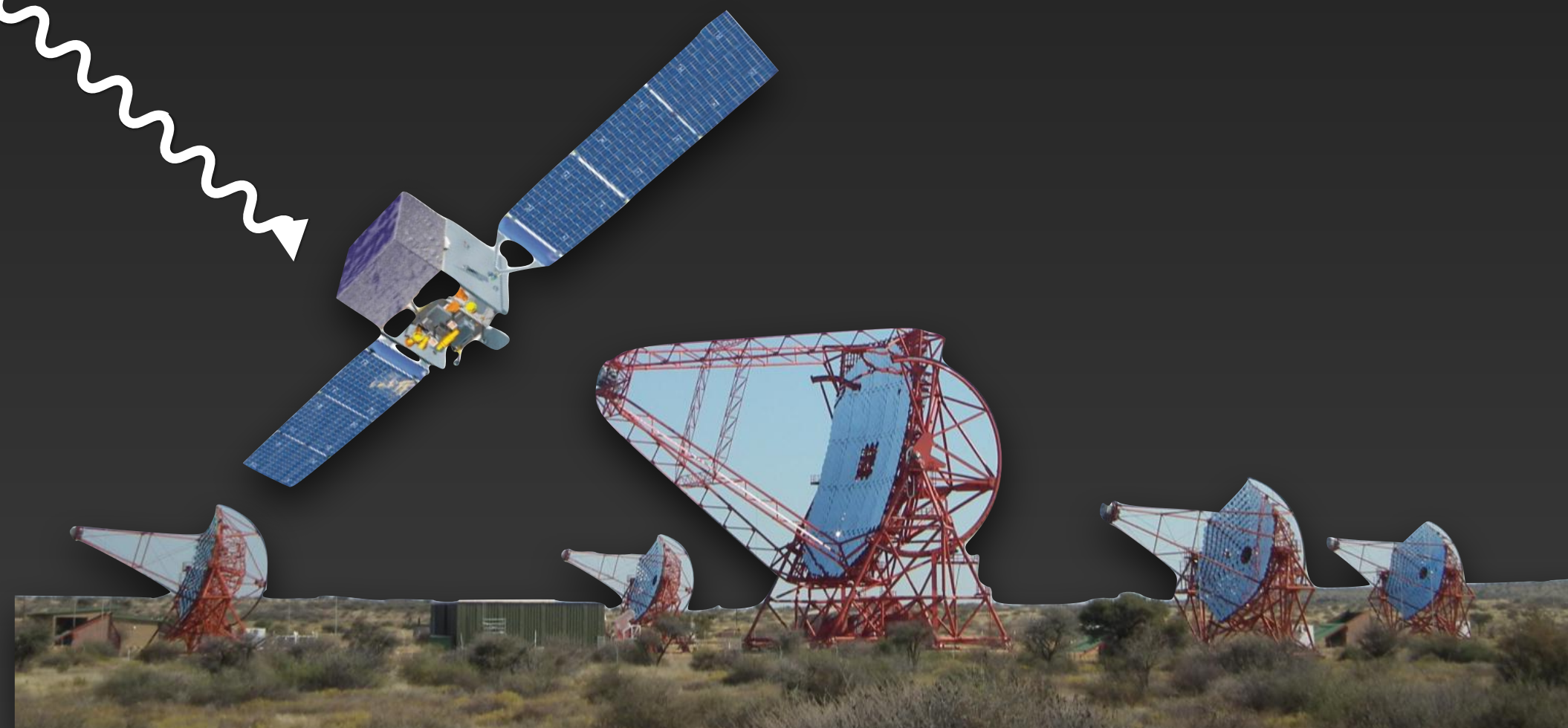
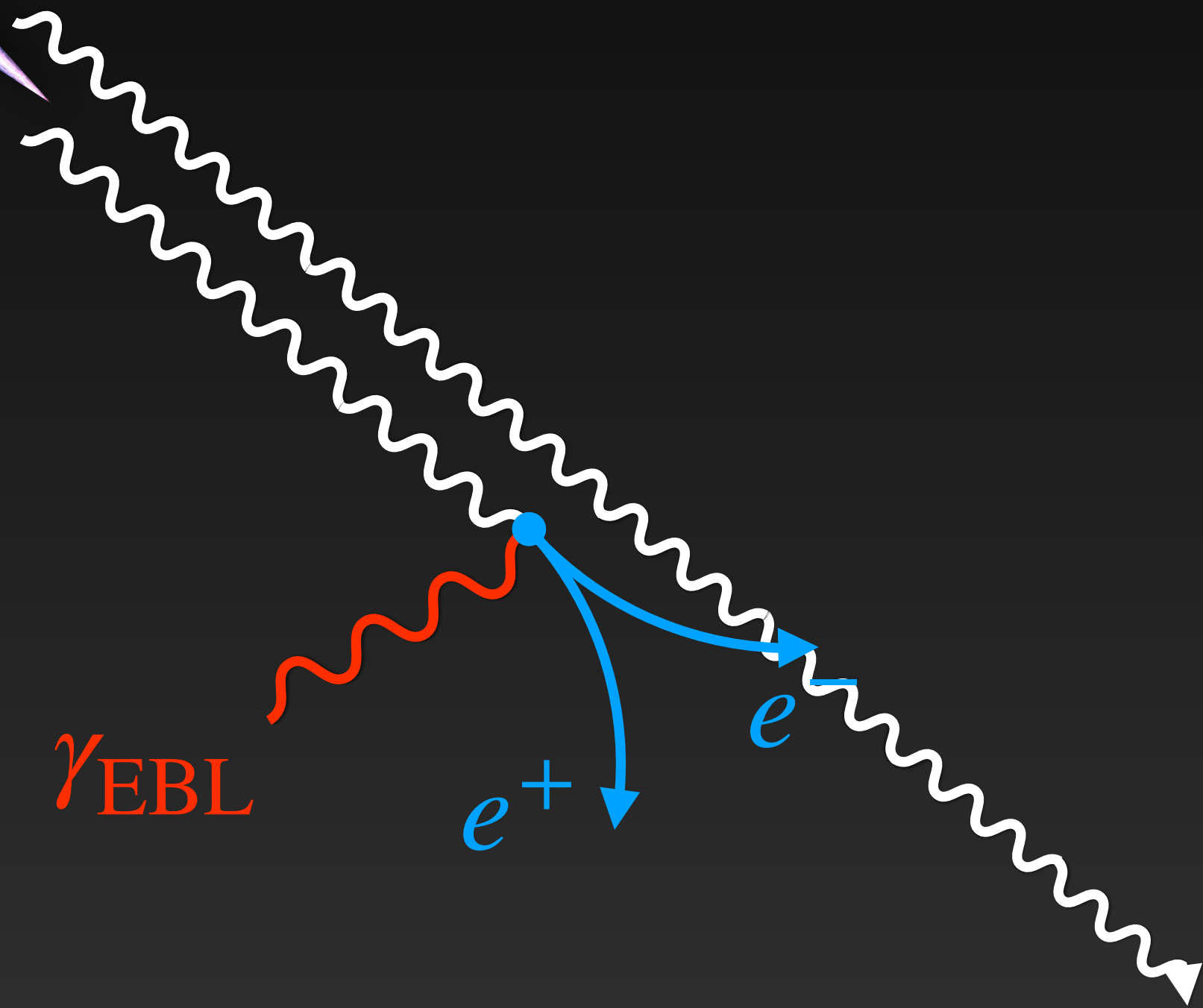
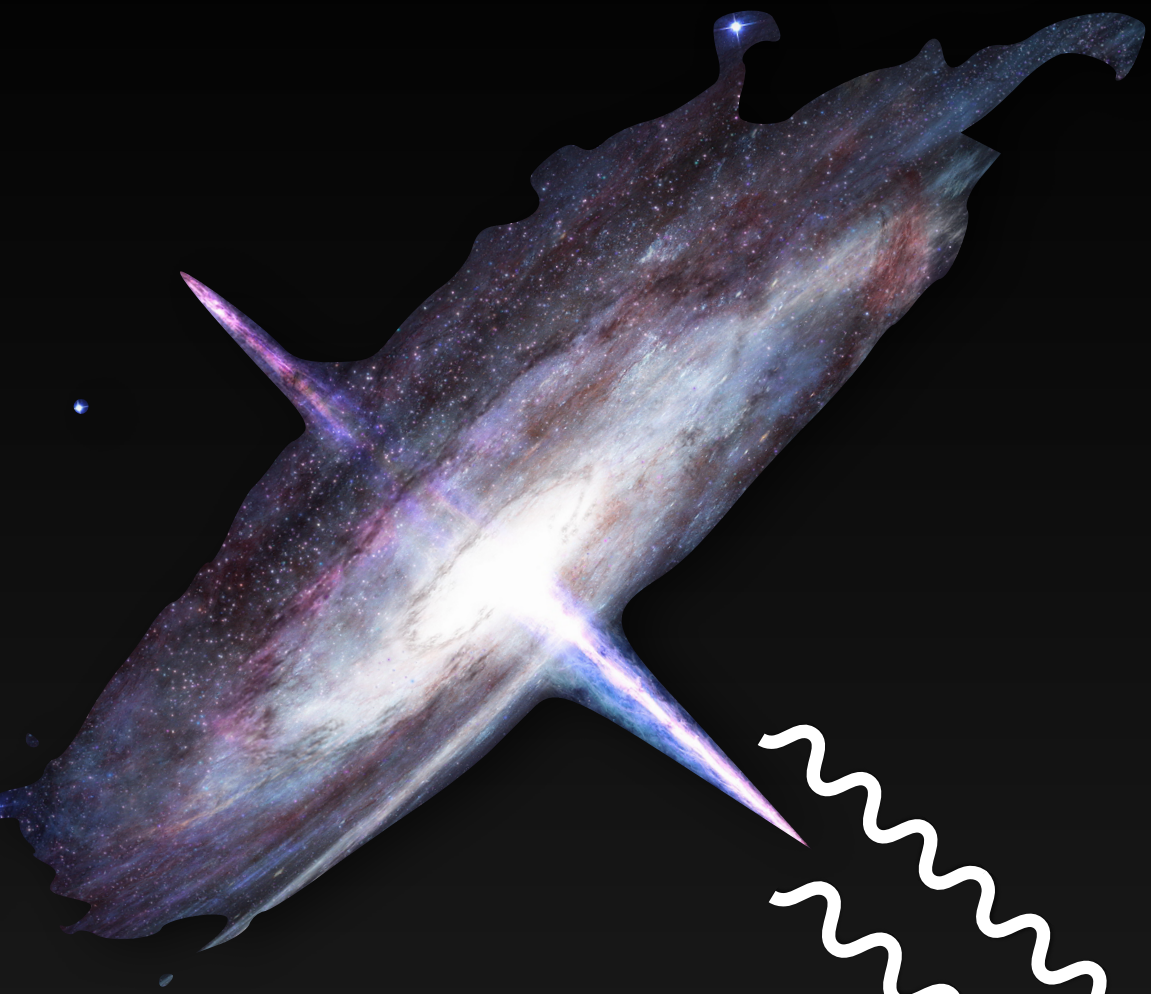
Indirect detection of the IGMF

Using gamma-ray observations of blazars



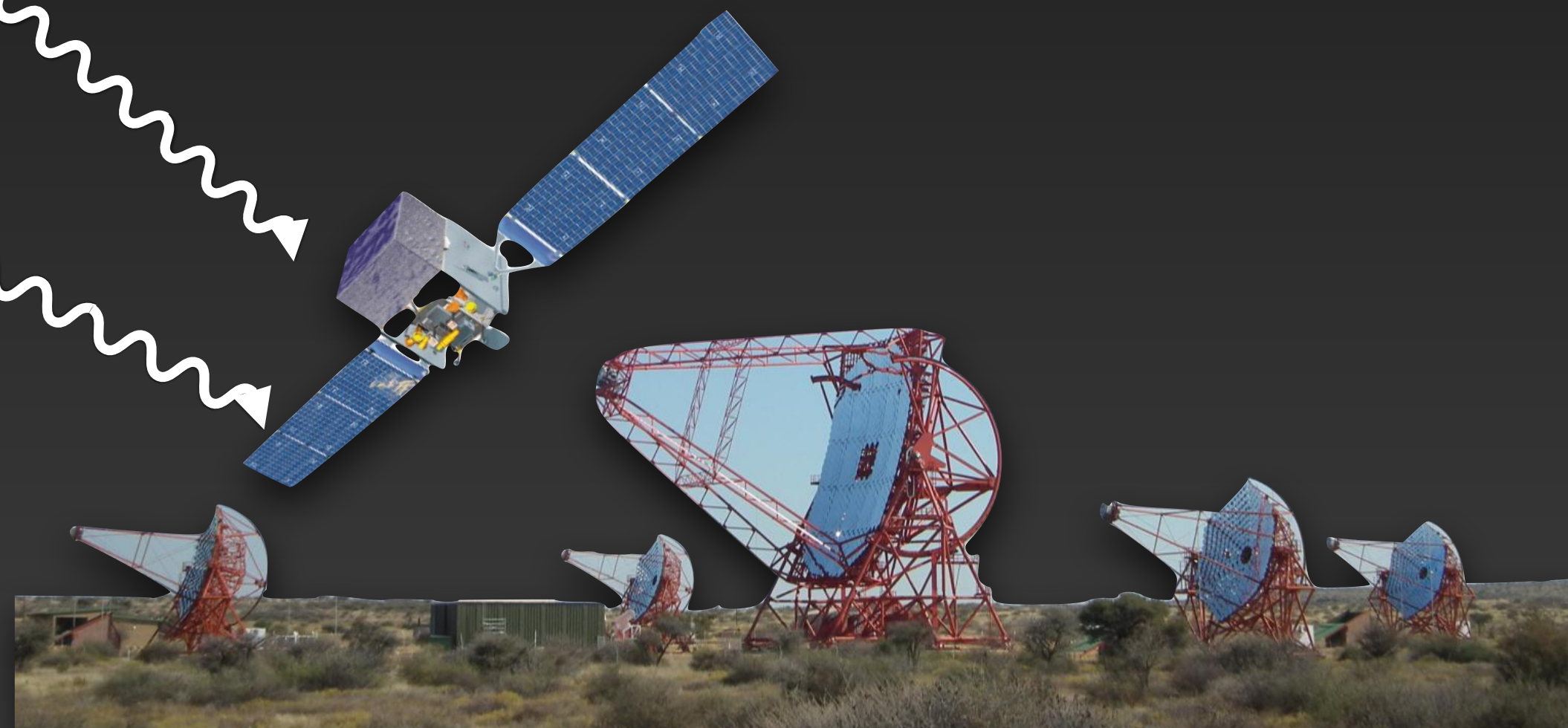
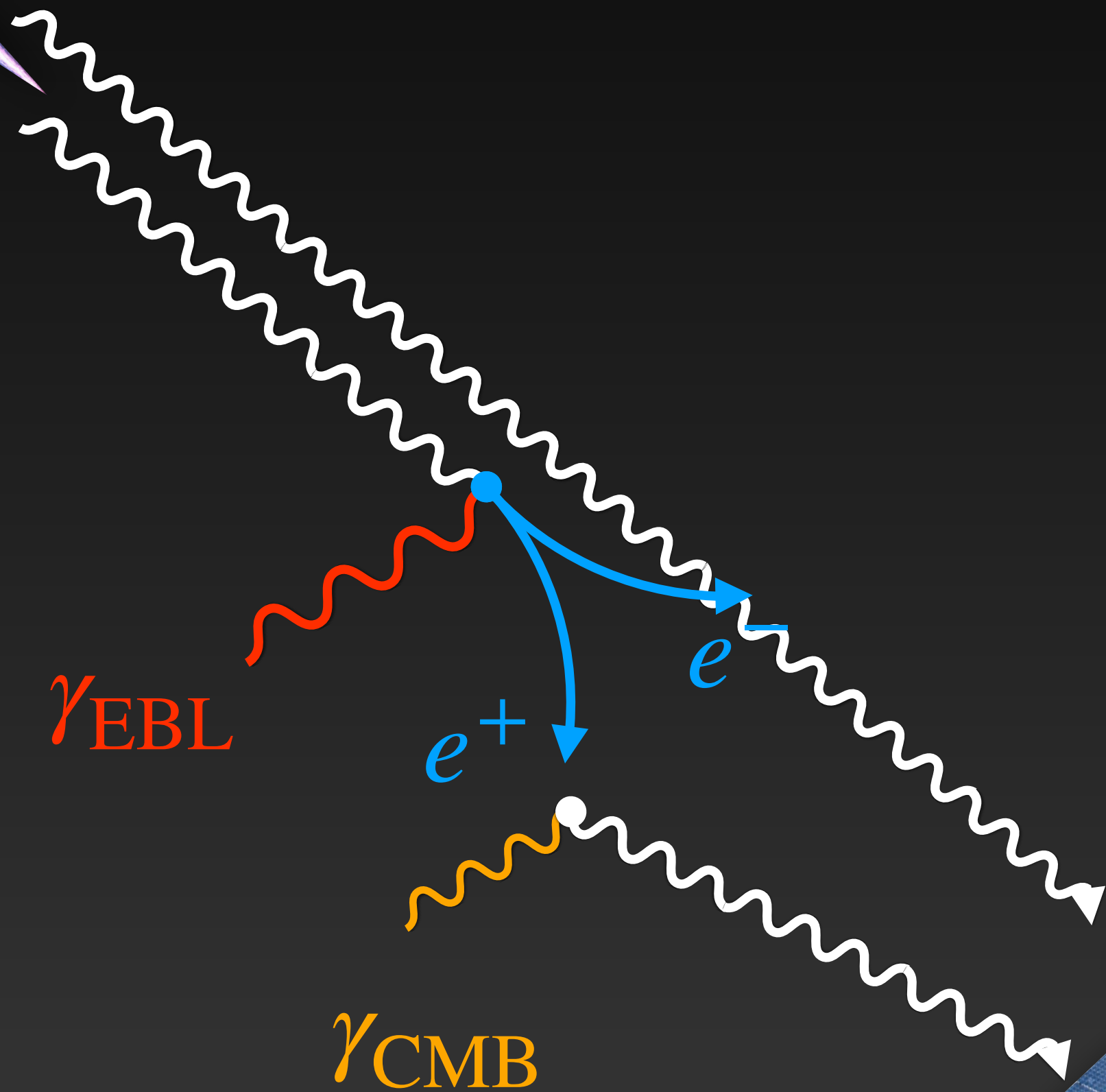
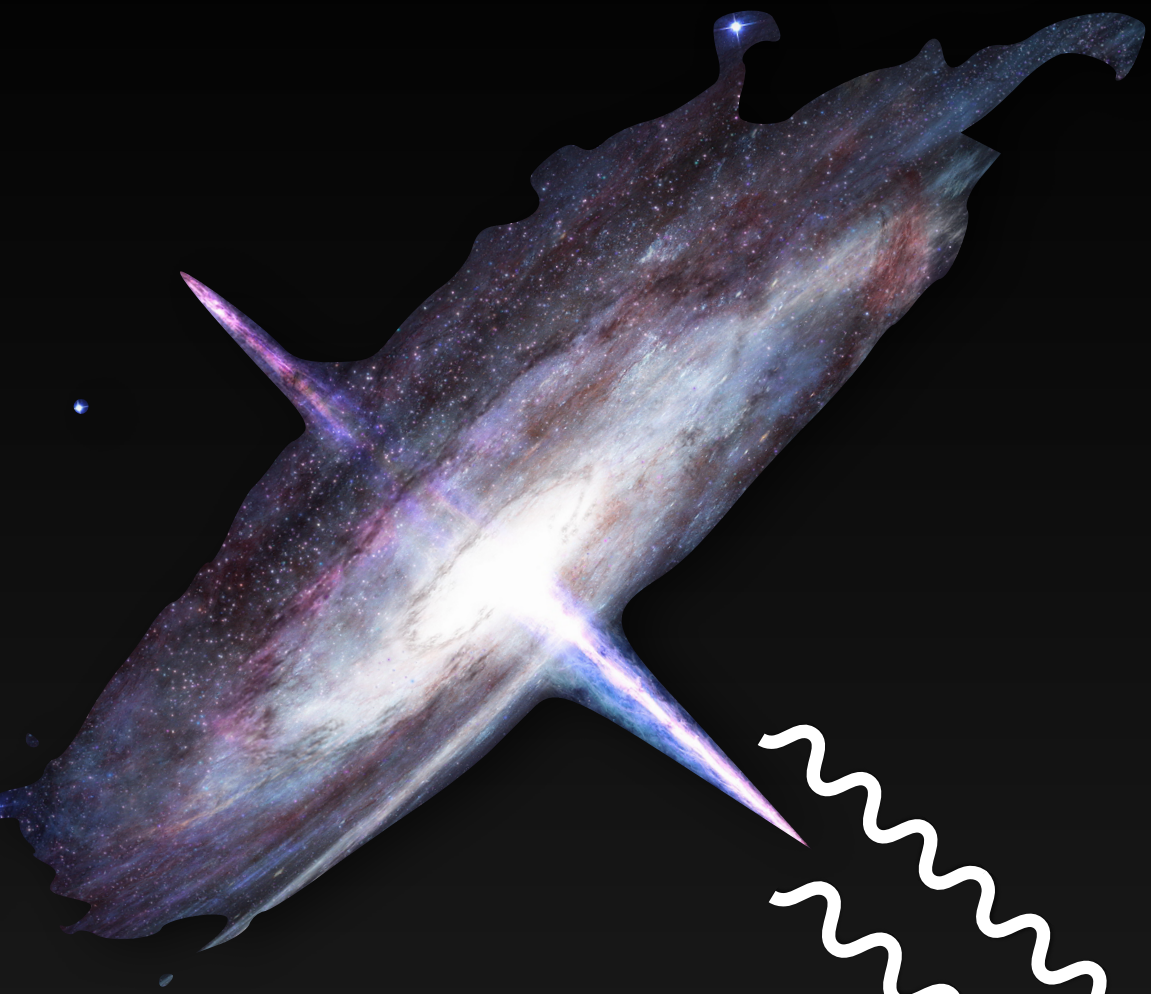
Indirect detection of the IGMF

Using gamma-ray observations of blazars



Indirect detection of the IGMF

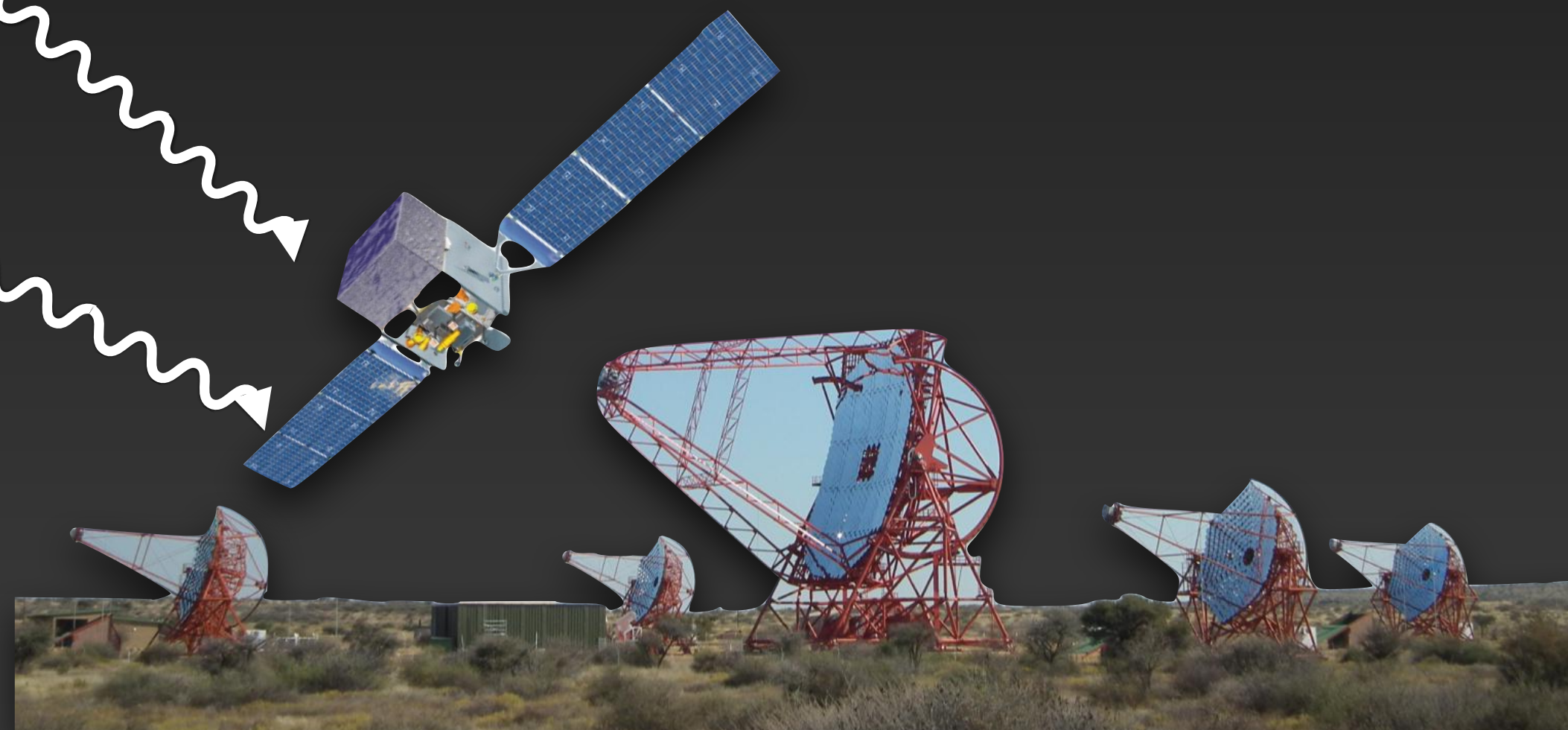
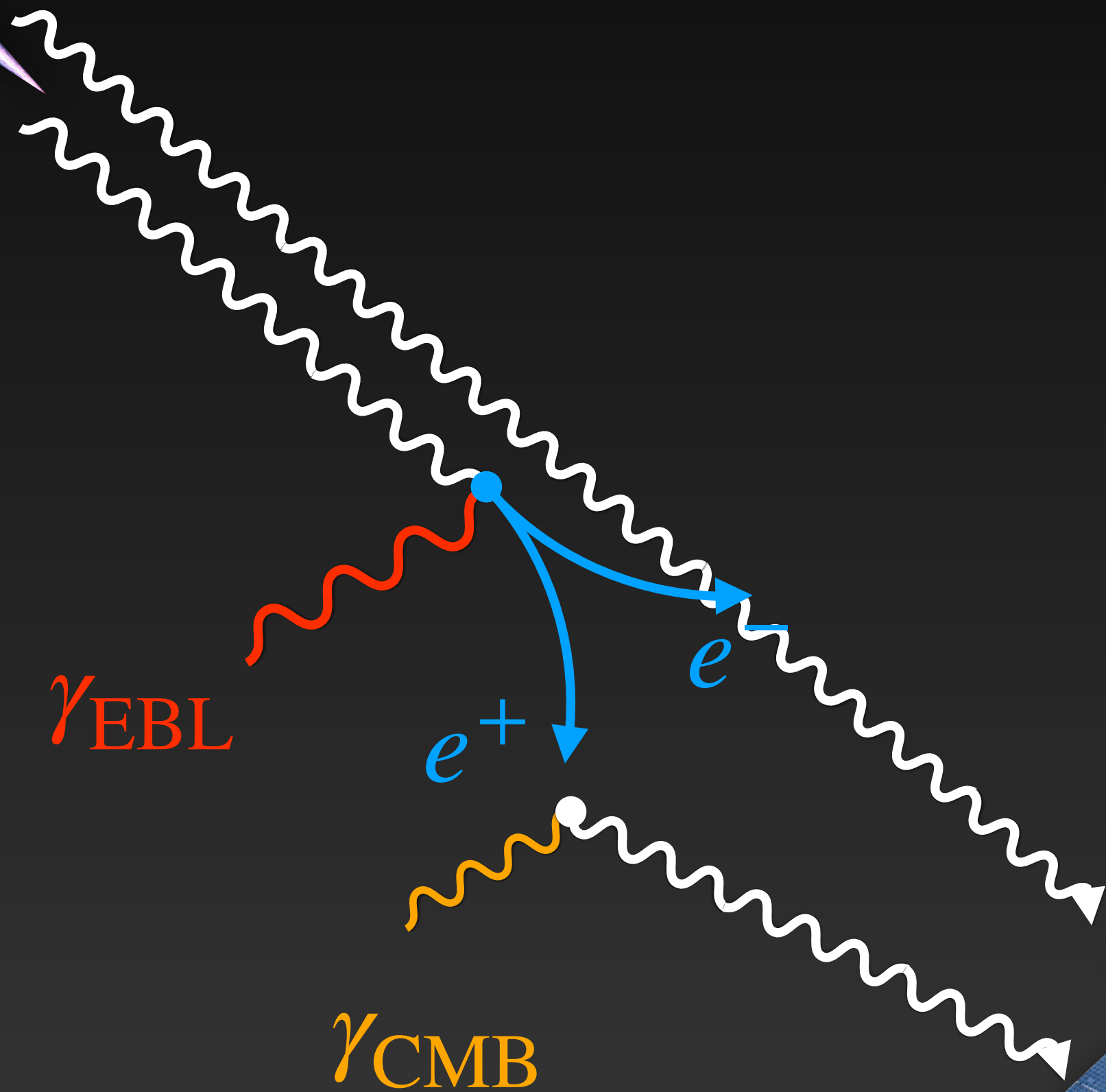
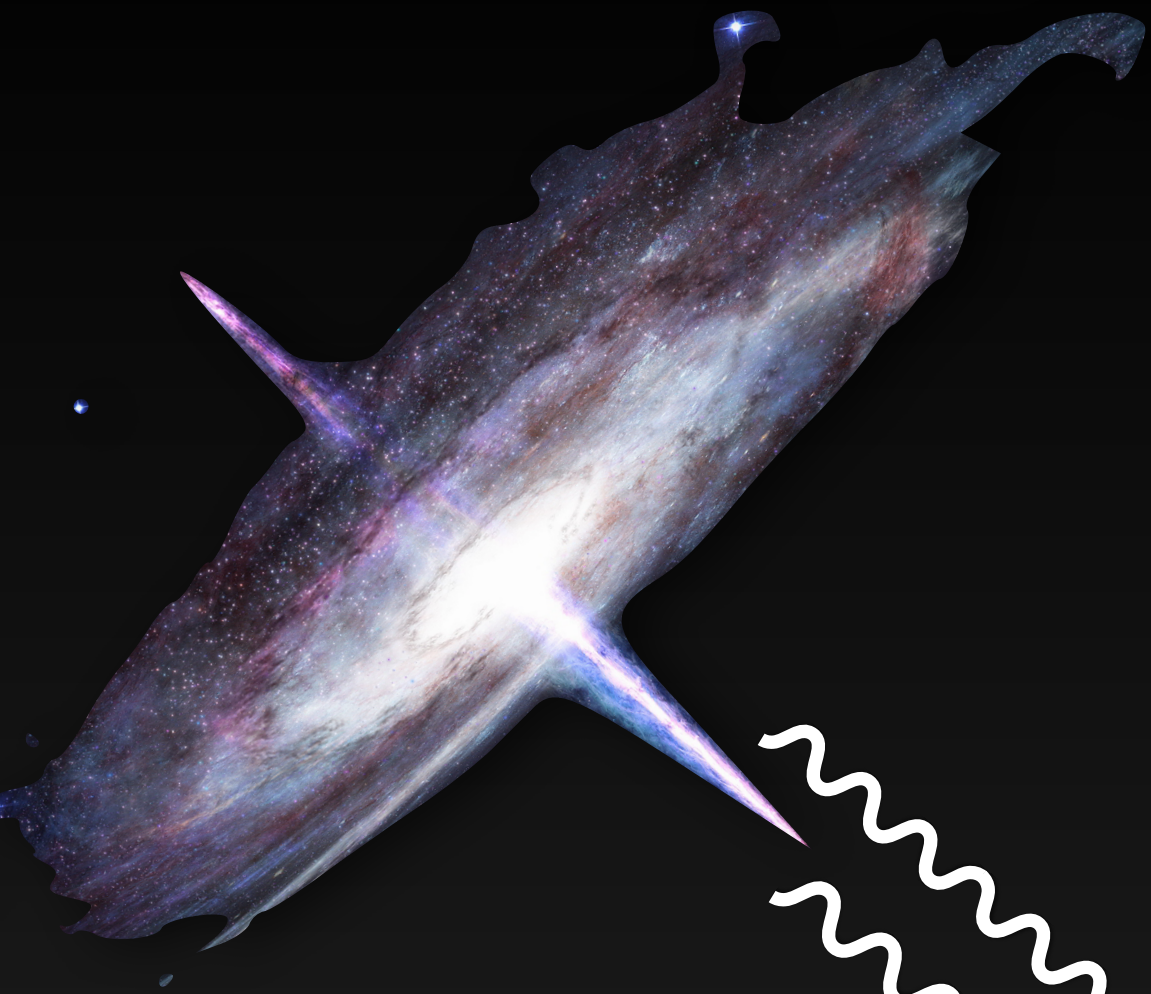
Using gamma-ray observations of blazars



Indirect detection of the IGMF

Using gamma-ray observations of blazars

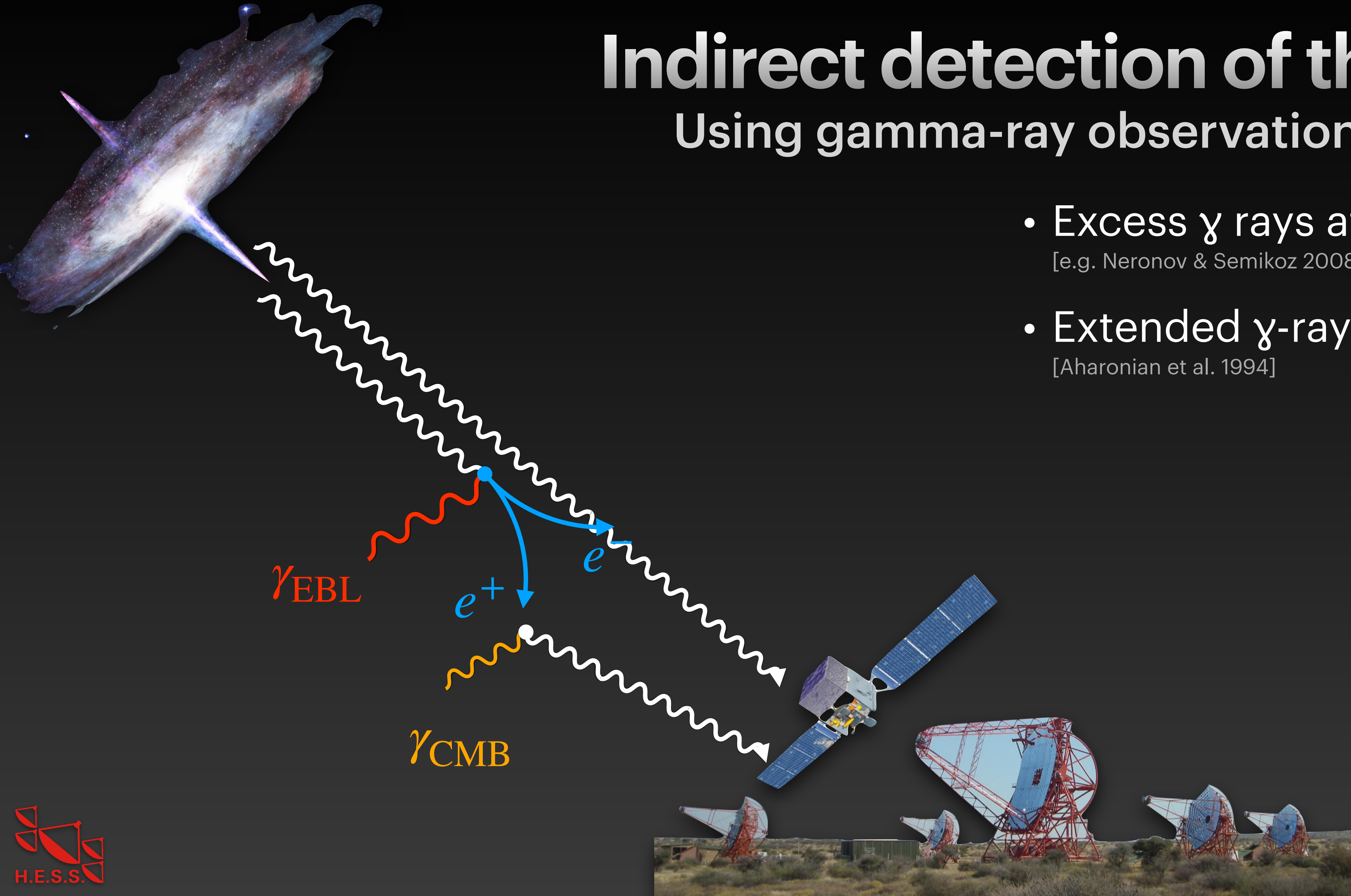
- Excess γ rays at lower energies
[e.g. Neronov & Semikoz 2008]



Indirect detection of the IGMF

Using gamma-ray observations of blazars

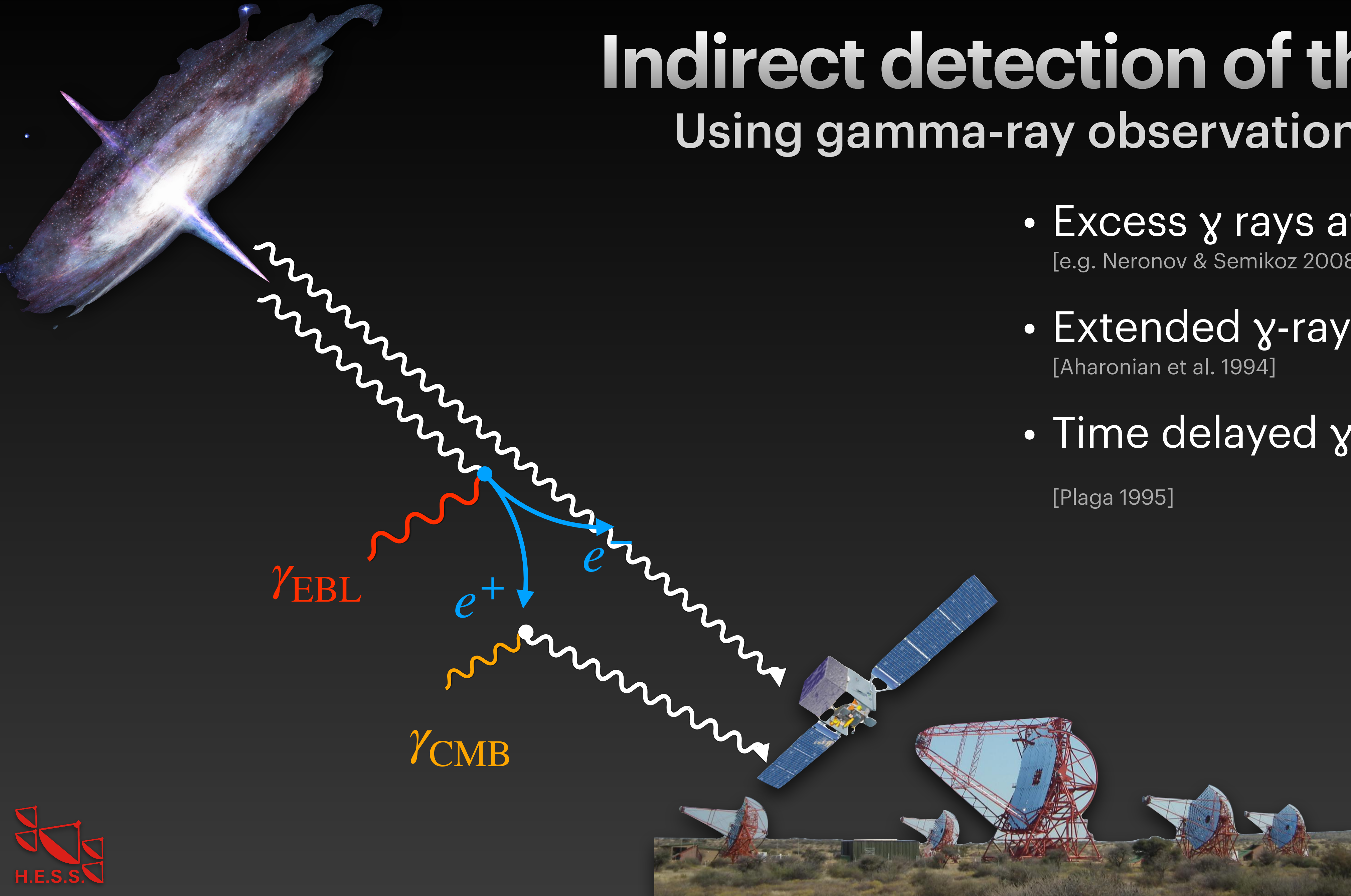
- Excess γ rays at lower energies
[e.g. Neronov & Semikoz 2008]
- Extended γ -ray halos
[Aharonian et al. 1994]



Indirect detection of the IGMF

Using gamma-ray observations of blazars

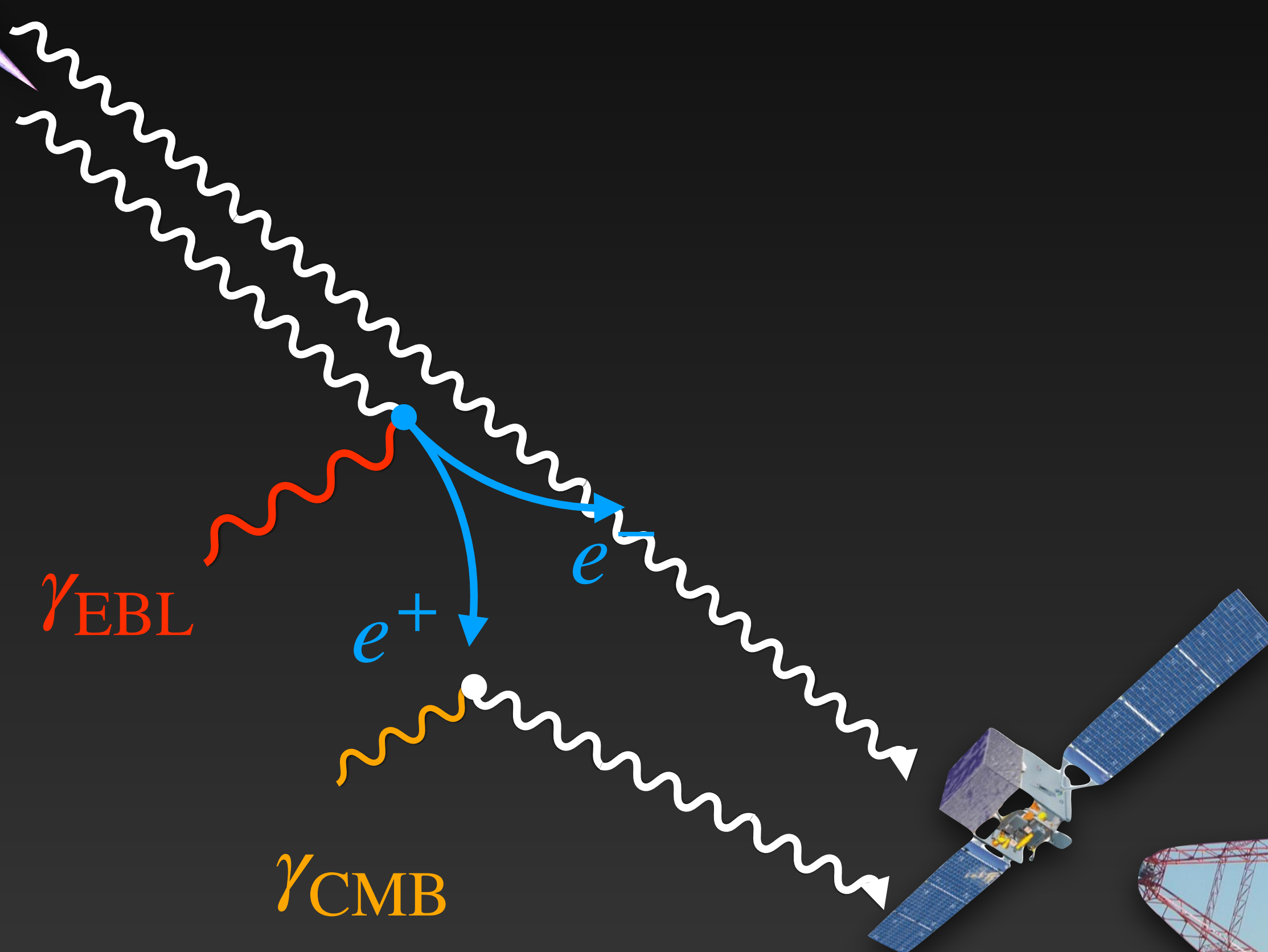
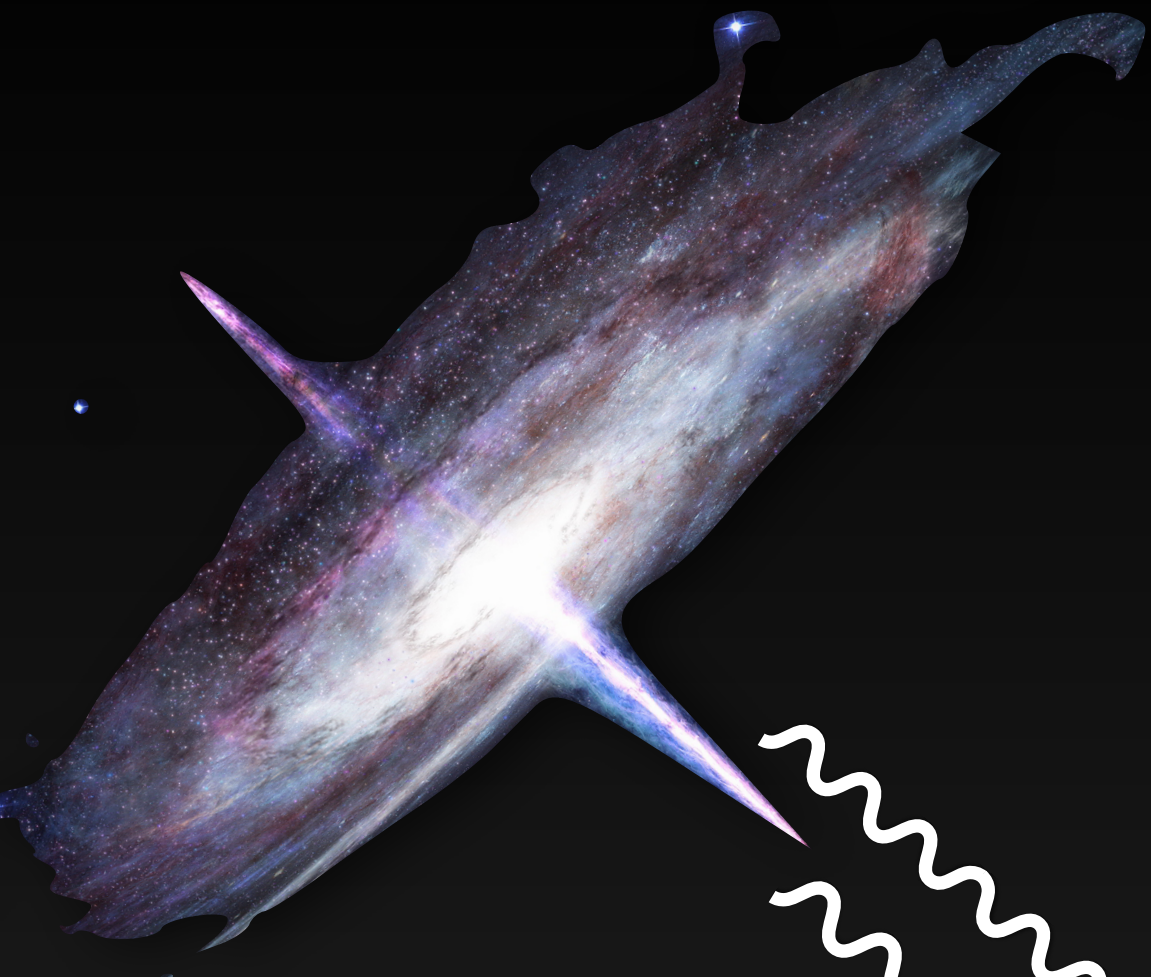
- Excess γ rays at lower energies
[e.g. Neronov & Semikoz 2008]
- Extended γ -ray halos
[Aharonian et al. 1994]
- Time delayed γ -ray emission
[Plaga 1995]



Indirect detection of the IGMF

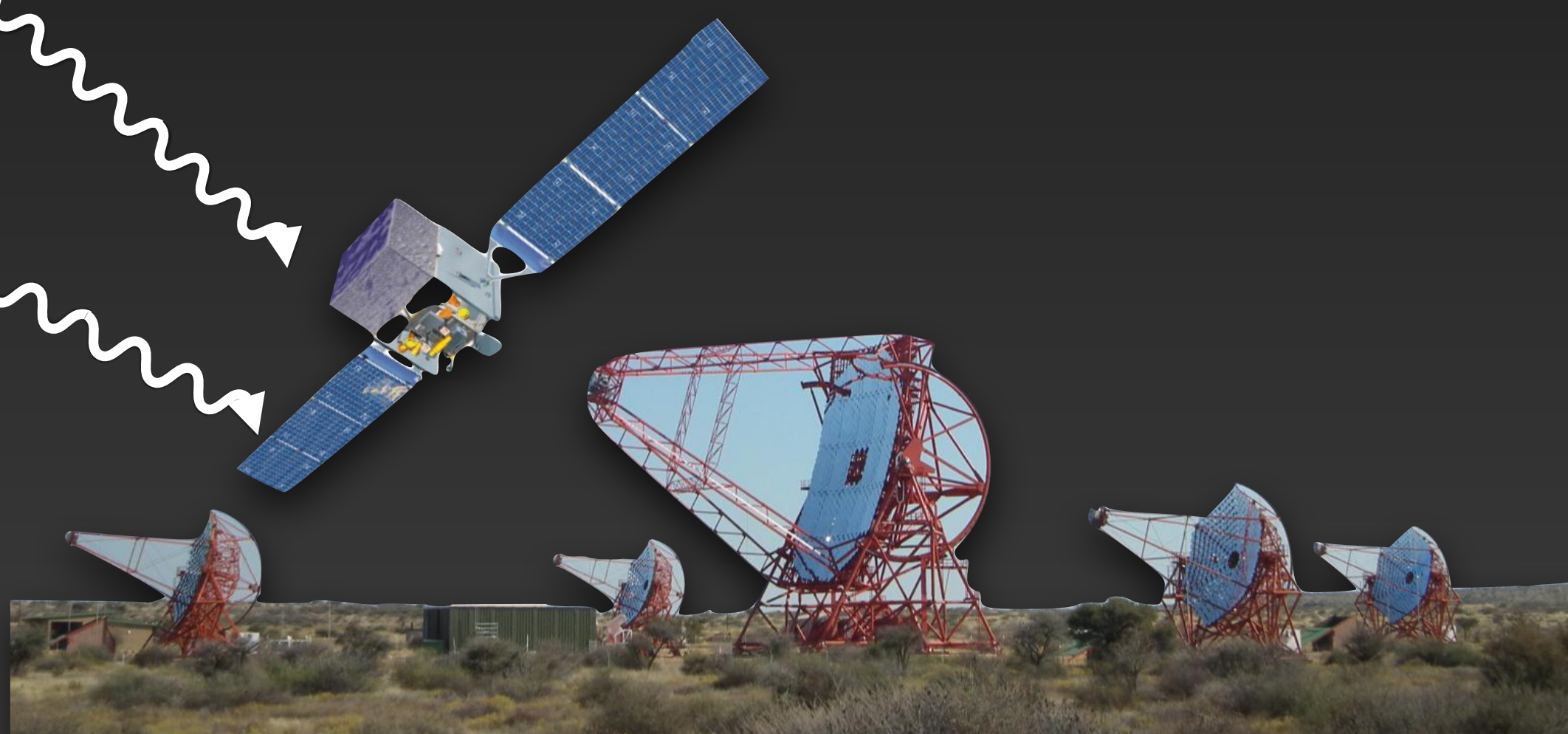
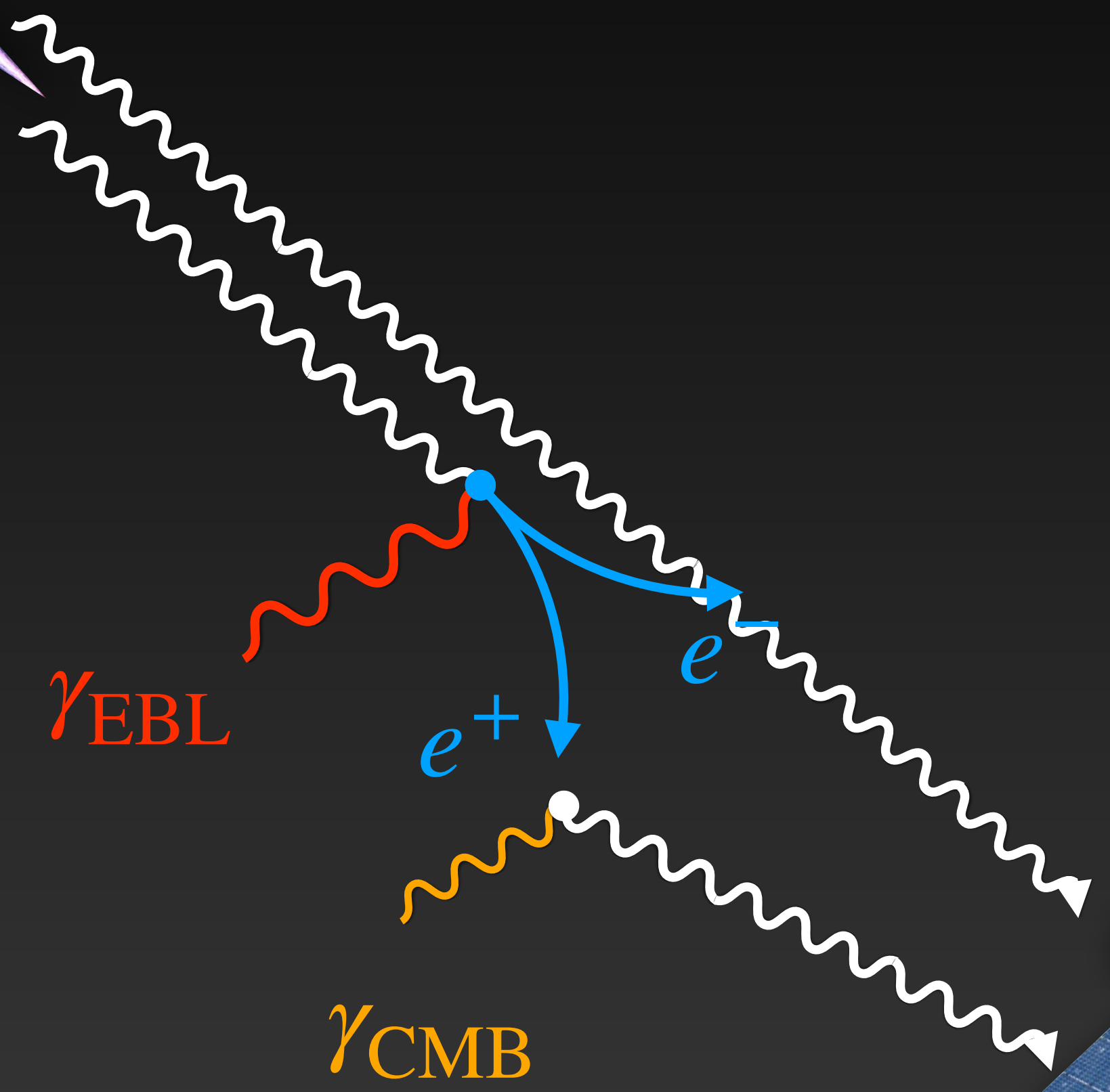
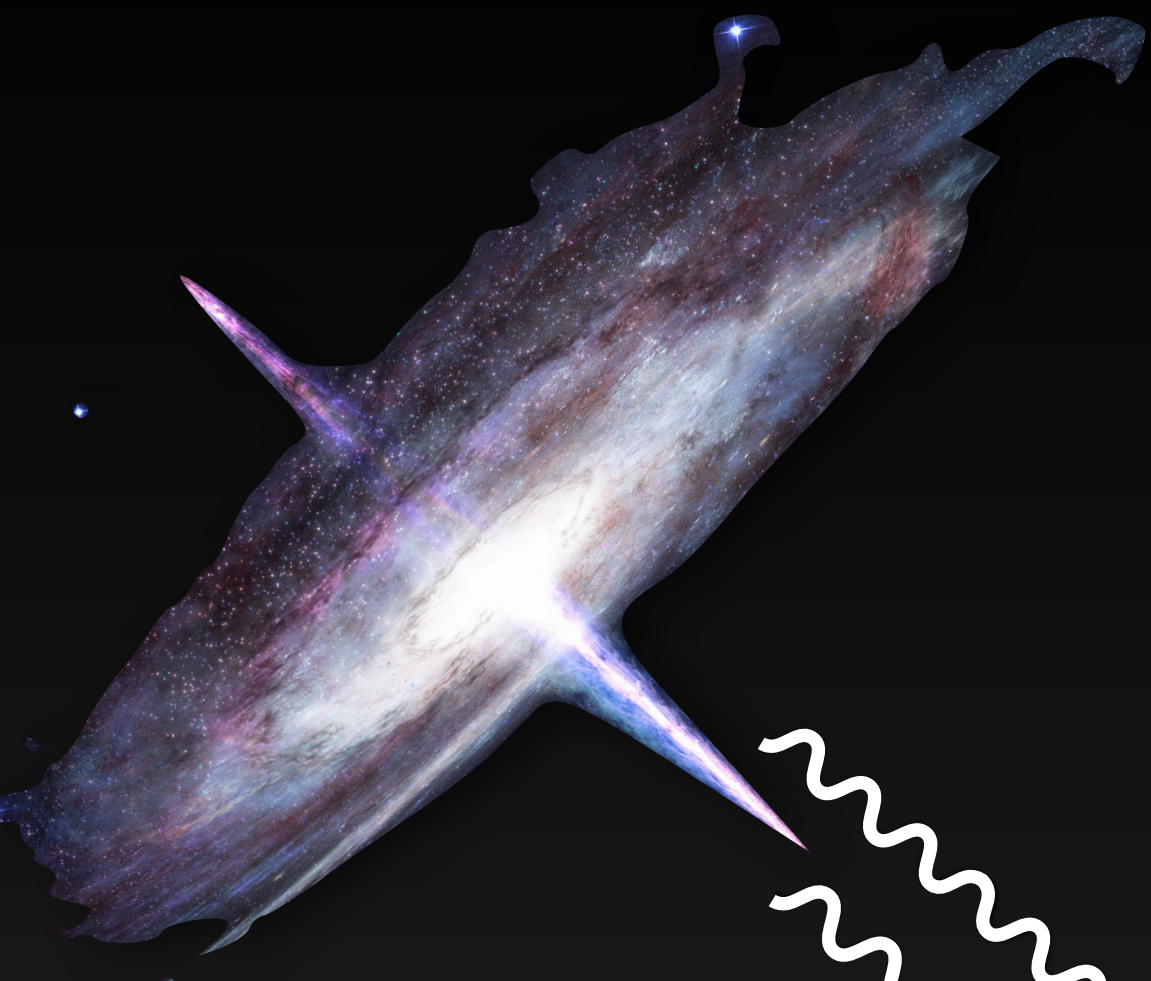
Using gamma-ray observations of blazars

- Excess γ rays at lower energies
[e.g. Neronov & Semikoz 2008]
- Extended γ -ray halos
[Aharonian et al. 1994]
- Time delayed γ -ray emission
[Plaga 1995]
- Biggest uncertainty: blazar duty cycle
[Dermer et al. 2011]



Goal: new constraints on the IGMF

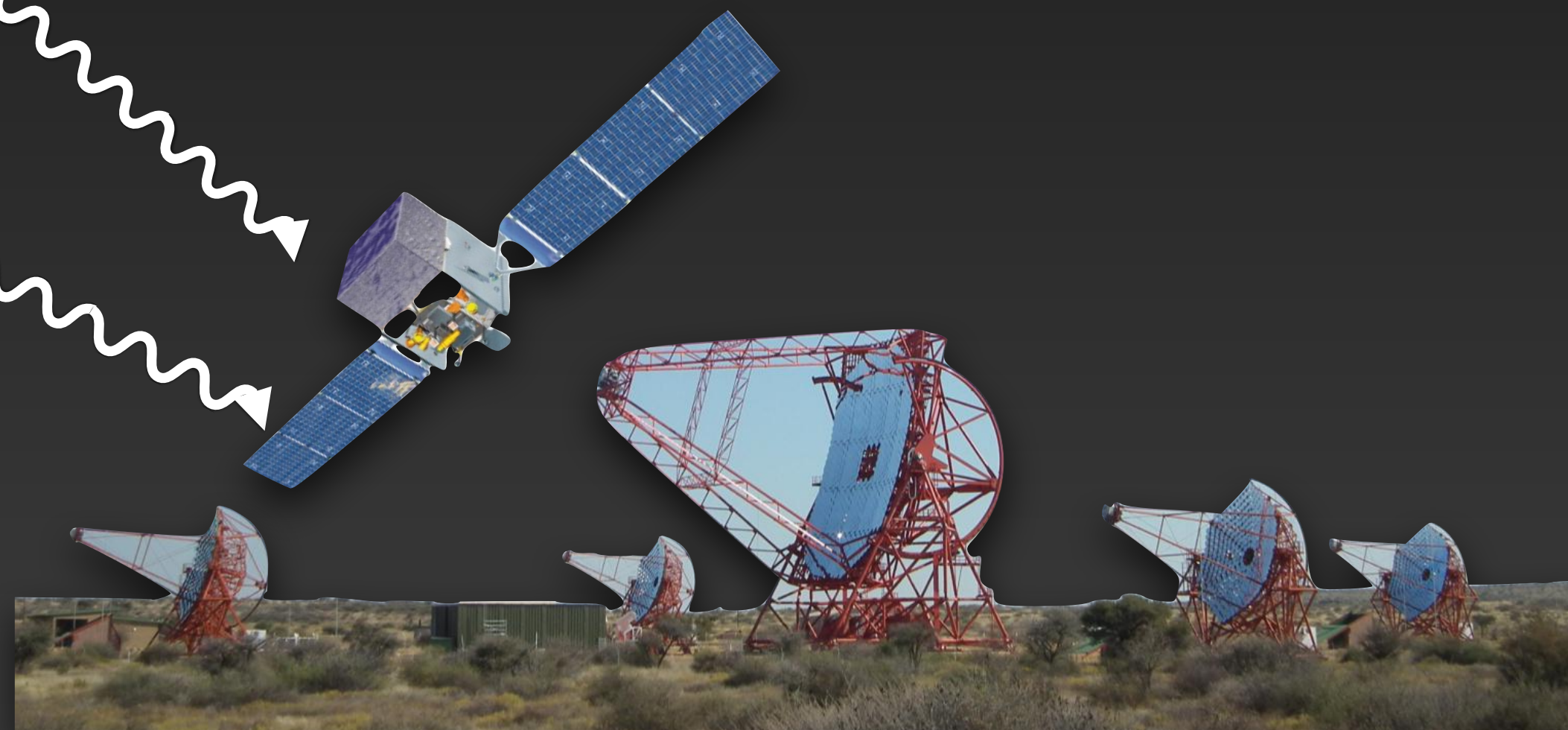
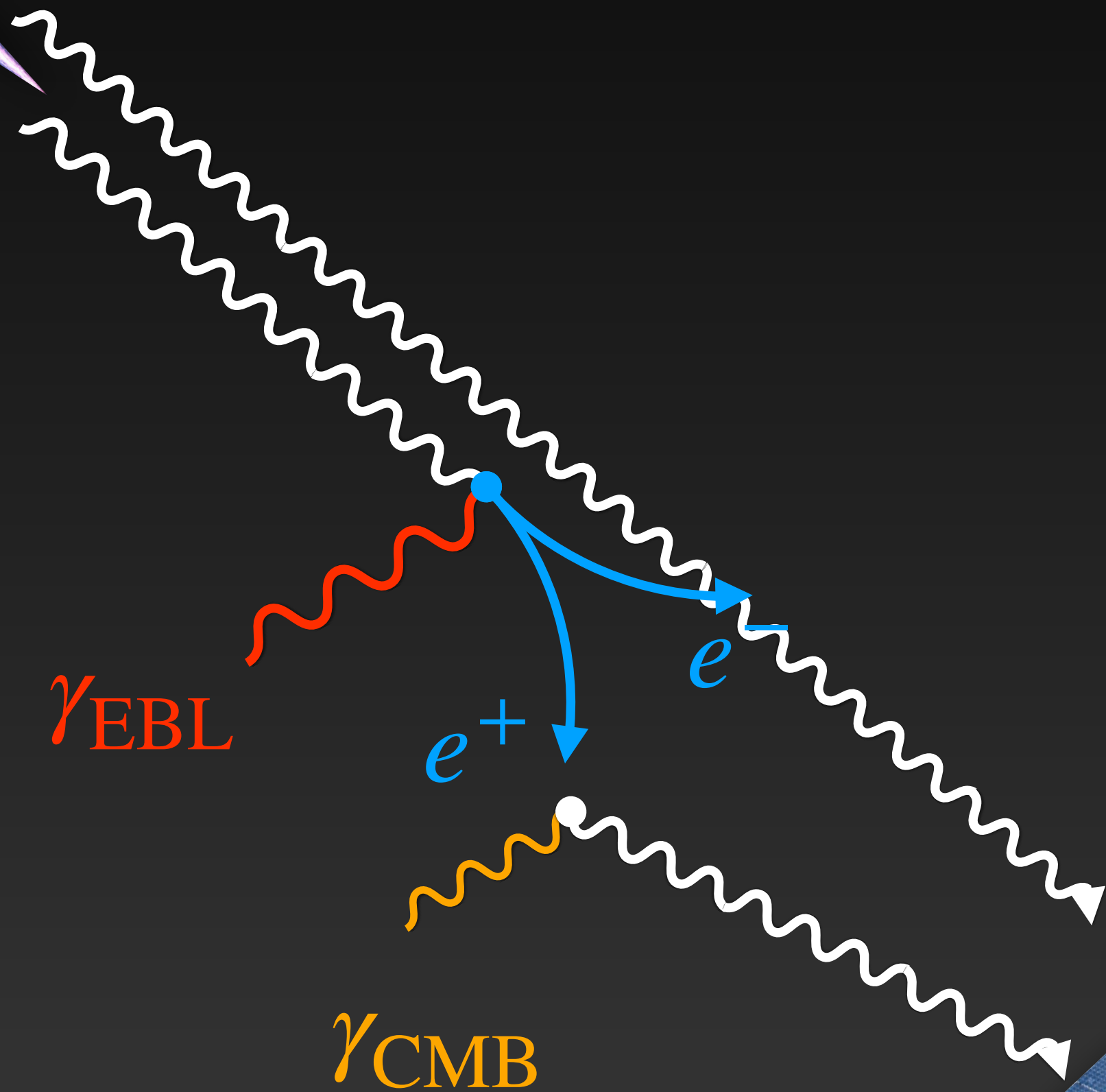
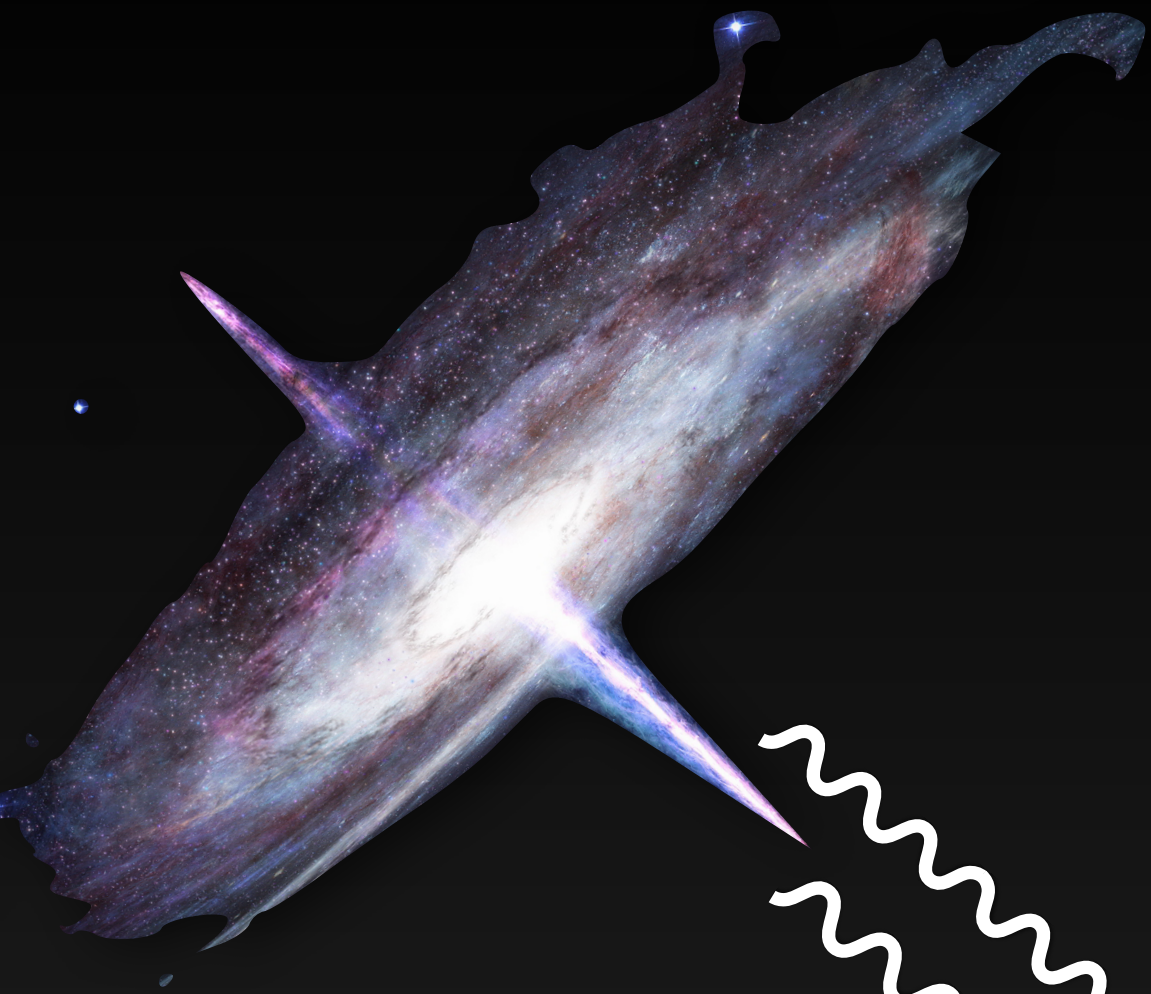
Using a combined maximum likelihood approach of H.E.S.S. and LAT data



Goal: new constraints on the IGMF

Using a combined maximum likelihood approach of H.E.S.S. and LAT data

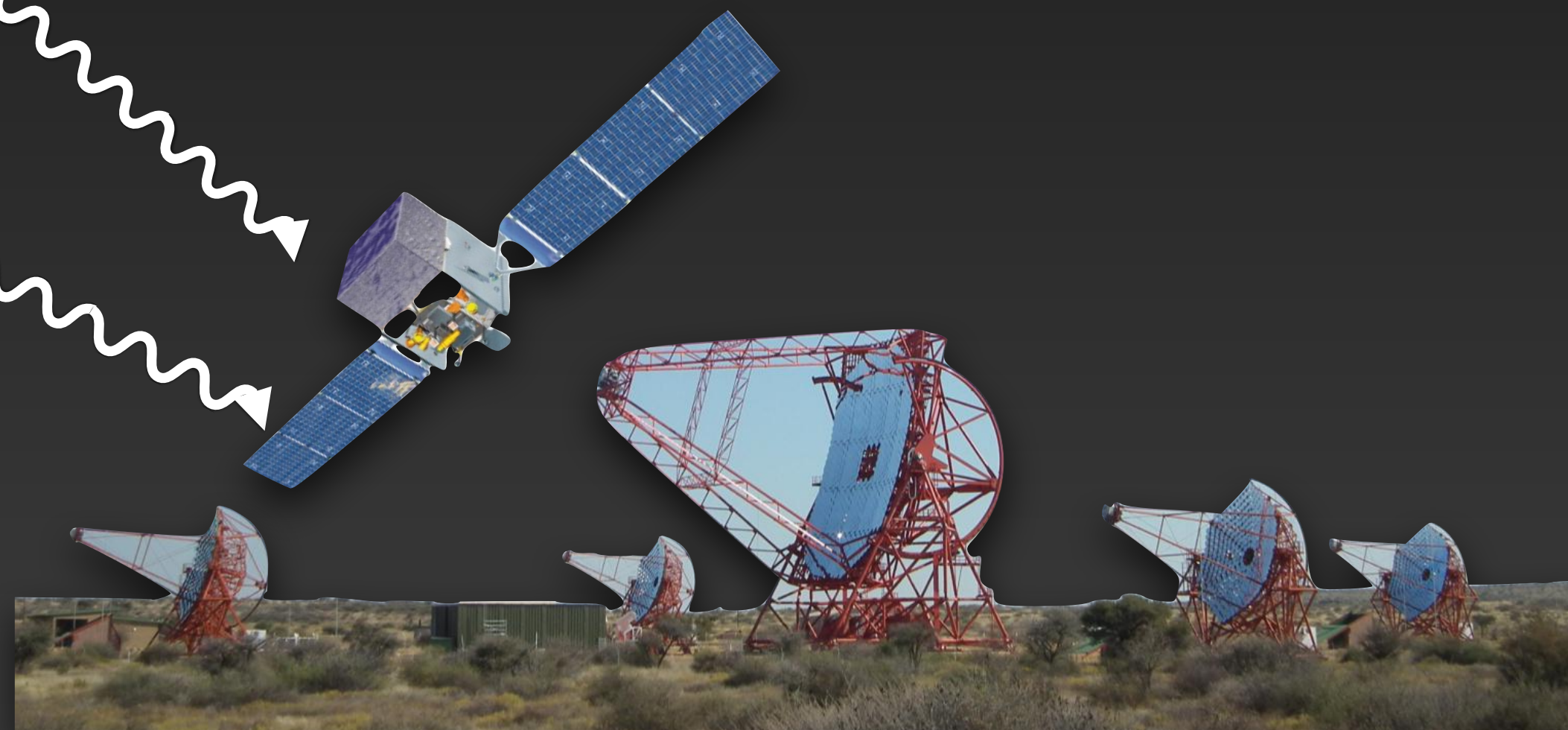
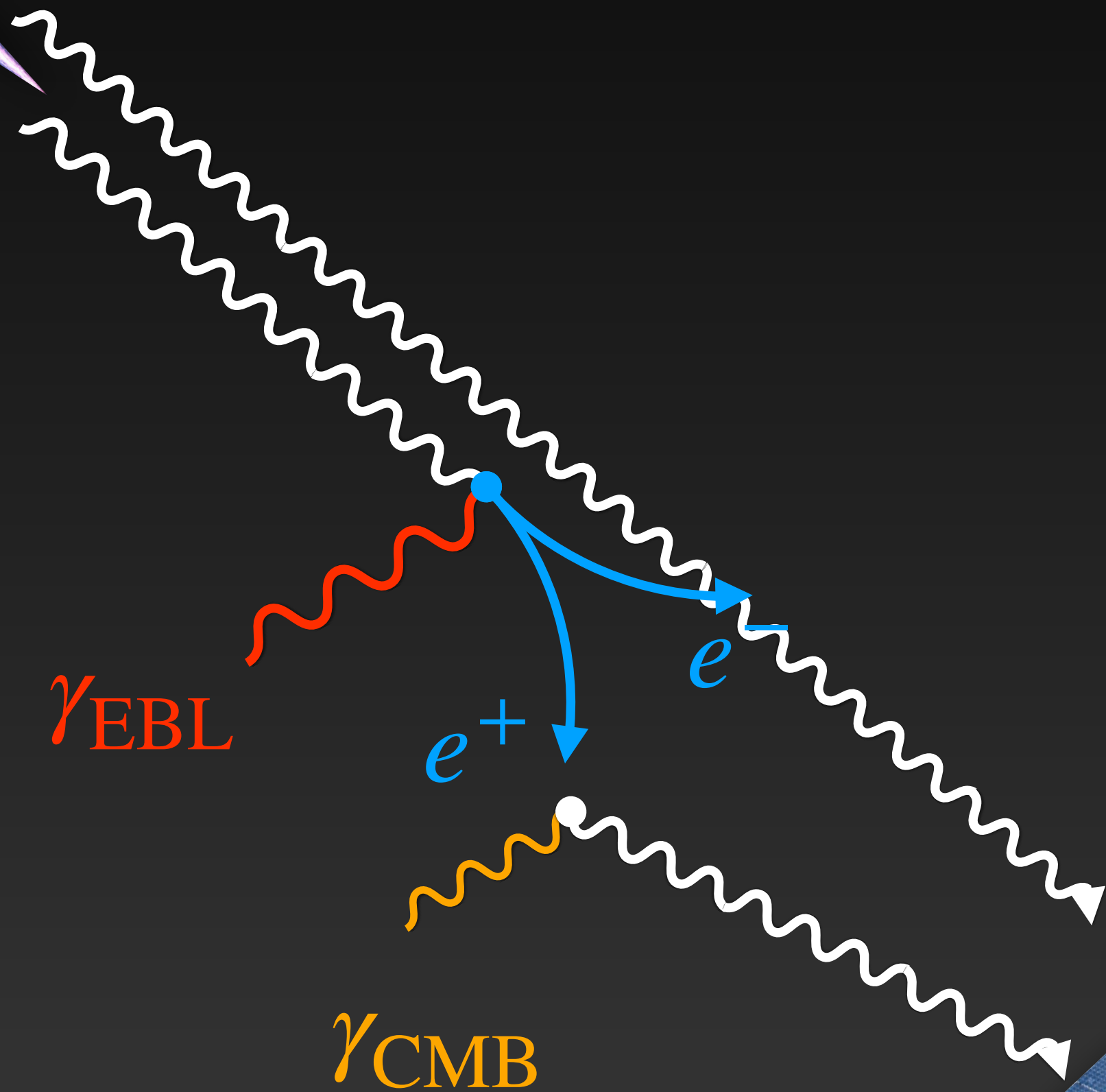
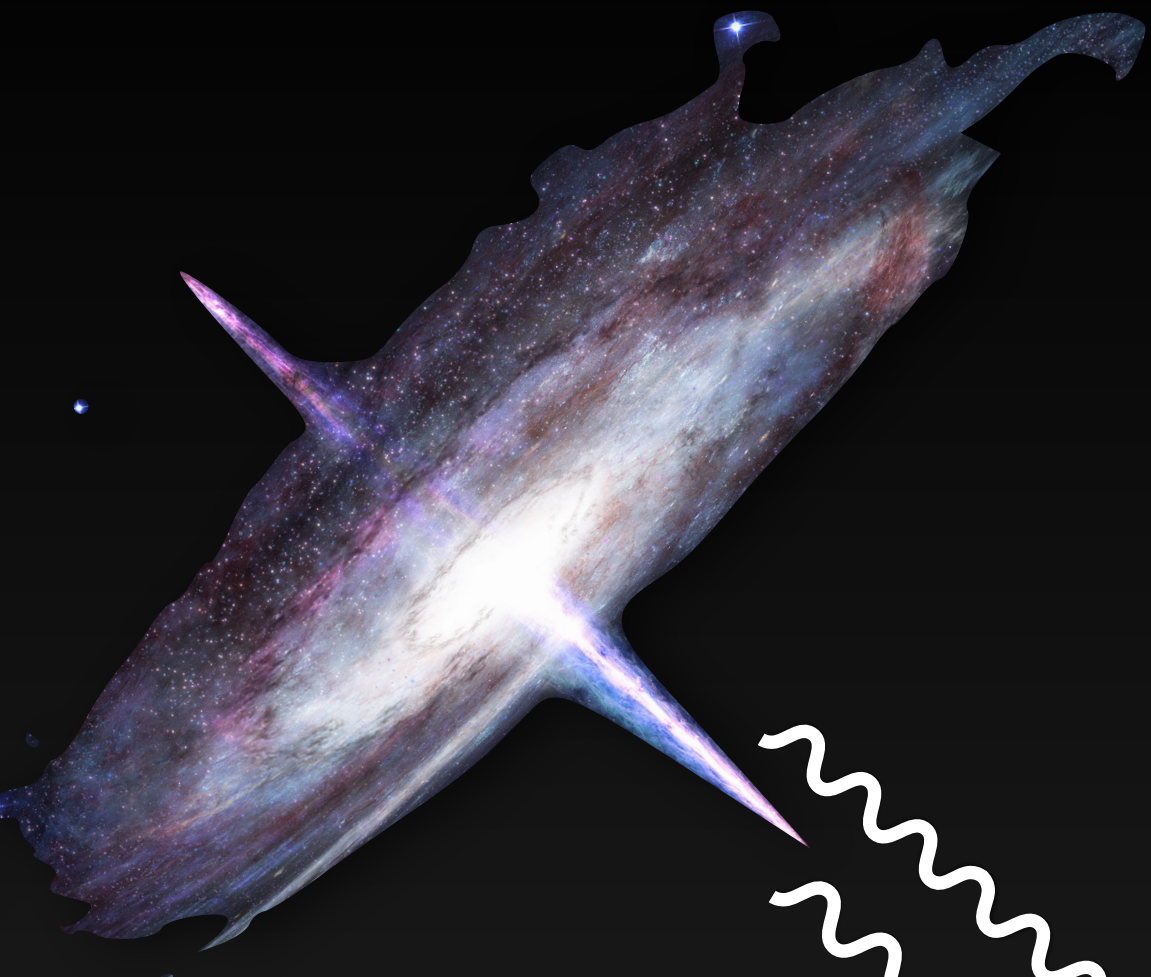
- Search for spatial and spectral halo signature



Goal: new constraints on the IGMF

Using a combined maximum likelihood approach of H.E.S.S. and LAT data

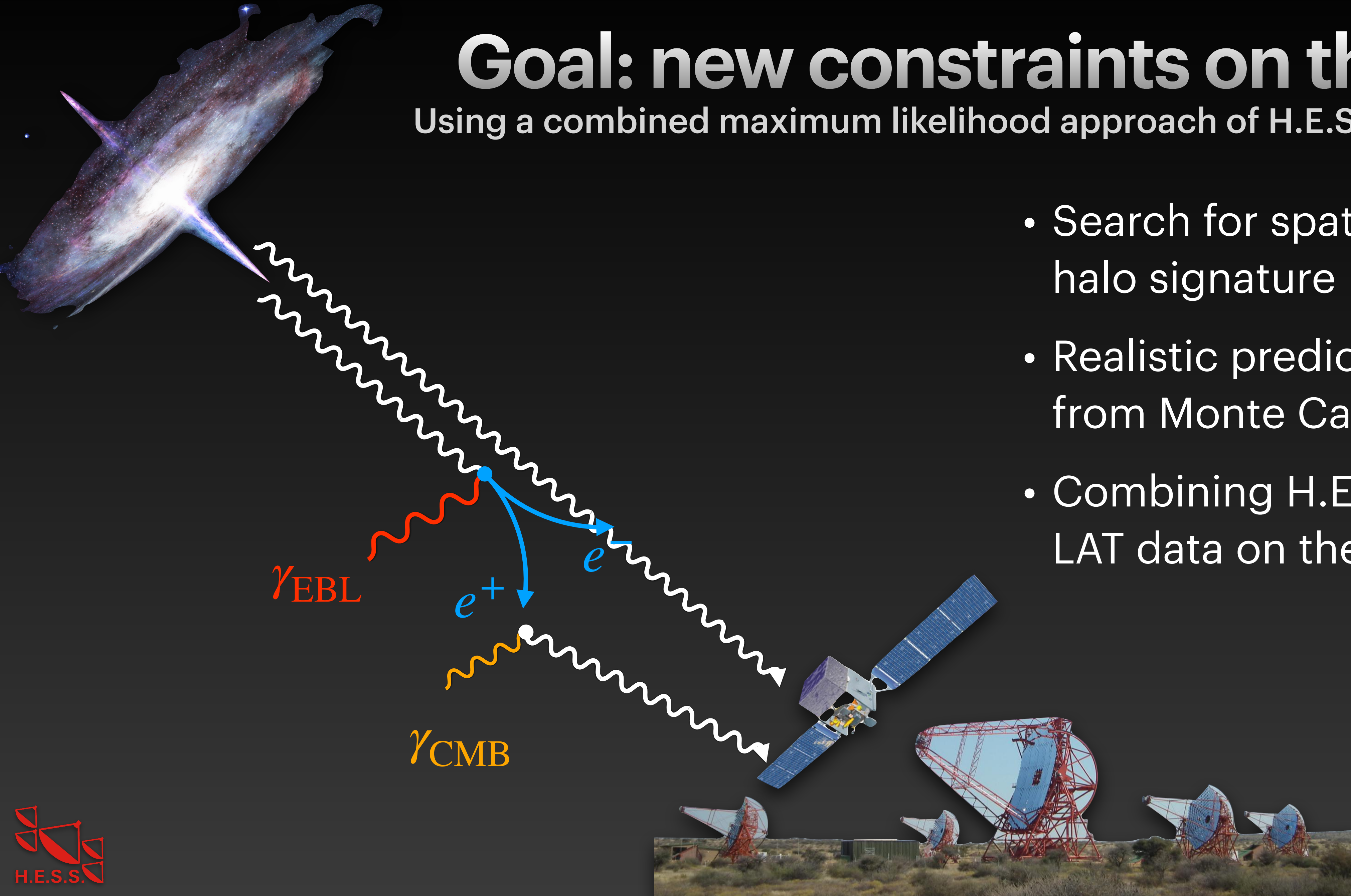
- Search for spatial and spectral halo signature
- Realistic predictions for halo from Monte Carlo Simulations



Goal: new constraints on the IGMF

Using a combined maximum likelihood approach of H.E.S.S. and LAT data

- Search for spatial and spectral halo signature
- Realistic predictions for halo from Monte Carlo Simulations
- Combining H.E.S.S. and Fermi-LAT data on the likelihood level



Source Selection

Source Selection

- **Demands:**

Source Selection

- **Demands:**
 - Emission at energies corresponding to high optical depth

Source Selection

- **Demands:**
 - Emission at energies corresponding to high optical depth
 - Stable gamma-ray emission in time as seen with the LAT

Source Selection

- **Demands:**
 - Emission at energies corresponding to high optical depth
 - Stable gamma-ray emission in time as seen with the LAT
 - \Rightarrow extreme HBL sources

Source Selection

- **Demands:**
 - Emission at energies corresponding to high optical depth
 - Stable gamma-ray emission in time as seen with the LAT
 - \Rightarrow extreme HBL sources
- **Source selection from 4LAC-DR2 catalog:**

Source Selection

- **Demands:**
 - Emission at energies corresponding to high optical depth
 - Stable gamma-ray emission in time as seen with the LAT
 - \Rightarrow extreme HBL sources
- **Source selection from 4LAC-DR2 catalog:**
 - Spectral type: power law & $\Gamma + \sigma_{\Gamma} < 2$

Source Selection

- **Demands:**
 - Emission at energies corresponding to high optical depth
 - Stable gamma-ray emission in time as seen with the LAT
 - \Rightarrow extreme HBL sources
- **Source selection from 4LAC-DR2 catalog:**
 - Spectral type: power law & $\Gamma + \sigma_{\Gamma} < 2$
 - Redshift known

Source Selection

- **Demands:**
 - Emission at energies corresponding to high optical depth
 - Stable gamma-ray emission in time as seen with the LAT
 - \Rightarrow extreme HBL sources
- **Source selection from 4LAC-DR2 catalog:**
 - Spectral type: power law & $\Gamma + \sigma_{\Gamma} < 2$
 - Redshift known
 - BL Lac source type with synchrotron peak $\nu_{\text{Sync}} > 10^{17}$ Hz

Source Selection

- **Demands:**
 - Emission at energies corresponding to high optical depth
 - Stable gamma-ray emission in time as seen with the LAT
 - \Rightarrow extreme HBL sources
- **Source selection from 4LAC-DR2 catalog:**
 - Spectral type: power law & $\Gamma + \sigma_{\Gamma} < 2$
 - Redshift known
 - BL Lac source type with synchrotron peak $\nu_{\text{sync}} > 10^{17}$ Hz
 - Chance probability < 99% that source is variable

Source Selection

- **Demands:**
 - Emission at energies corresponding to high optical depth
 - Stable gamma-ray emission in time as seen with the LAT
 - \Rightarrow extreme HBL sources
- **Source selection from 4LAC-DR2 catalog:**
 - Spectral type: power law & $\Gamma + \sigma_{\Gamma} < 2$
 - Redshift known
 - BL Lac source type with synchrotron peak $\nu_{\text{sync}} > 10^{17}$ Hz
 - Chance probability < 99% that source is variable
 - Sources with TeV counterpart observed with H.E.S.S.

Source Selection

- **Demands:**
 - Emission at energies corresponding to high optical depth
 - Stable gamma-ray emission in time as seen with the LAT
 - \Rightarrow extreme HBL sources
- **Source selection from 4LAC-DR2 catalog:**
 - Spectral type: power law & $\Gamma + \sigma_{\Gamma} < 2$
 - Redshift known
 - BL Lac source type with synchrotron peak $\nu_{\text{Sync}} > 10^{17}$ Hz
 - Chance probability < 99% that source is variable
 - Sources with TeV counterpart observed with H.E.S.S.

Resulting sources:

Source Name	Redshift
1ES 0229+200	0,139
1ES 0347-121	0,188
PKS 0548-322	0,069
1ES 1101-232	0,186
H 2356-309	0,165

Modeling the halo with CRPropa3

Modeling the halo with CRPropa3

- CRPropa 3 Monte Carlo Code used to generate 4D (spatial + energy + delay time) halo templates

Modeling the halo with CRPropa3

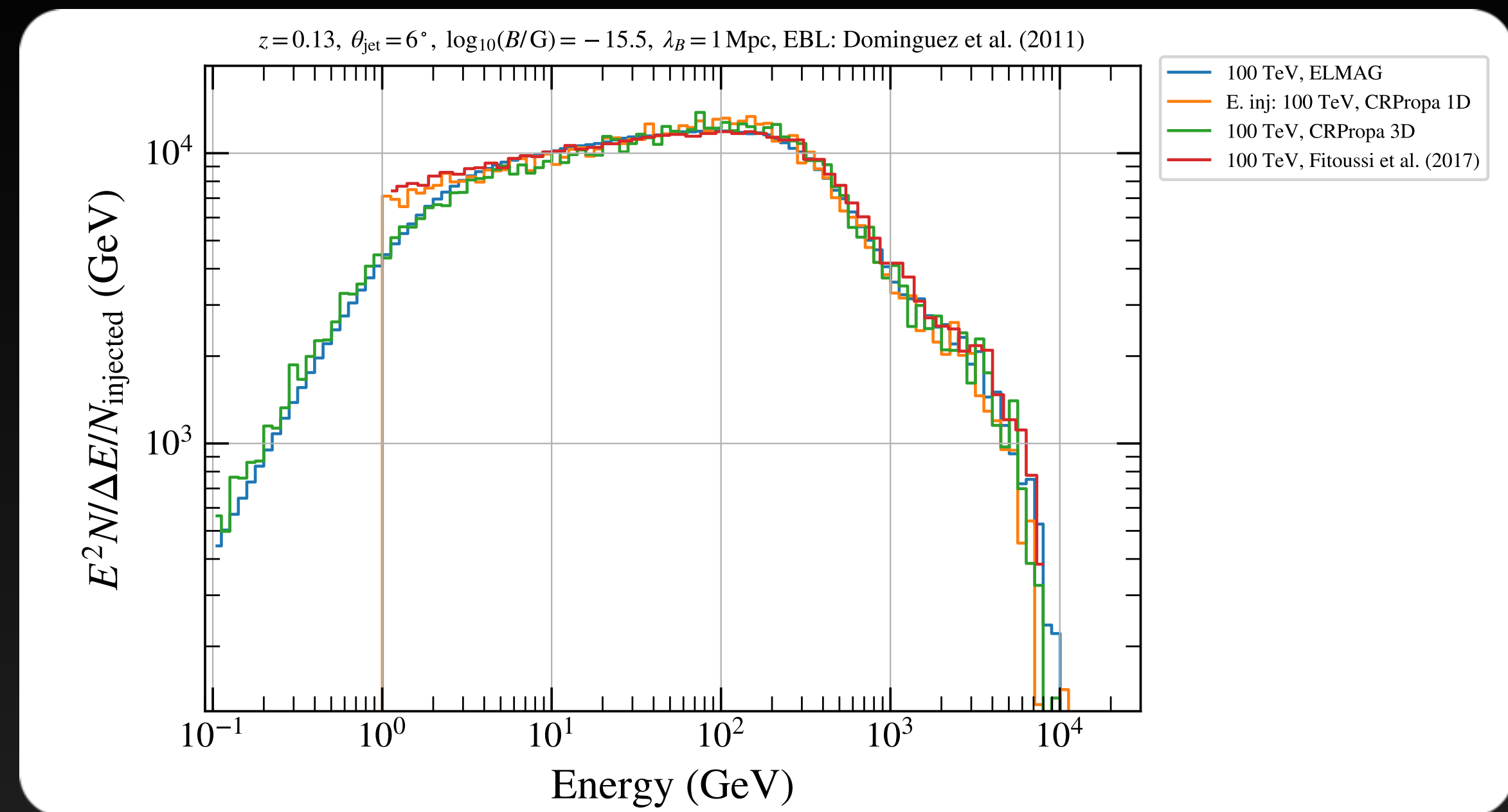
- CRPropa 3 Monte Carlo Code used to generate 4D (spatial + energy + delay time) halo templates
- All relevant particle interactions included

Modeling the halo with CRPropa3

- CRPropa 3 Monte Carlo Code used to generate 4D (spatial + energy + delay time) halo templates
- All relevant particle interactions included
- Halo templates generated for all sources for $B = 10^{-16} \text{ G}, \dots, 10^{-13} \text{ G}$ for $\lambda_B = 1 \text{ Mpc}$ and EBL model of Dominguez et al. (2011)

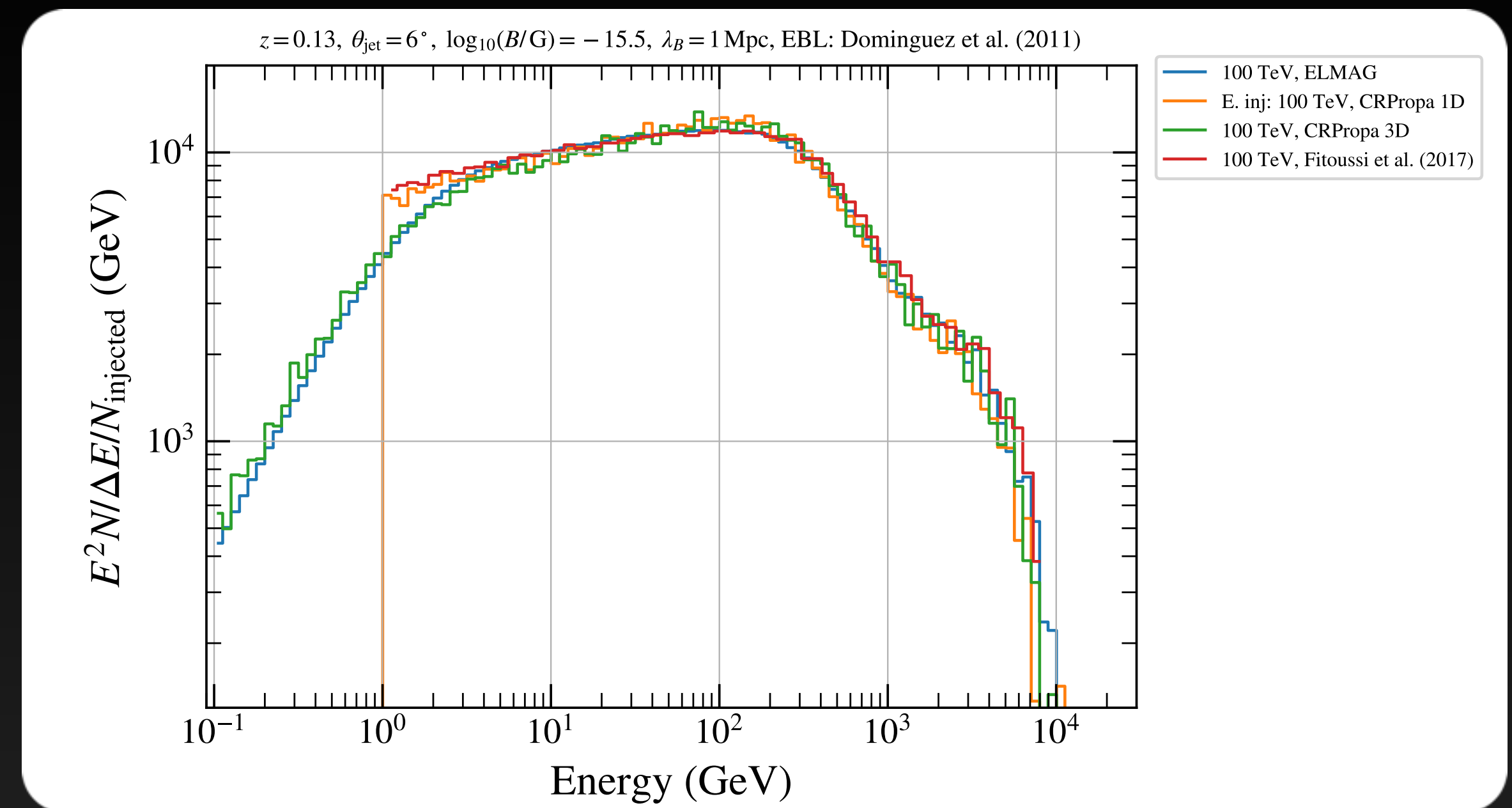
Modeling the halo with CRPropa3

- CRPropa 3 Monte Carlo Code used to generate 4D (spatial + energy + delay time) halo templates
- All relevant particle interactions included
- Halo templates generated for all sources for $B = 10^{-16} \text{ G}, \dots, 10^{-13} \text{ G}$ for $\lambda_B = 1 \text{ Mpc}$ and EBL model of Dominguez et al. (2011)



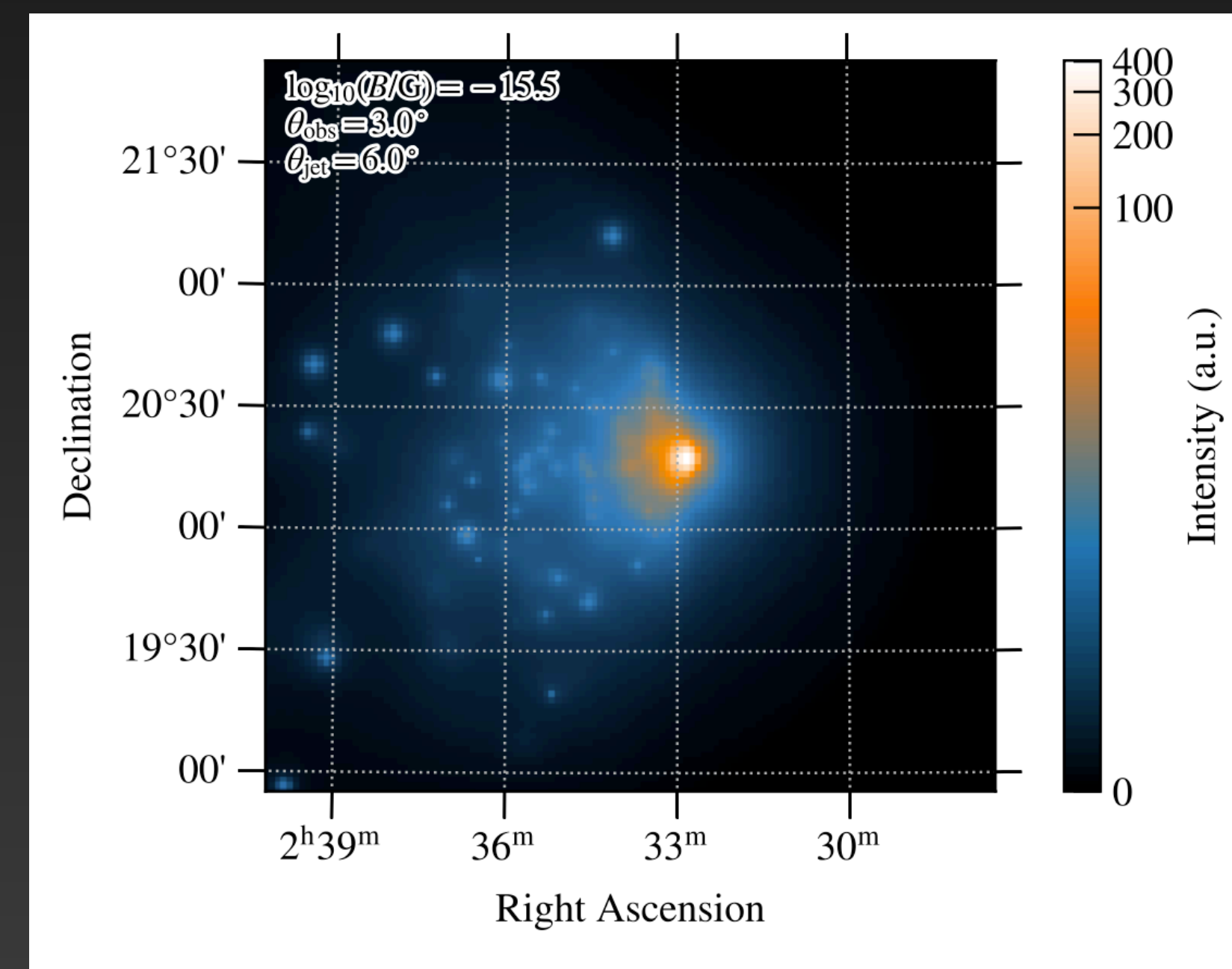
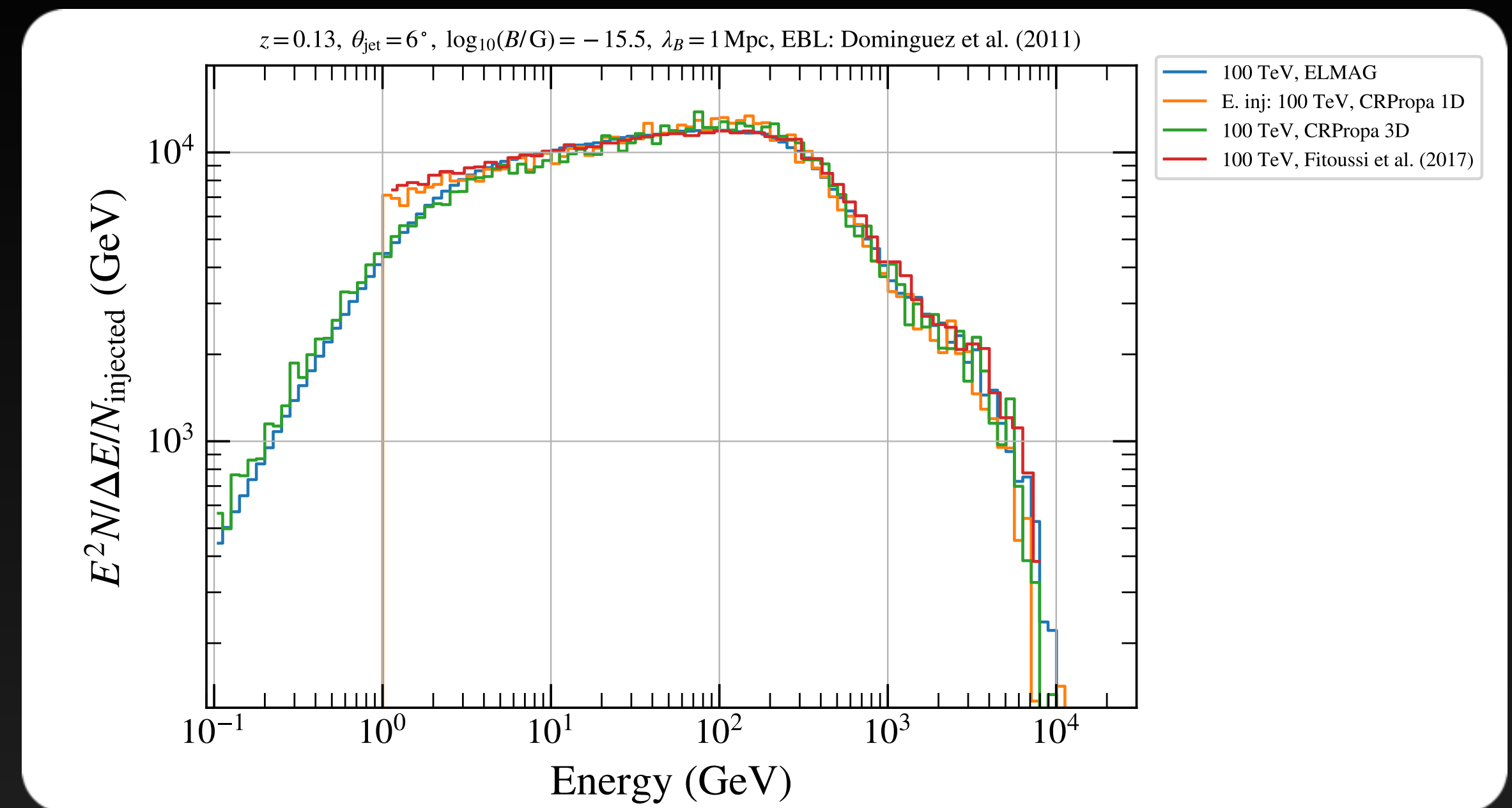
Modeling the halo with CRPropa3

- CRPropa 3 Monte Carlo Code used to generate 4D (spatial + energy + delay time) halo templates
- All relevant particle interactions included
- Halo templates generated for all sources for $B = 10^{-16} \text{ G}, \dots, 10^{-13} \text{ G}$ for $\lambda_B = 1 \text{ Mpc}$ and EBL model of Dominguez et al. (2011)
- Developed python wrapper in order to:
 - Reweight simulations for different input spectra [Ackermann et al. 2018]
 - Smooth sky maps adaptively [Ebeling et al. 2006]
 - Change orientation between source and observer in post processing [Alves Batista et al. 2016]
 - Change blazar activity time



Modeling the halo with CRPropa3

- CRPropa 3 Monte Carlo Code used to generate 4D (spatial + energy + delay time) halo templates
- All relevant particle interactions included
- Halo templates generated for all sources for $B = 10^{-16} \text{ G}, \dots, 10^{-13} \text{ G}$ for $\lambda_B = 1 \text{ Mpc}$ and EBL model of Dominguez et al. (2011)
- Developed python wrapper in order to:
 - Reweight simulations for different input spectra [Ackermann et al. 2018]
 - Smooth sky maps adaptively [Ebeling et al. 2006]
 - Change orientation between source and observer in post processing [Alves Batista et al. 2016]
 - Change blazar activity time



Fermi-LAT data selection

Parameter	Selection
Time range	11.5 years
Energy Range	> 1 GeV
ROI size	6° x 6°
Max. Zenith angle	100°
Filter	DATA_QUAL>0 && LAT_CONFIG==1
Spatial binning	0.025° / pixel
Energy binning	8 bins per decade
Event Class / IRFs	P8R3_SOURCE_V3, inflight PSF
Event types	PSF0-2, PSF3

Extracting LAT likelihoods in the presence of a halo

Extracting LAT likelihoods in the presence of a halo

- First step: standard LAT point source analysis

Extracting LAT likelihoods in the presence of a halo

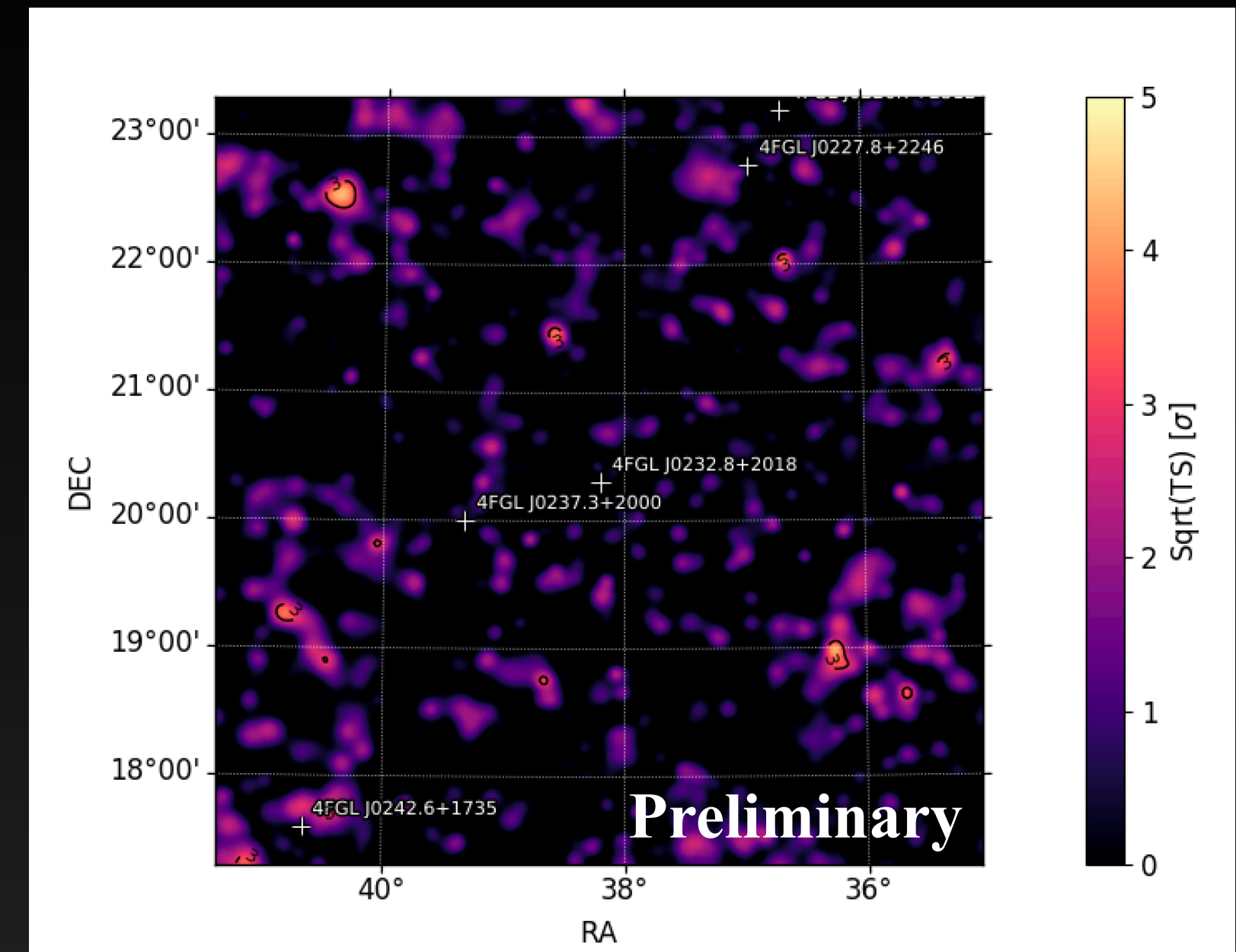
- First step: standard LAT point source analysis
- Source spectrum: $\phi_{\text{obs}} = N(E/E_0)^{-\Gamma} \exp(-\tau)$

Extracting LAT likelihoods in the presence of a halo

- First step: standard LAT point source analysis
- Source spectrum: $\phi_{\text{obs}} = N(E/E_0)^{-\Gamma} \exp(-\tau)$
- Sources appear well described by point sources

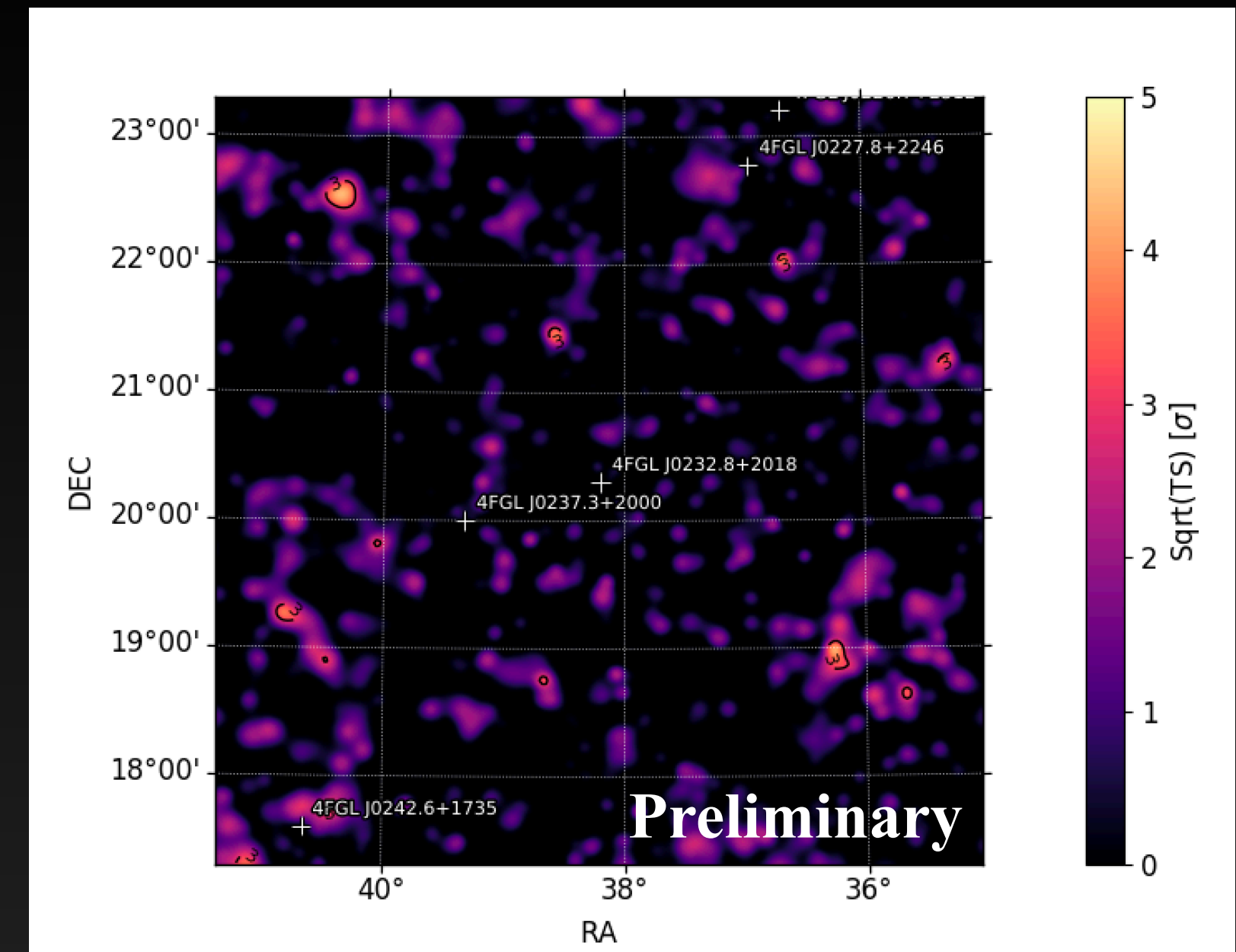
Extracting LAT likelihoods in the presence of a halo

- First step: standard LAT point source analysis
- Source spectrum: $\phi_{\text{obs}} = N(E/E_0)^{-\Gamma} \exp(-\tau)$
- Sources appear well described by point sources



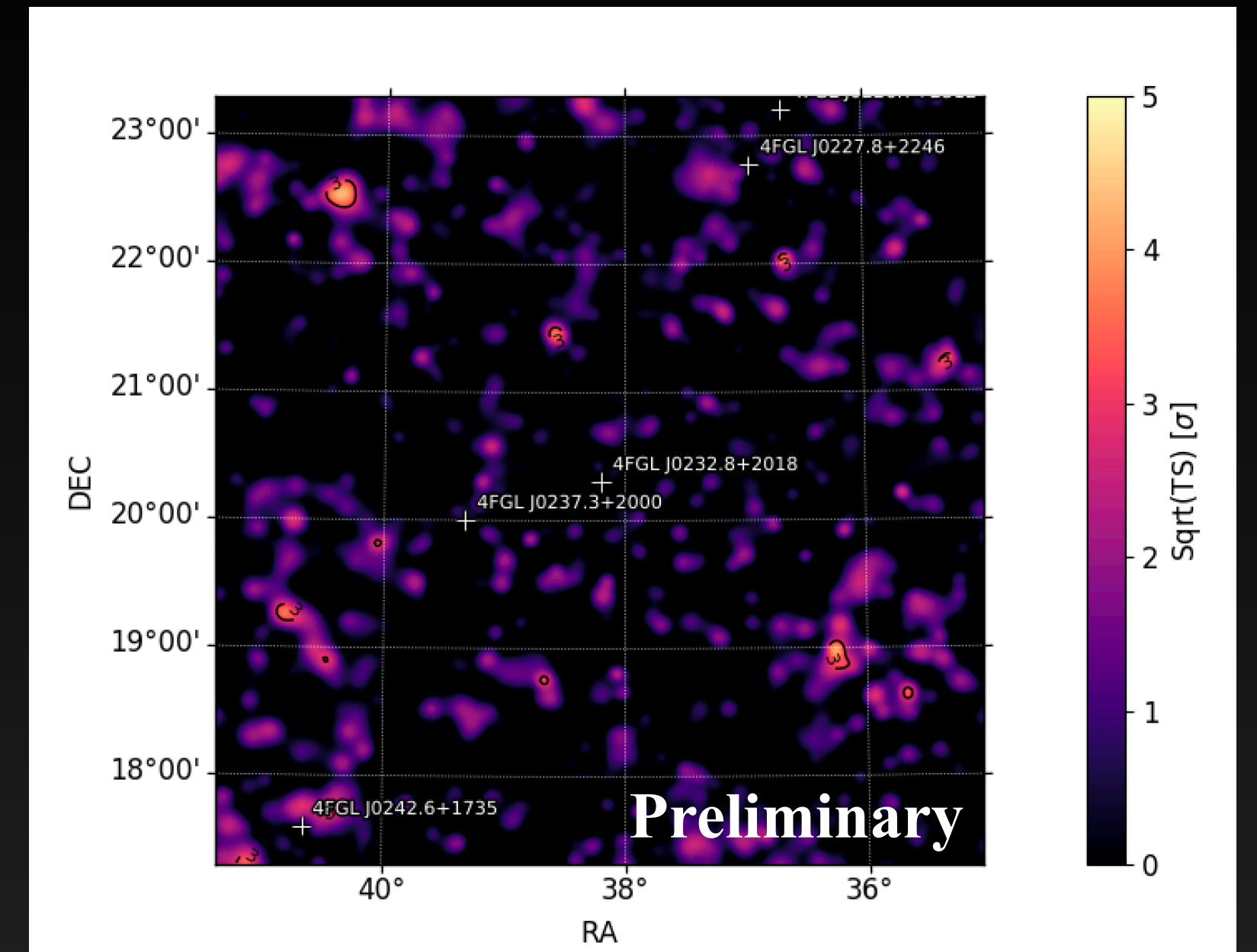
Extracting LAT likelihoods in the presence of a halo

- First step: standard LAT point source analysis
- Source spectrum: $\phi_{\text{obs}} = N(E/E_0)^{-\Gamma} \exp(-\tau)$
- Sources appear well described by point sources
- For each simulated IGMF strength:



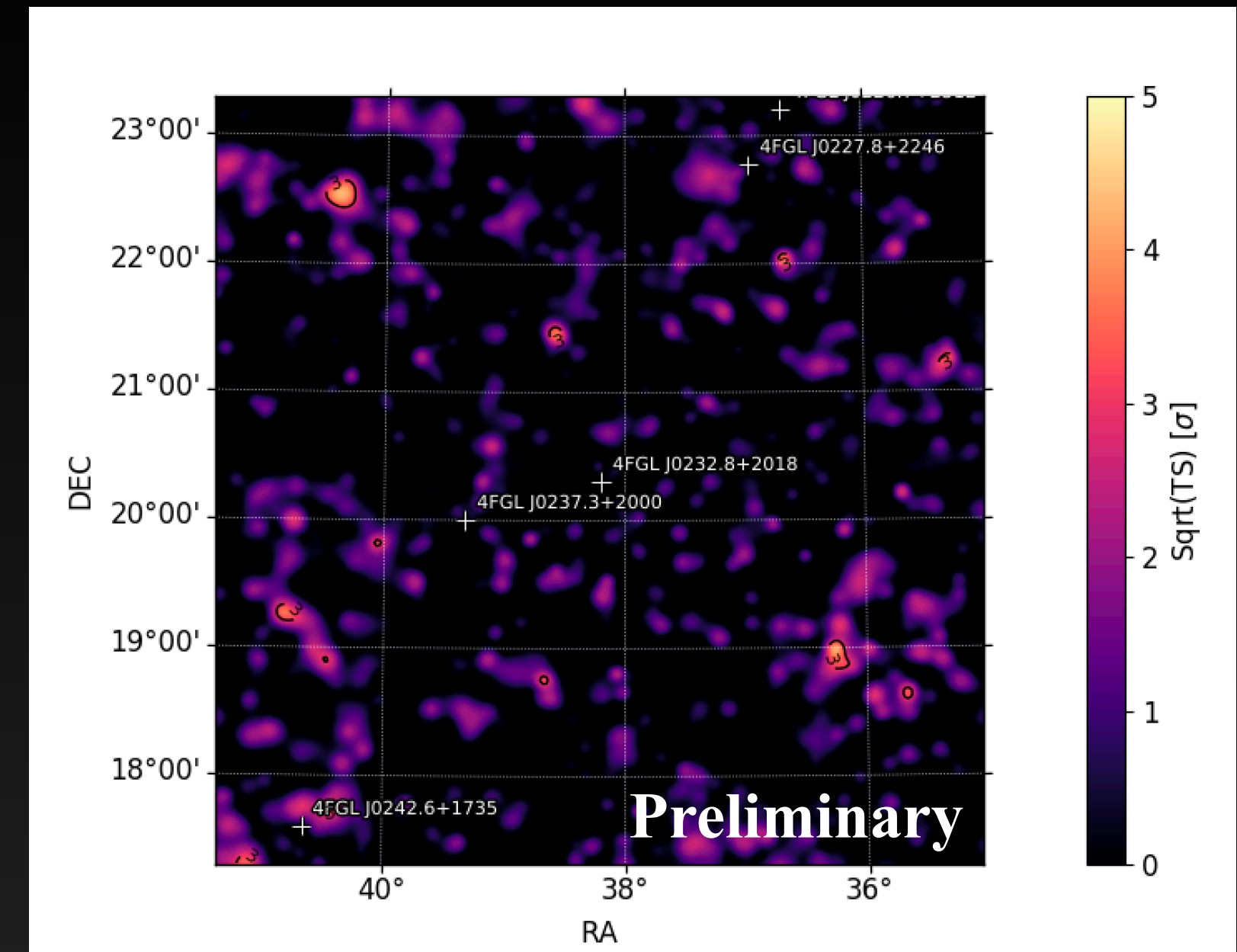
Extracting LAT likelihoods in the presence of a halo

- First step: standard LAT point source analysis
- Source spectrum: $\phi_{\text{obs}} = N(E/E_0)^{-\Gamma} \exp(-\tau)$
- Sources appear well described by point sources
- For each simulated IGMF strength:
 - Change point source model to $\phi_{\text{obs}} = N(E/E_0)^{-\Gamma} \exp(-E/E_{\text{cut}}) \exp(-\tau)$



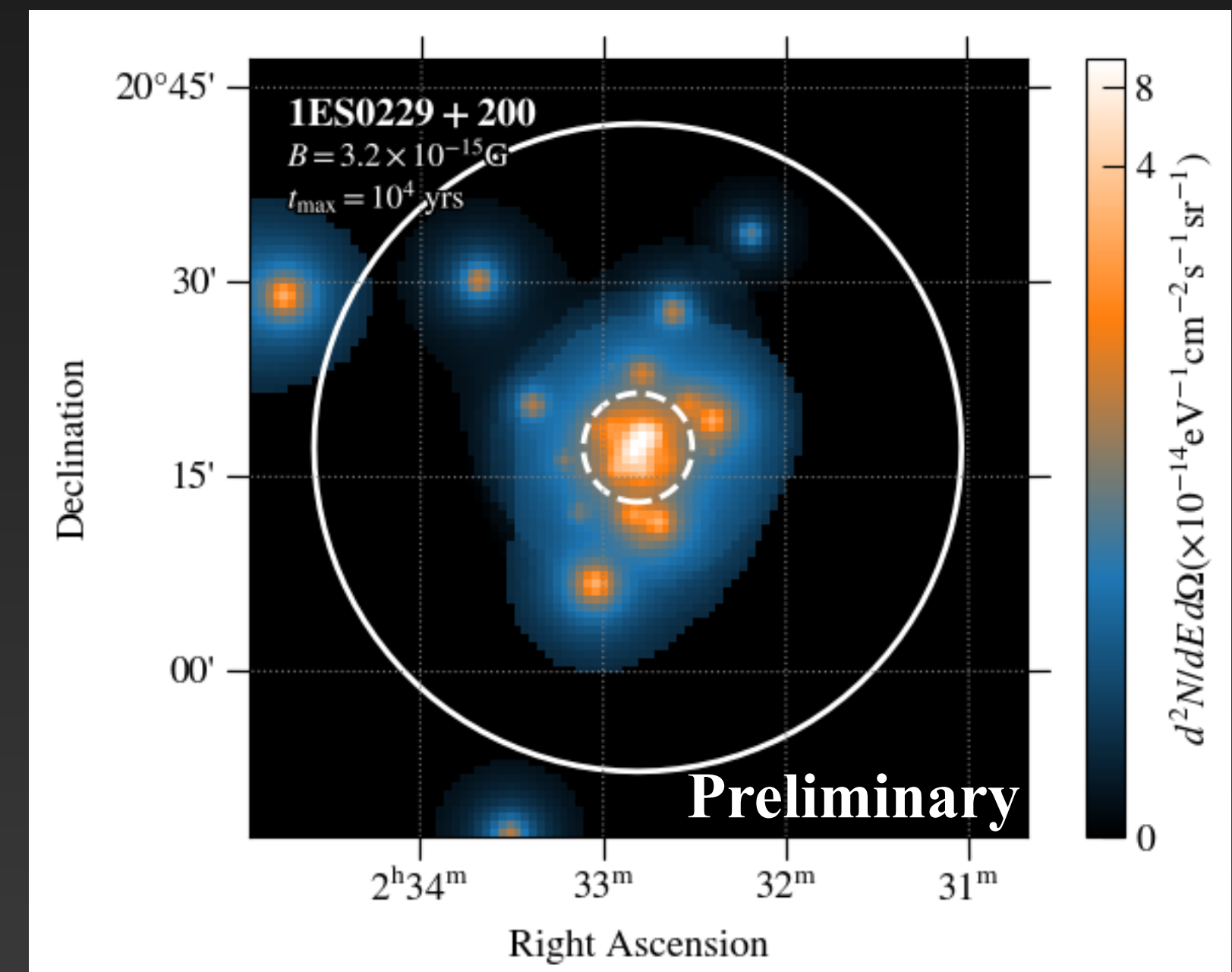
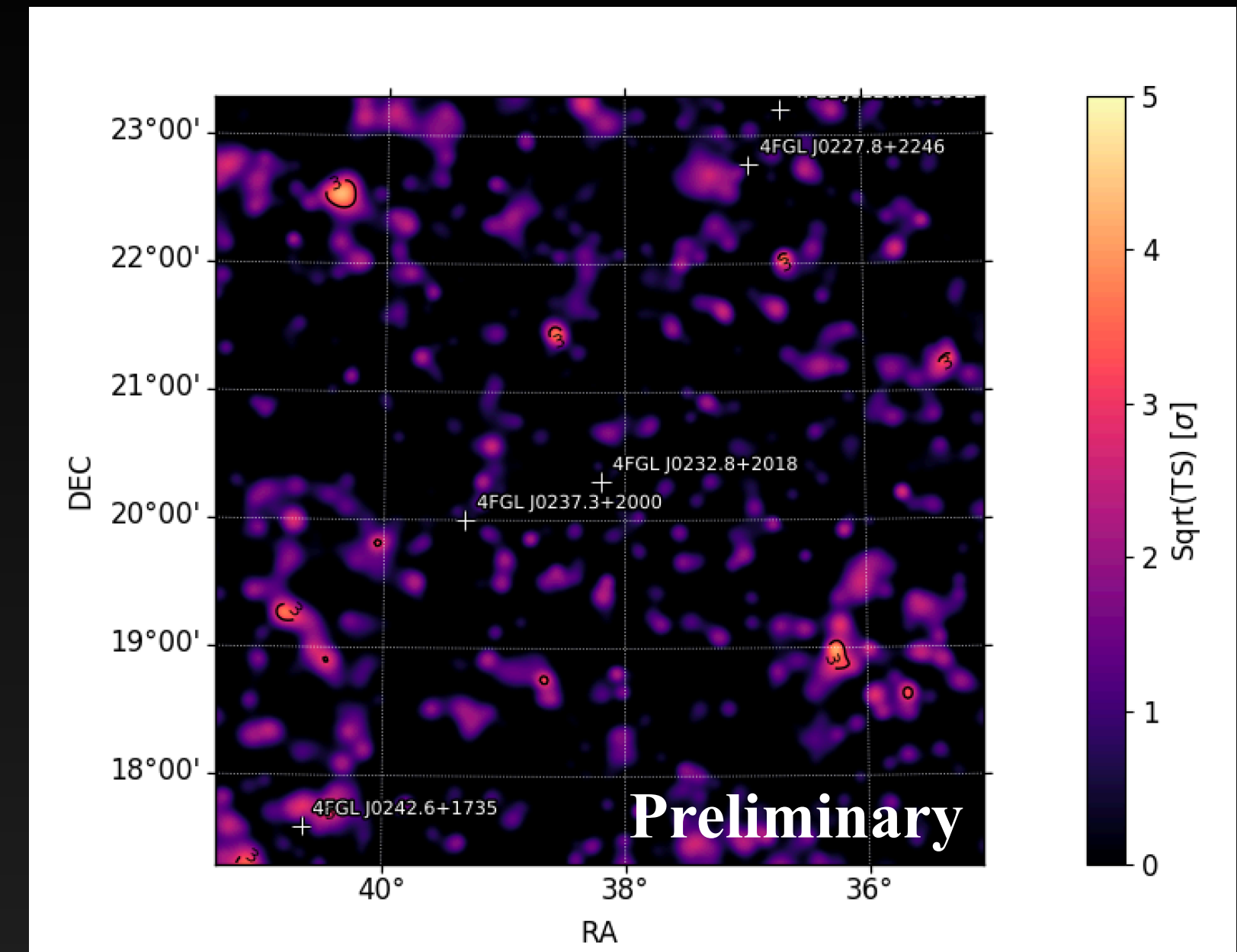
Extracting LAT likelihoods in the presence of a halo

- First step: standard LAT point source analysis
- Source spectrum: $\phi_{\text{obs}} = N(E/E_0)^{-\Gamma} \exp(-\tau)$
- Sources appear well described by point sources
- For each simulated IGMF strength:
 - Change point source model to $\phi_{\text{obs}} = N(E/E_0)^{-\Gamma} \exp(-E/E_{\text{cut}}) \exp(-\tau)$
 - Loop over spectral parameters, add corresponding halo template, extract likelihood of fit, $\ln \mathcal{L}_{\text{LAT}}$



Extracting LAT likelihoods in the presence of a halo

- First step: standard LAT point source analysis
- Source spectrum: $\phi_{\text{obs}} = N(E/E_0)^{-\Gamma} \exp(-\tau)$
- Sources appear well described by point sources
- For each simulated IGMF strength:
 - Change point source model to $\phi_{\text{obs}} = N(E/E_0)^{-\Gamma} \exp(-E/E_{\text{cut}}) \exp(-\tau)$
 - Loop over spectral parameters, add corresponding halo template, extract likelihood of fit, $\ln \mathcal{L}_{\text{LAT}}$



H.E.S.S. Data sets

- Data taken with small telescopes up to 2018 considered here
- Analysis performed using gammapy [Deil et al. 2017]
- Source spectra ϕ_{obs} well described by power law including EBL absorption,

$$\phi_{\text{obs}} = N(E/E_0)^{-\Gamma} \exp(-\tau)$$

Preliminary

Source	Life time (hours)	Detection significance	Power law index Γ
1ES 0229+200	144,1	16.5 σ	1.76 \pm 0.12
1ES 0347-121	59,2	16.1 σ	2.12 \pm 0.15
PKS 0548-322	53,9	10.2 σ	1.92 \pm 0.12
1ES 1101-232	71,9	18.7 σ	1.66 \pm 0.09
H 2356-309	150,5	23.4 σ	2.10 \pm 0.09

Combined H.E.S.S. and LAT analysis

Combined H.E.S.S. and LAT analysis

- Intrinsic blazar model:

$$\phi(E) = N \left(\frac{E}{E_0} \right)^{-\Gamma} \exp \left(-\frac{E}{E_{\text{cut}}} \right)$$

Combined H.E.S.S. and LAT analysis

- Intrinsic blazar model:

$$\phi(E) = N \left(\frac{E}{E_0} \right)^{-\Gamma} \exp \left(-\frac{E}{E_{\text{cut}}} \right)$$

- Total source model:

$$\phi_{\text{tot}}(E, B) = \phi(E) \exp(-\tau) + \phi_{\text{halo}}(E, B)$$

Combined H.E.S.S. and LAT analysis

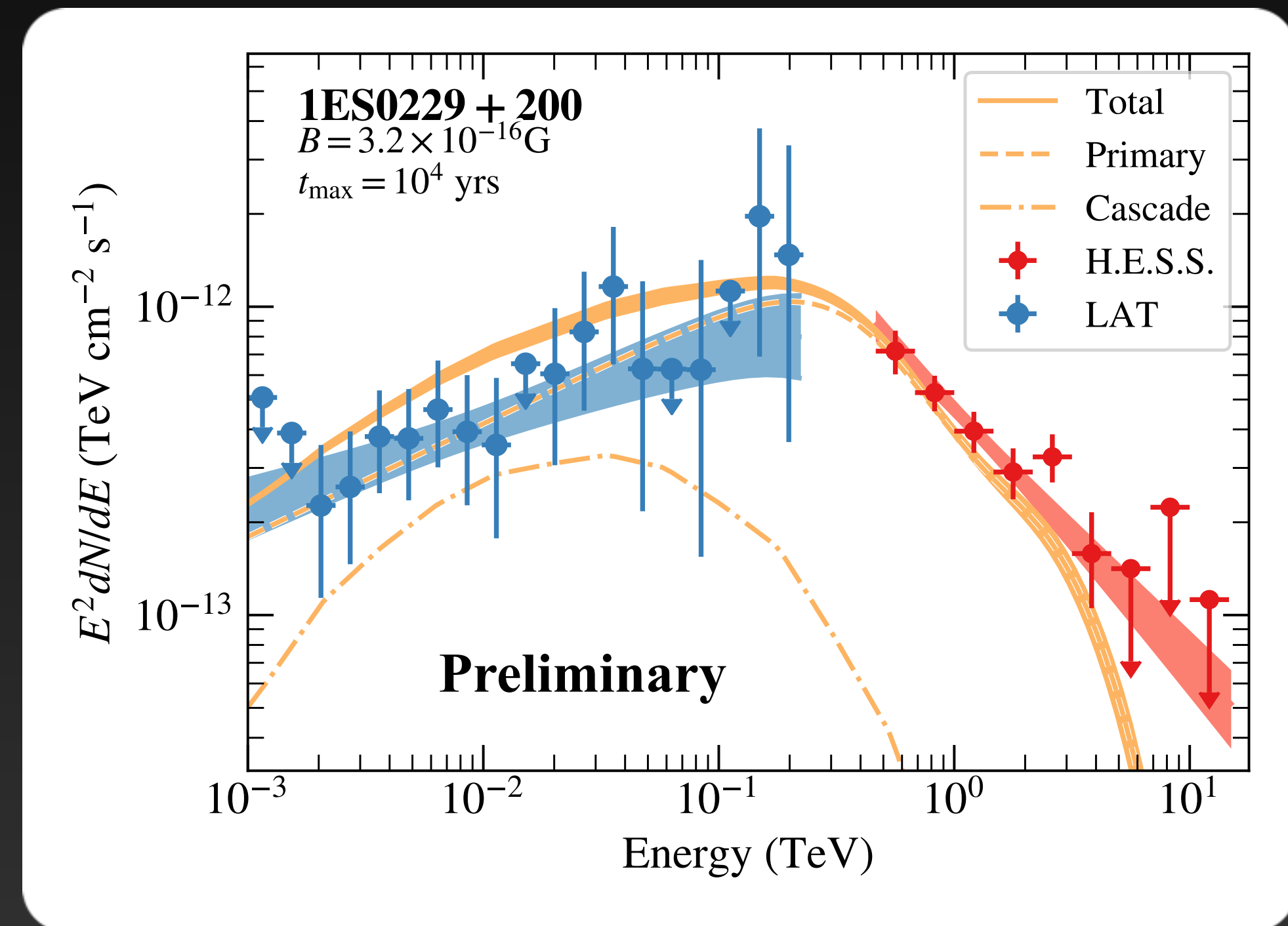
- Intrinsic blazar model:

$$\phi(E) = N \left(\frac{E}{E_0} \right)^{-\Gamma} \exp \left(-\frac{E}{E_{\text{cut}}} \right)$$

- Total source model:

$$\phi_{\text{tot}}(E, B) = \phi(E) \exp(-\tau) + \phi_{\text{halo}}(E, B)$$

- Halo flux taken from CRPropa3 simulation; depends on spectral parameters, blazar activity time...



Combined H.E.S.S. and LAT analysis

- Intrinsic blazar model:

$$\phi(E) = N \left(\frac{E}{E_0} \right)^{-\Gamma} \exp \left(-\frac{E}{E_{\text{cut}}} \right)$$

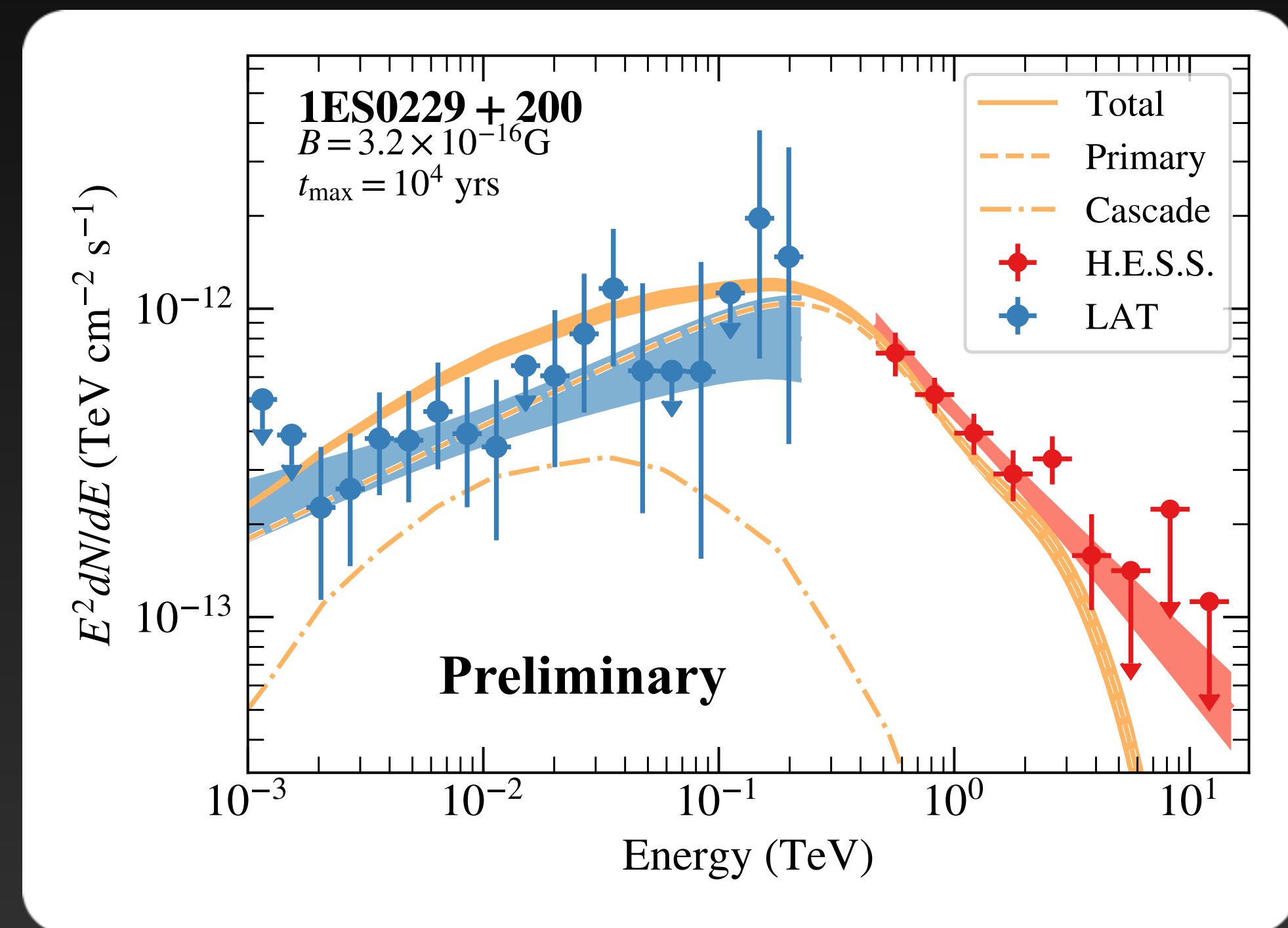
- Total source model:

$$\phi_{\text{tot}}(E, B) = \phi(E) \exp(-\tau) + \phi_{\text{halo}}(E, B)$$

- Halo flux taken from CRPropa3 simulation; depends on spectral parameters, blazar activity time...

- Spectral parameters optimized using combined H.E.S.S. and LAT likelihoods:

$$\ln \mathcal{L} = \ln \mathcal{L}_{\text{LAT}} + \ln \mathcal{L}_{\text{H.E.S.S.}}$$



Combined H.E.S.S. and LAT analysis

- Intrinsic blazar model:

$$\phi(E) = N \left(\frac{E}{E_0} \right)^{-\Gamma} \exp \left(-\frac{E}{E_{\text{cut}}} \right)$$

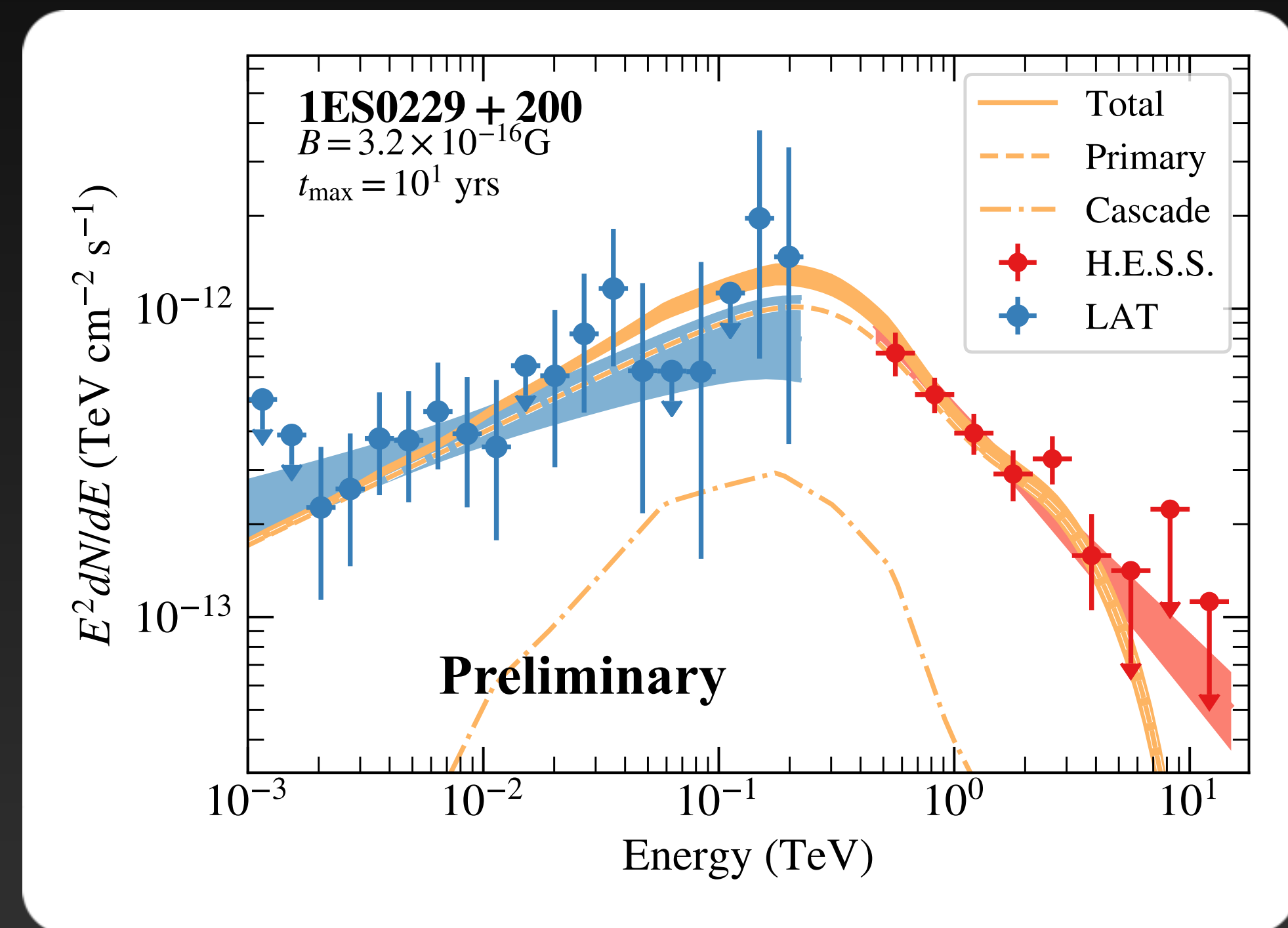
- Total source model:

$$\phi_{\text{tot}}(E, B) = \phi(E) \exp(-\tau) + \phi_{\text{halo}}(E, B)$$

- Halo flux taken from CRPropa3 simulation; depends on spectral parameters, blazar activity time...

- Spectral parameters optimized using combined H.E.S.S. and LAT likelihoods:

$$\ln \mathcal{L} = \ln \mathcal{L}_{\text{LAT}} + \ln \mathcal{L}_{\text{H.E.S.S.}}$$



Combined H.E.S.S. and LAT analysis

- Intrinsic blazar model:

$$\phi(E) = N \left(\frac{E}{E_0} \right)^{-\Gamma} \exp \left(-\frac{E}{E_{\text{cut}}} \right)$$

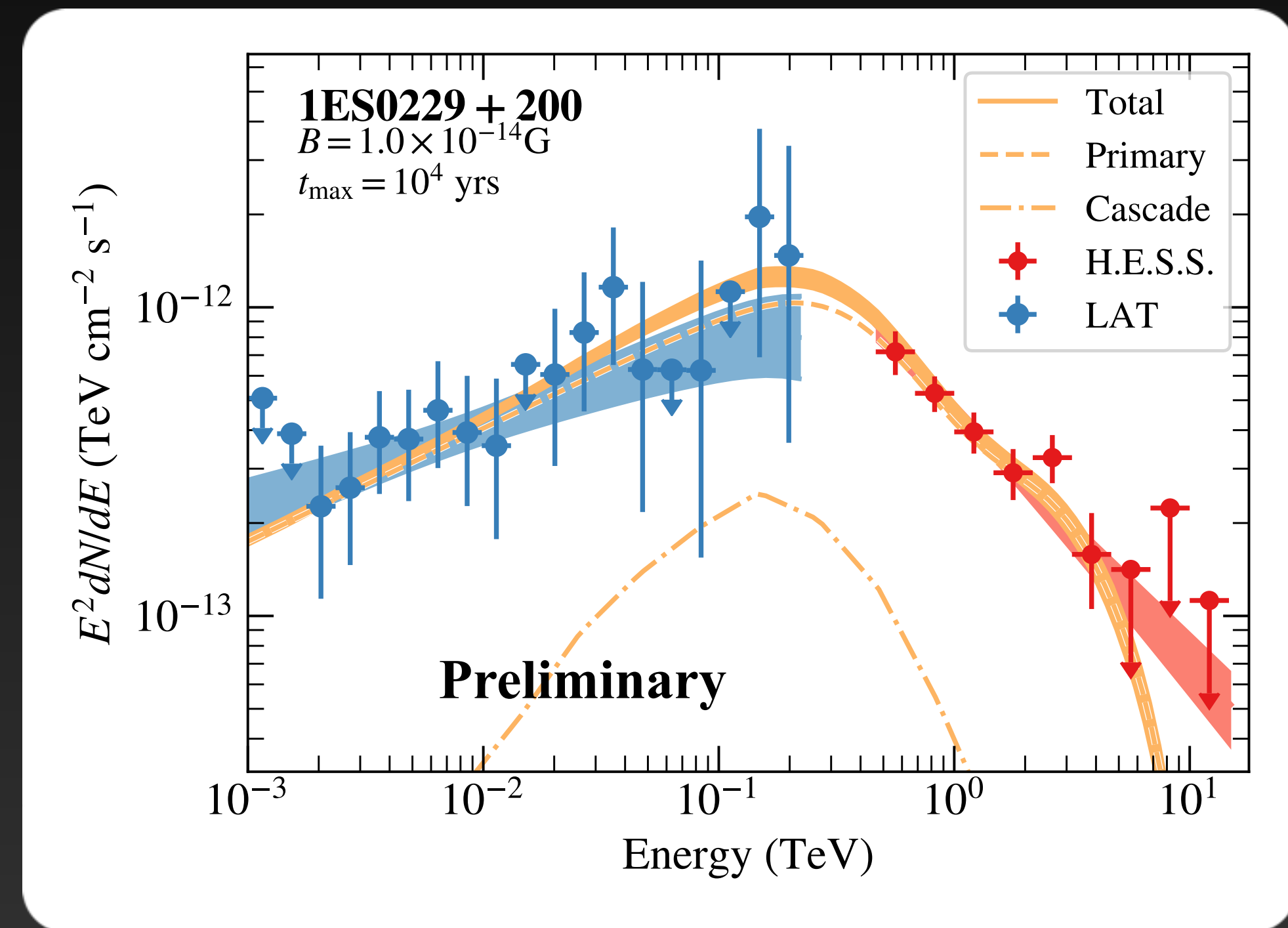
- Total source model:

$$\phi_{\text{tot}}(E, B) = \phi(E) \exp(-\tau) + \phi_{\text{halo}}(E, B)$$

- Halo flux taken from CRPropa3 simulation; depends on spectral parameters, blazar activity time...

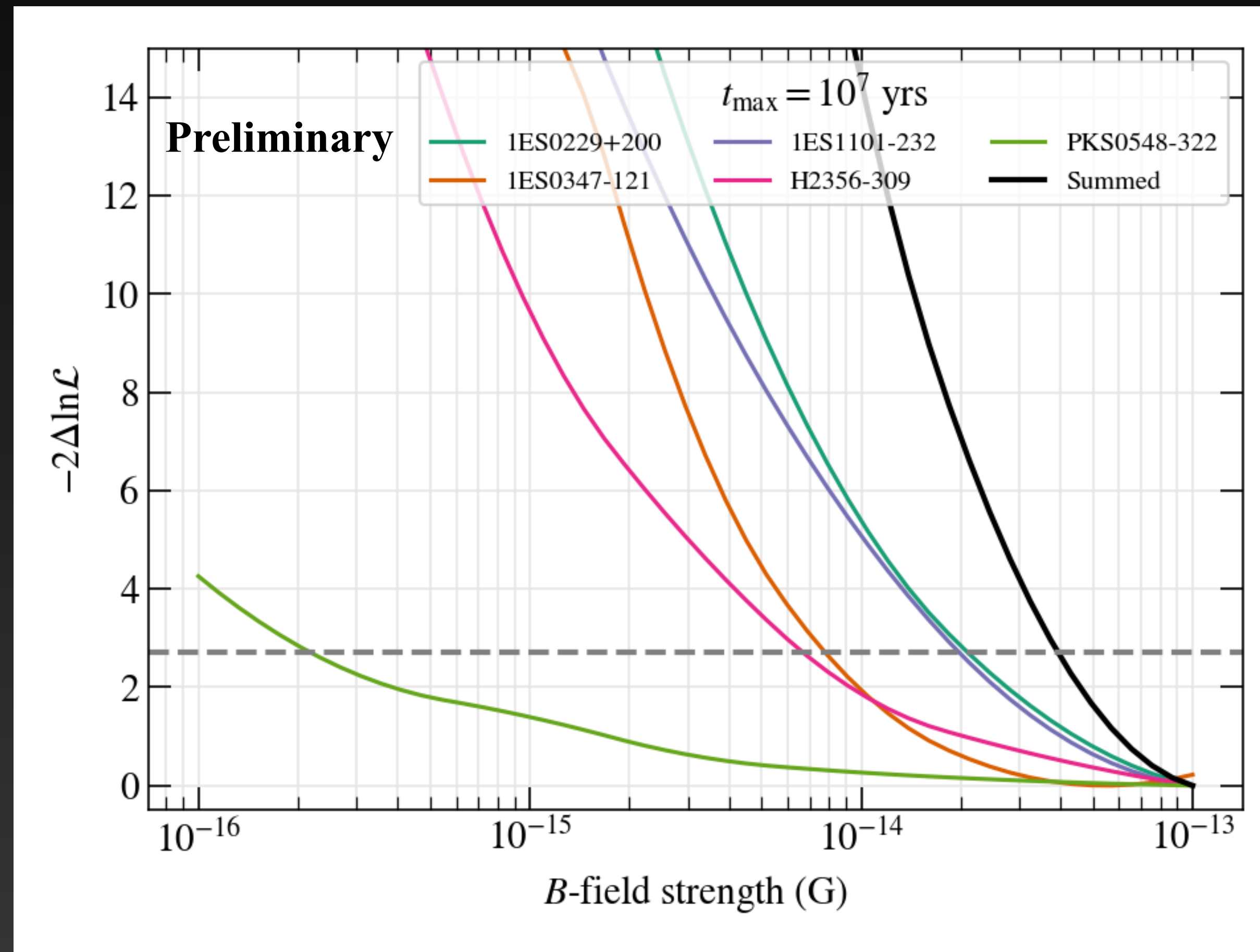
- Spectral parameters optimized using combined H.E.S.S. and LAT likelihoods:

$$\ln \mathcal{L} = \ln \mathcal{L}_{\text{LAT}} + \ln \mathcal{L}_{\text{H.E.S.S.}}$$



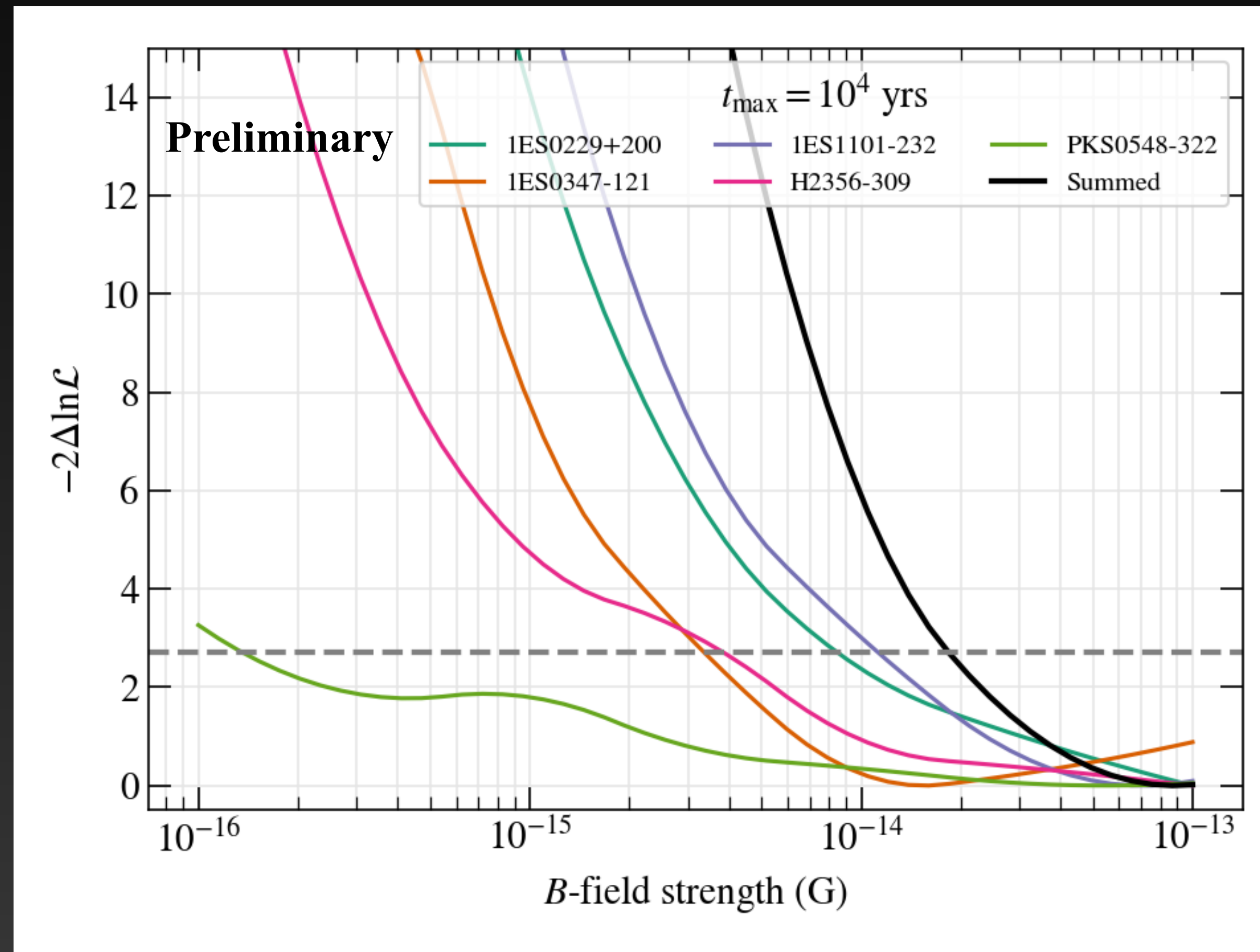
Results: lower limits on IGMF

Data does not prefer presence of halo



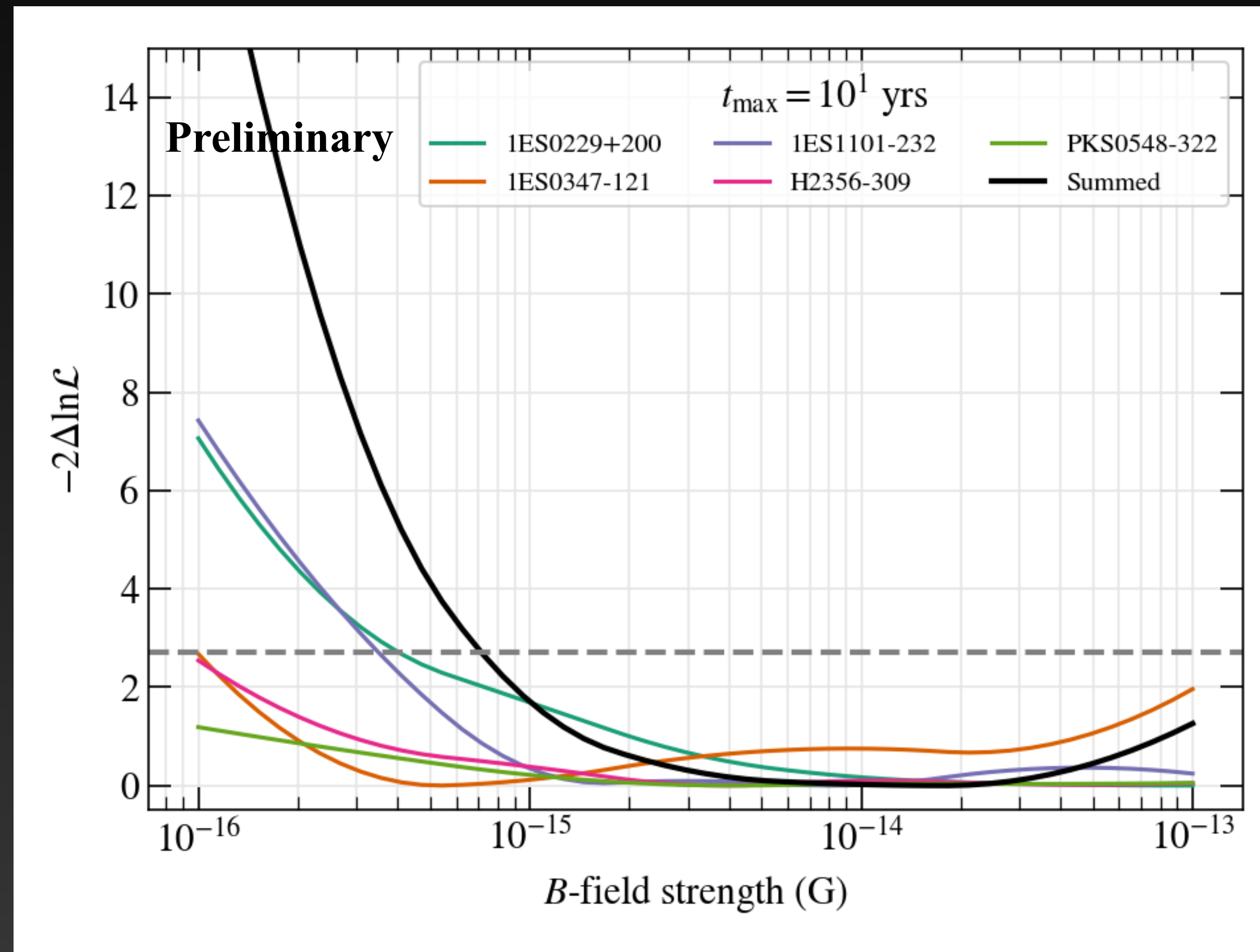
Results: lower limits on IGMF

Data does not prefer presence of halo



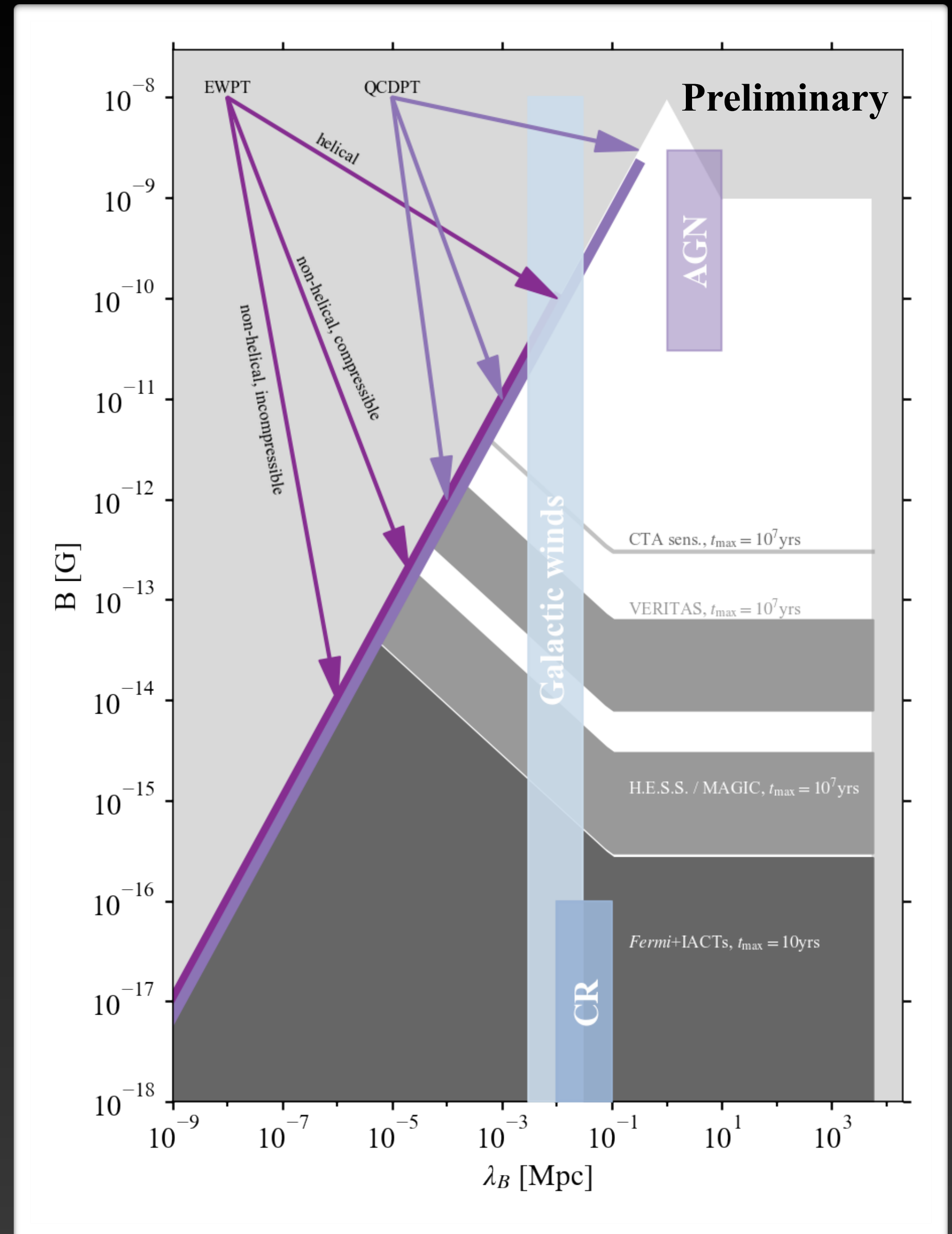
Results: lower limits on IGMF

Data does not prefer presence of halo



Conclusions

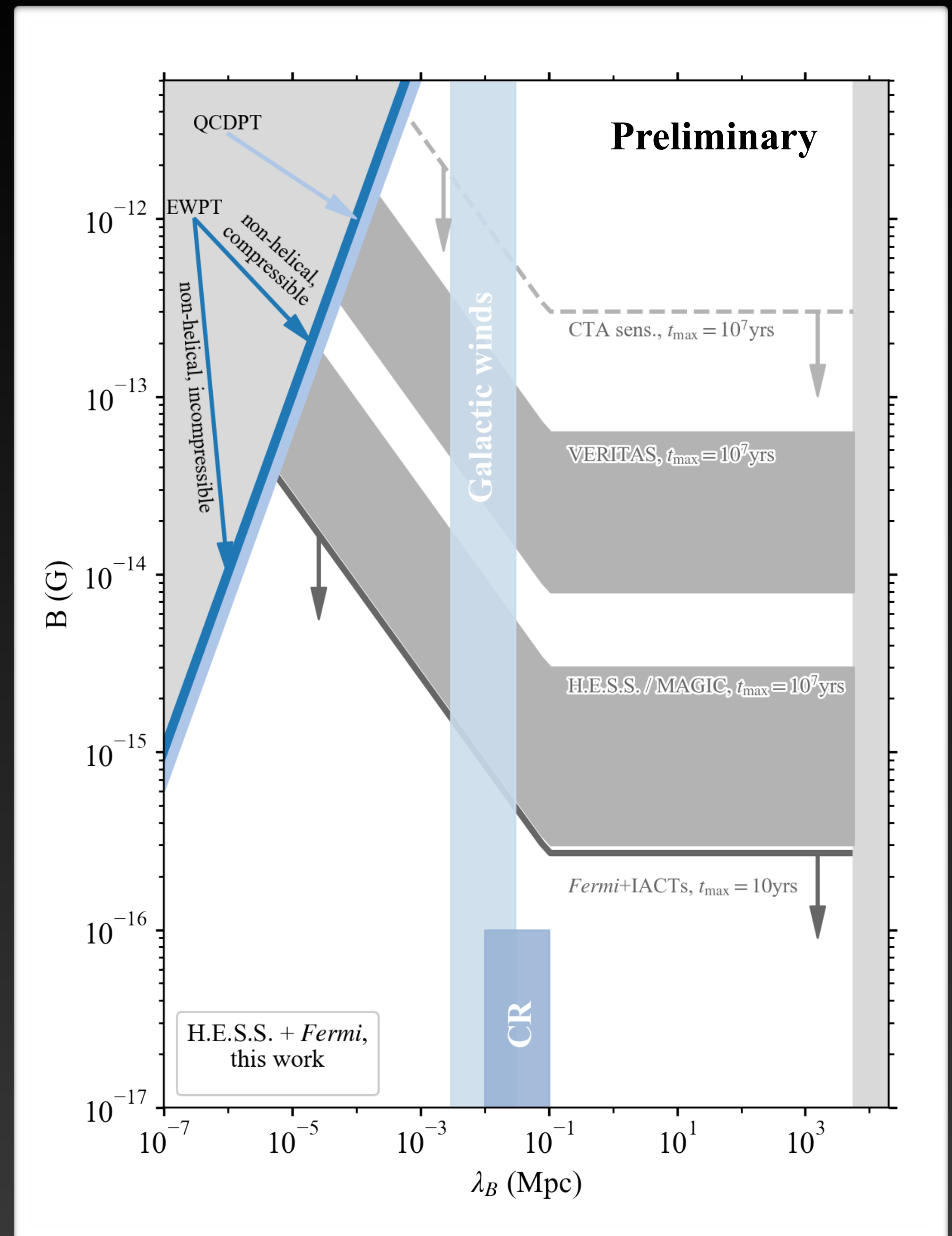
- CRPropa3 simulations used to generate realistic cascade templates
- No halo detected in combined LAT and H.E.S.S. data
- If pairs lose energy through scattering CMB photons, B fields weaker than $B \lesssim 7 \times 10^{-16} \text{ G}$ for $t_{\text{max}} = 10 \text{ yr}$ are ruled out
- Previous constraints improved by factor of 2



[Adapted from Durrer & Neronov 2013 and Abdalla et al. 2021]

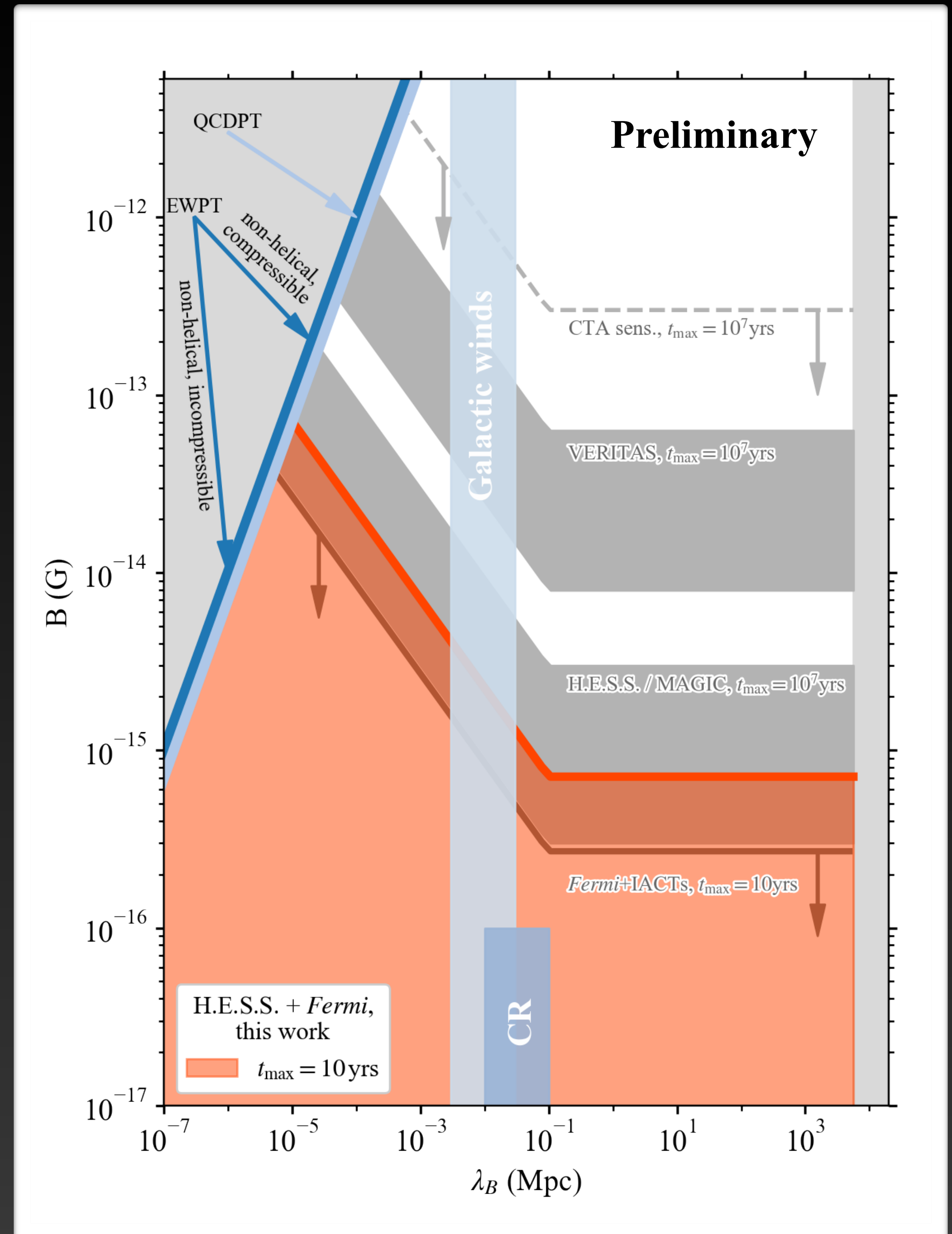
Conclusions

- CRPropa3 simulations used to generate realistic cascade templates
- No halo detected in combined LAT and H.E.S.S. data
- If pairs lose energy through scattering CMB photons, B fields weaker than $B \lesssim 7 \times 10^{-16} \text{ G}$ for $t_{\text{max}} = 10 \text{ yr}$ are ruled out
- Previous constraints improved by factor of 2



Conclusions

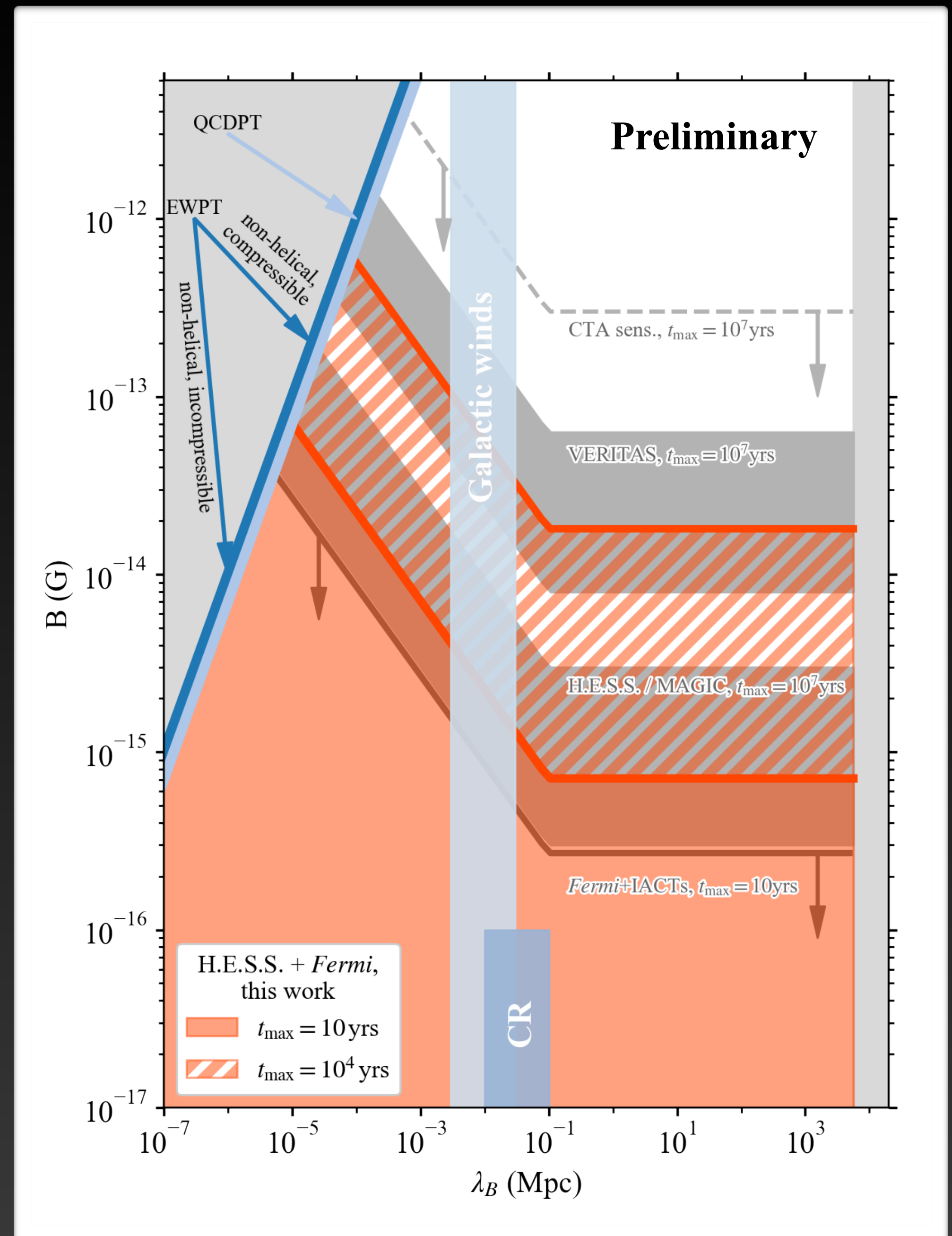
- CRPropa3 simulations used to generate realistic cascade templates
- No halo detected in combined LAT and H.E.S.S. data
- If pairs lose energy through scattering CMB photons, B fields weaker than $B \lesssim 7 \times 10^{-16} \text{ G}$ for $t_{\text{max}} = 10 \text{ yr}$ are ruled out
- Previous constraints improved by factor of 2



[Adapted from Durrer & Neronov 2013 and Abdalla et al. 2021]

Conclusions

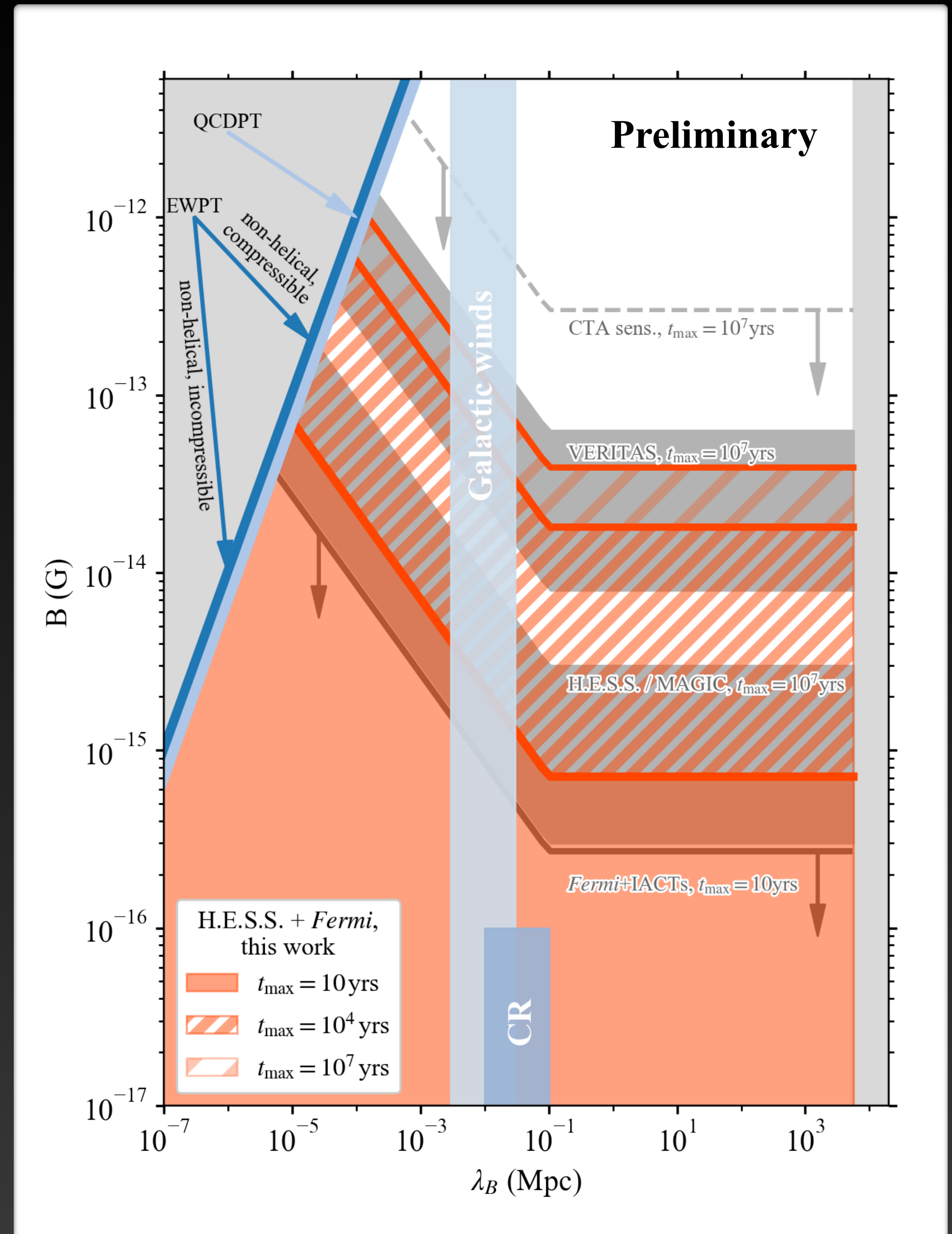
- CRPropa3 simulations used to generate realistic cascade templates
- No halo detected in combined LAT and H.E.S.S. data
- If pairs lose energy through scattering CMB photons, B fields weaker than $B \lesssim 7 \times 10^{-16} \text{ G}$ for $t_{\text{max}} = 10 \text{ yr}$ are ruled out
- Previous constraints improved by factor of 2



[Adapted from Durrer & Neronov 2013 and Abdalla et al. 2021]

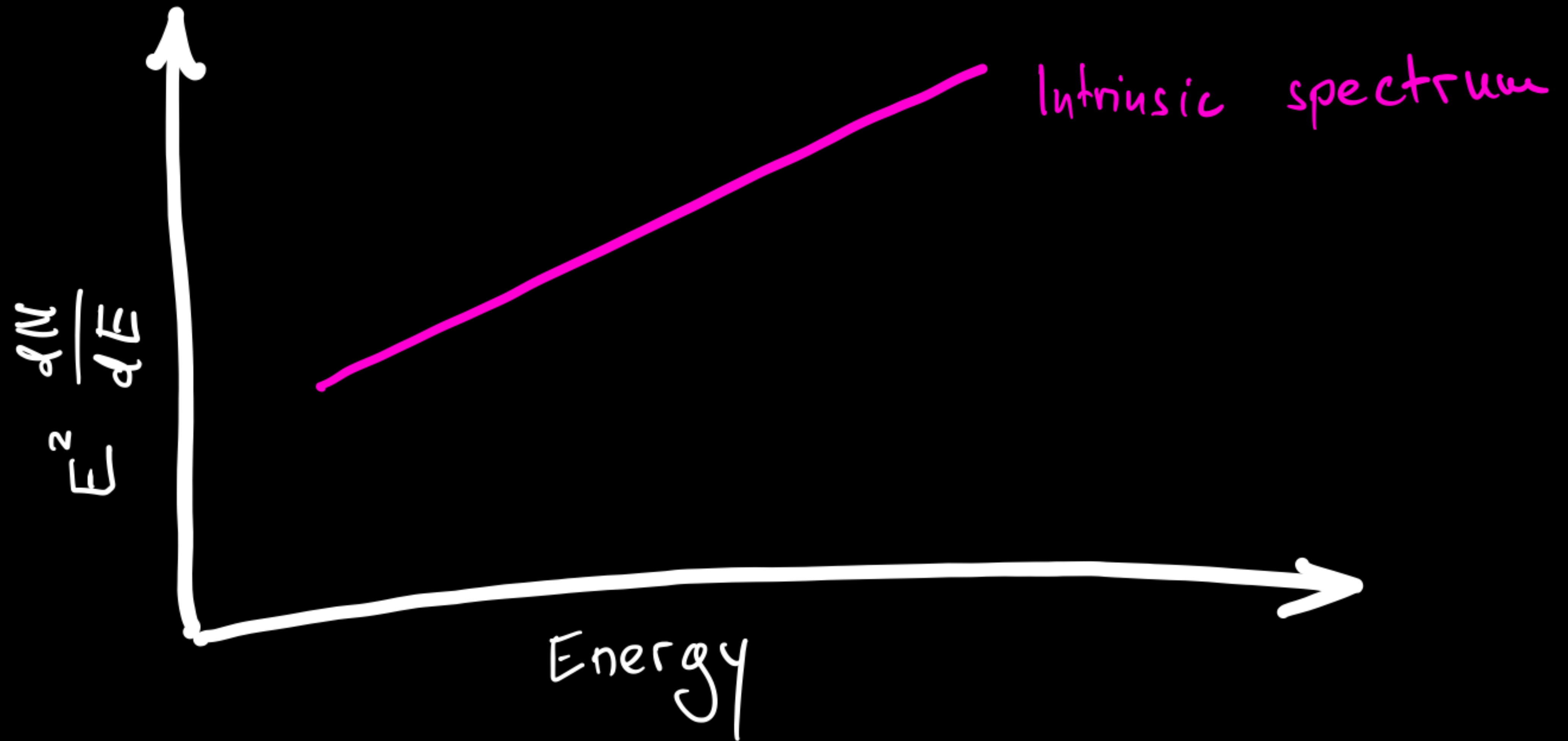
Conclusions

- CRPropa3 simulations used to generate realistic cascade templates
- No halo detected in combined LAT and H.E.S.S. data
- If pairs lose energy through scattering CMB photons, B fields weaker than $B \lesssim 7 \times 10^{-16} \text{ G}$ for $t_{\text{max}} = 10 \text{ yr}$ are ruled out
- Previous constraints improved by factor of 2

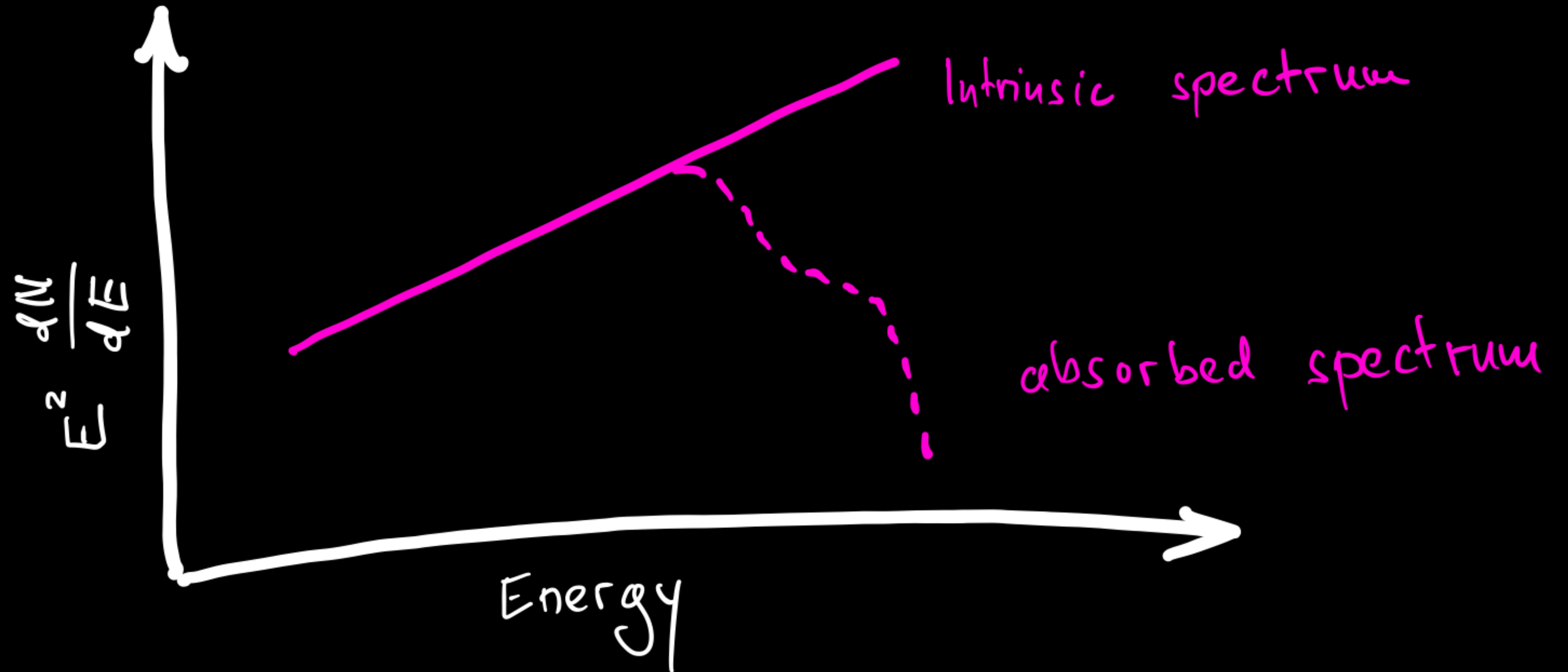


Back up

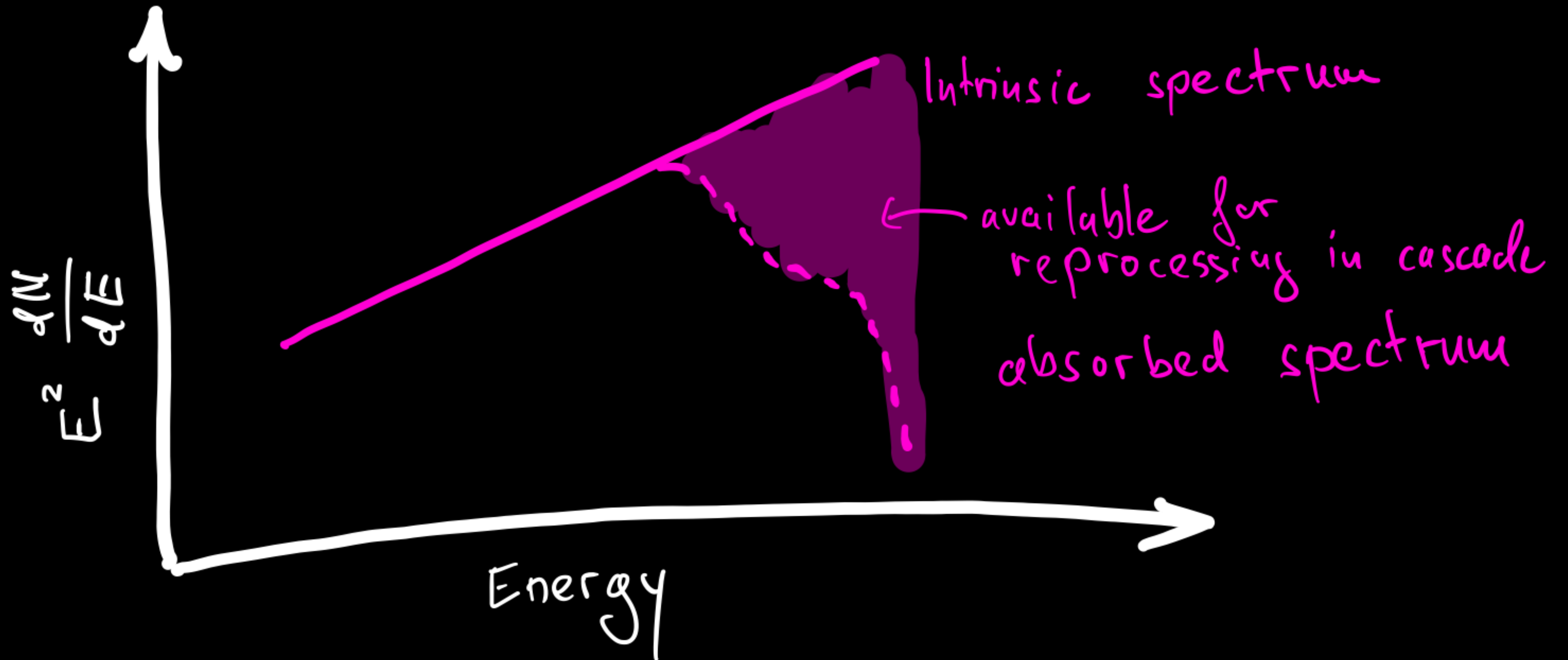
Basic idea



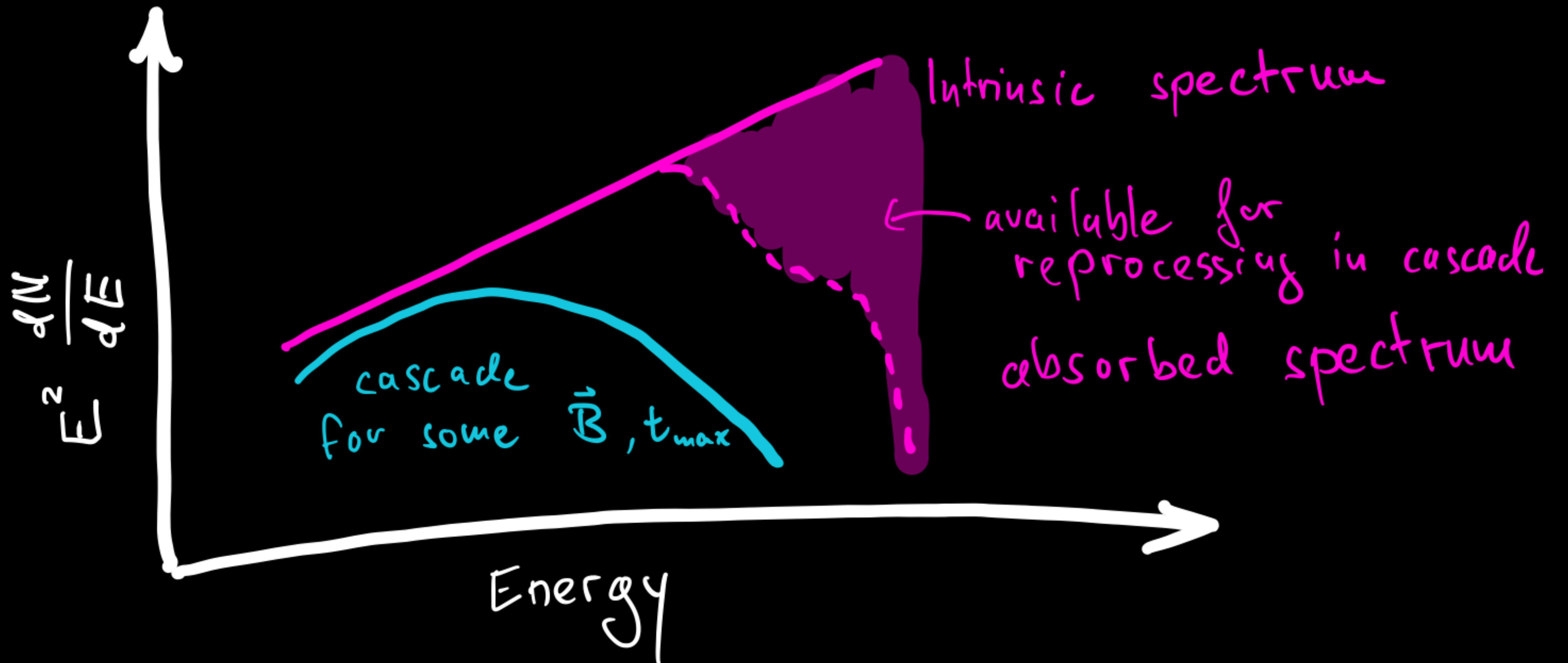
Basic idea



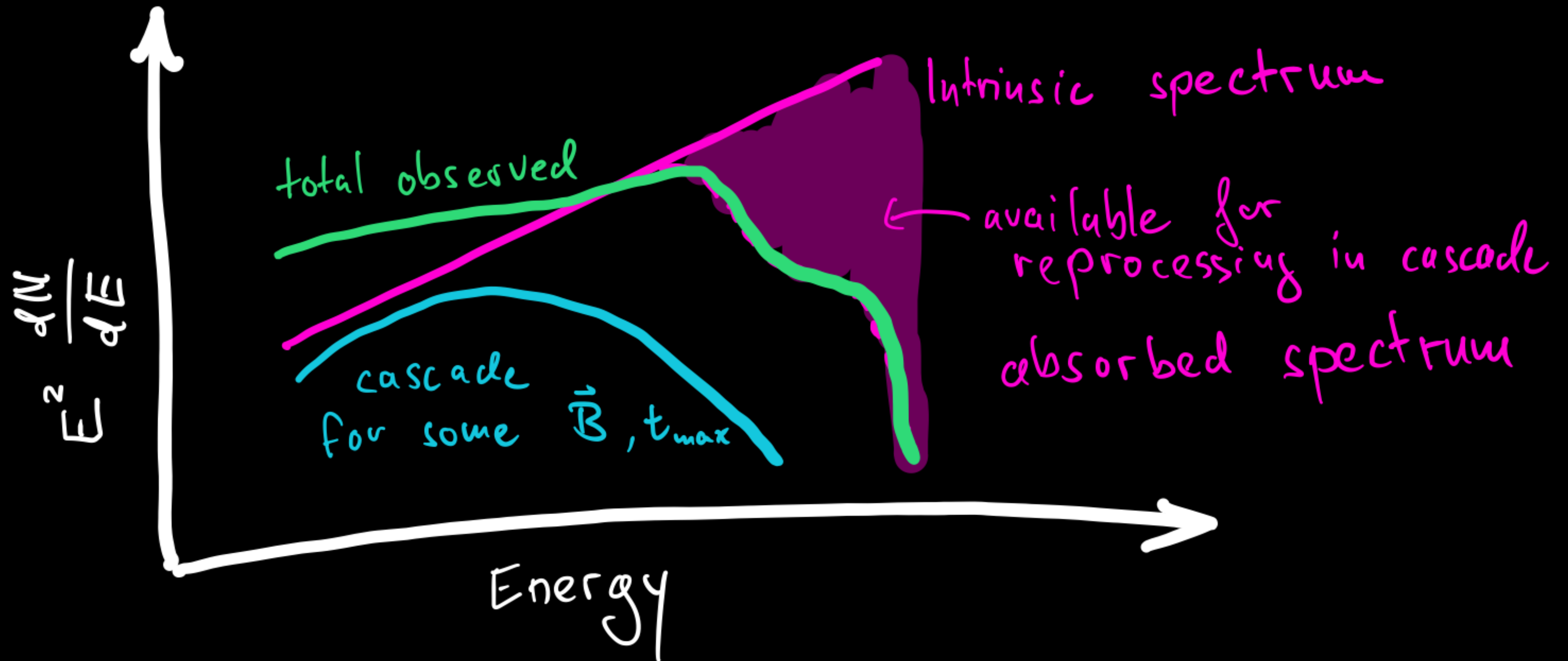
Basic idea



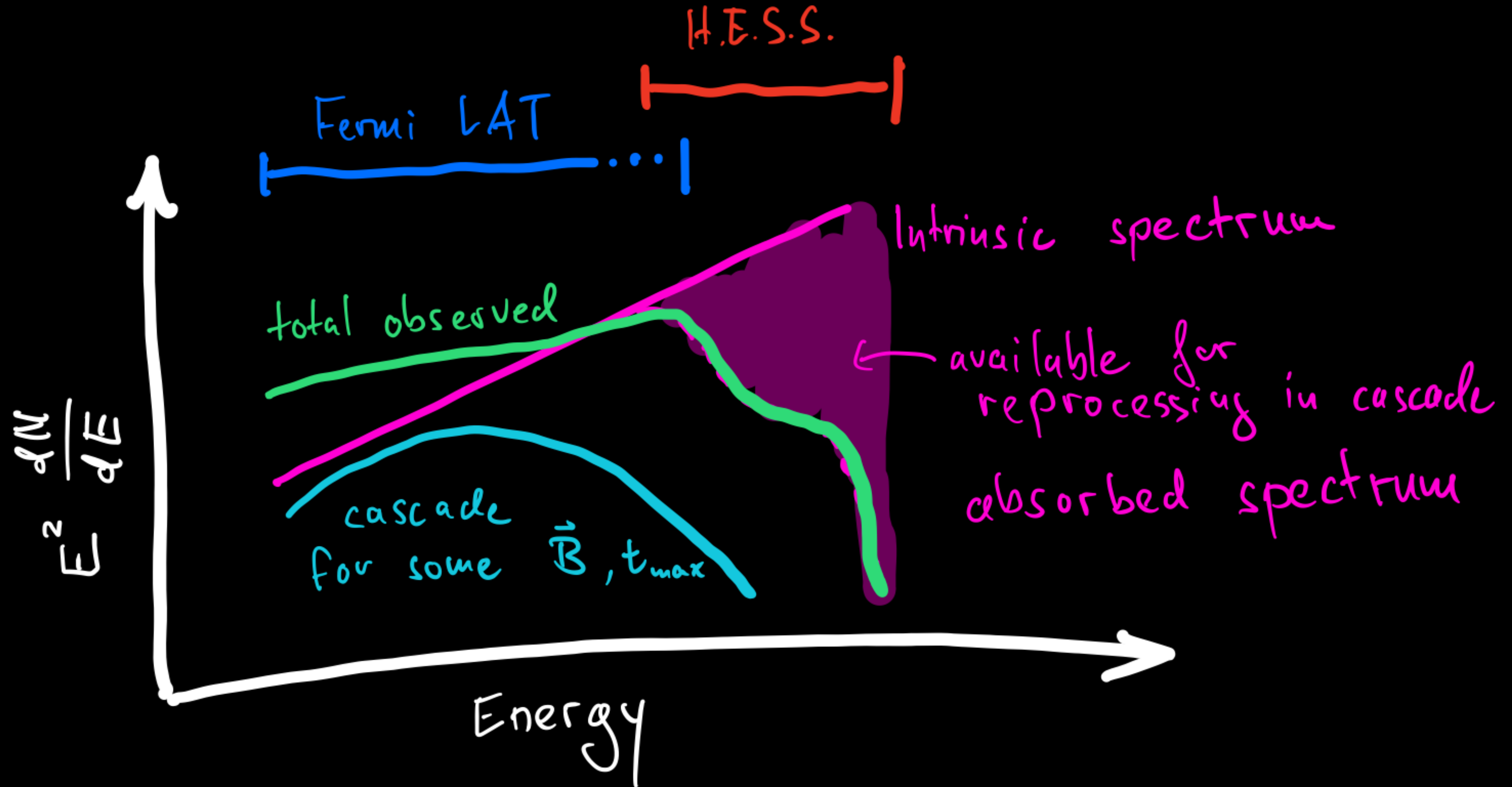
Basic idea



Basic idea



Basic idea



Fermi-LAT analysis with halo component

Start from optimized ROI without halo

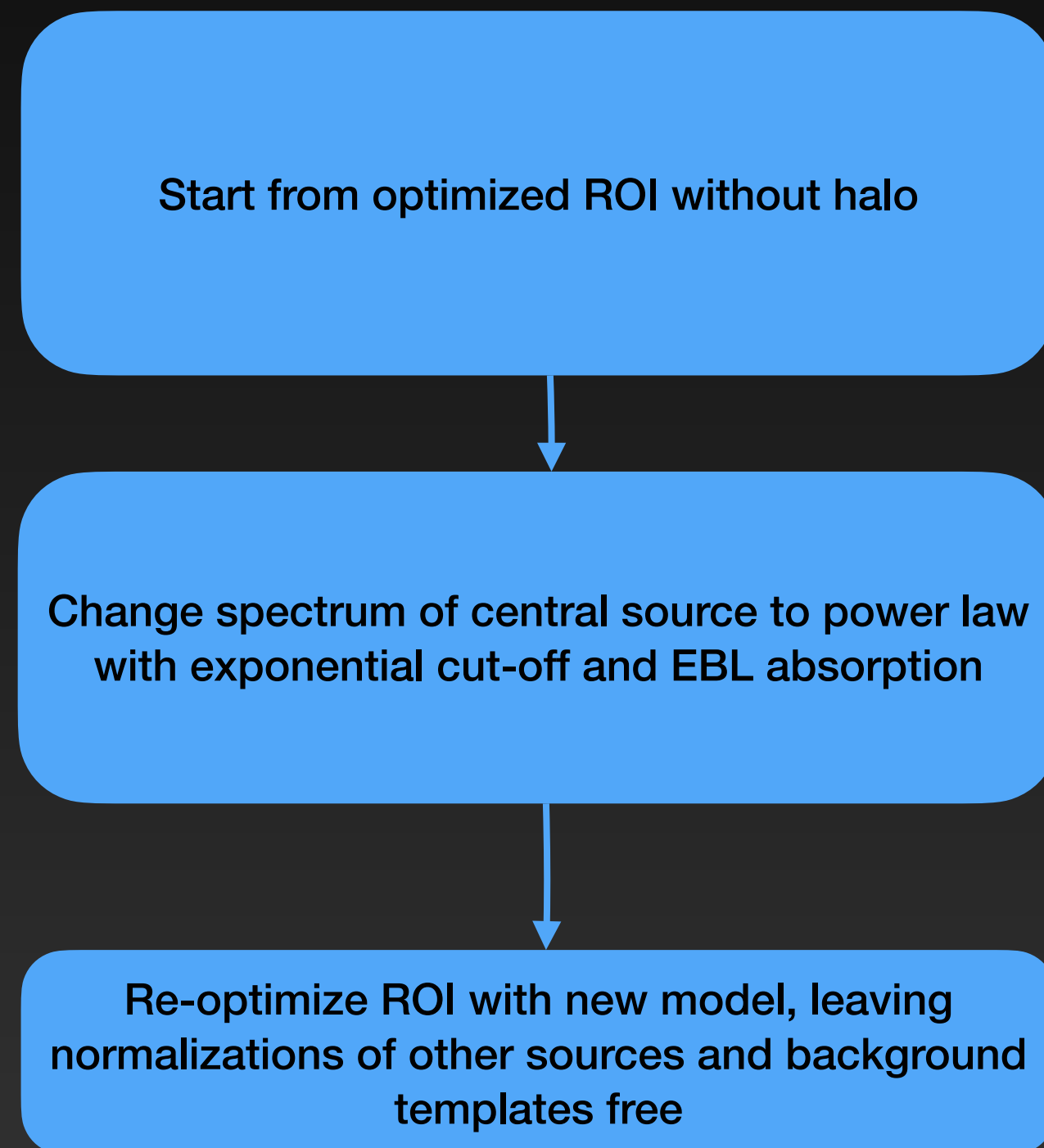
Fermi-LAT analysis with halo component

Start from optimized ROI without halo

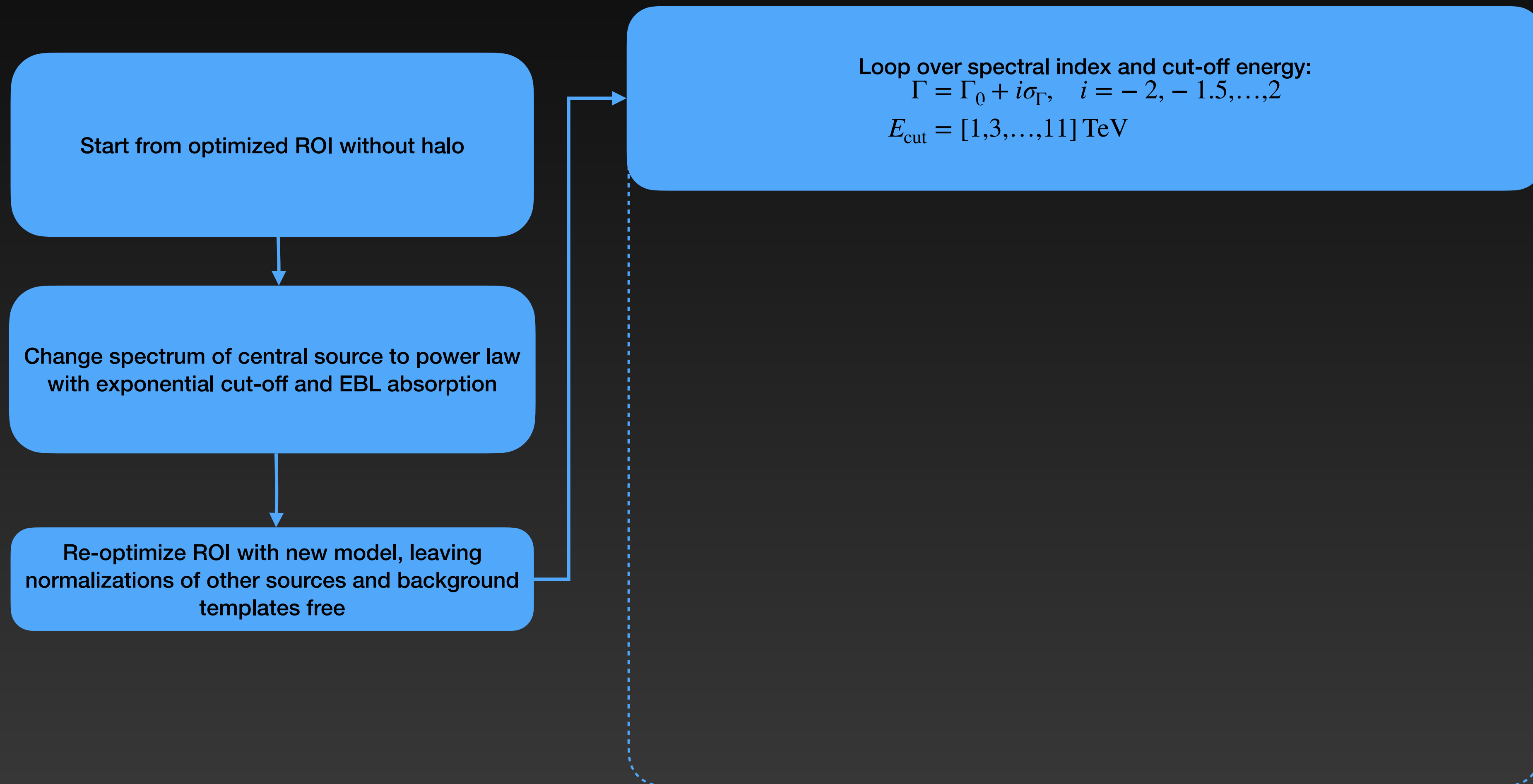


Change spectrum of central source to power law with exponential cut-off and EBL absorption

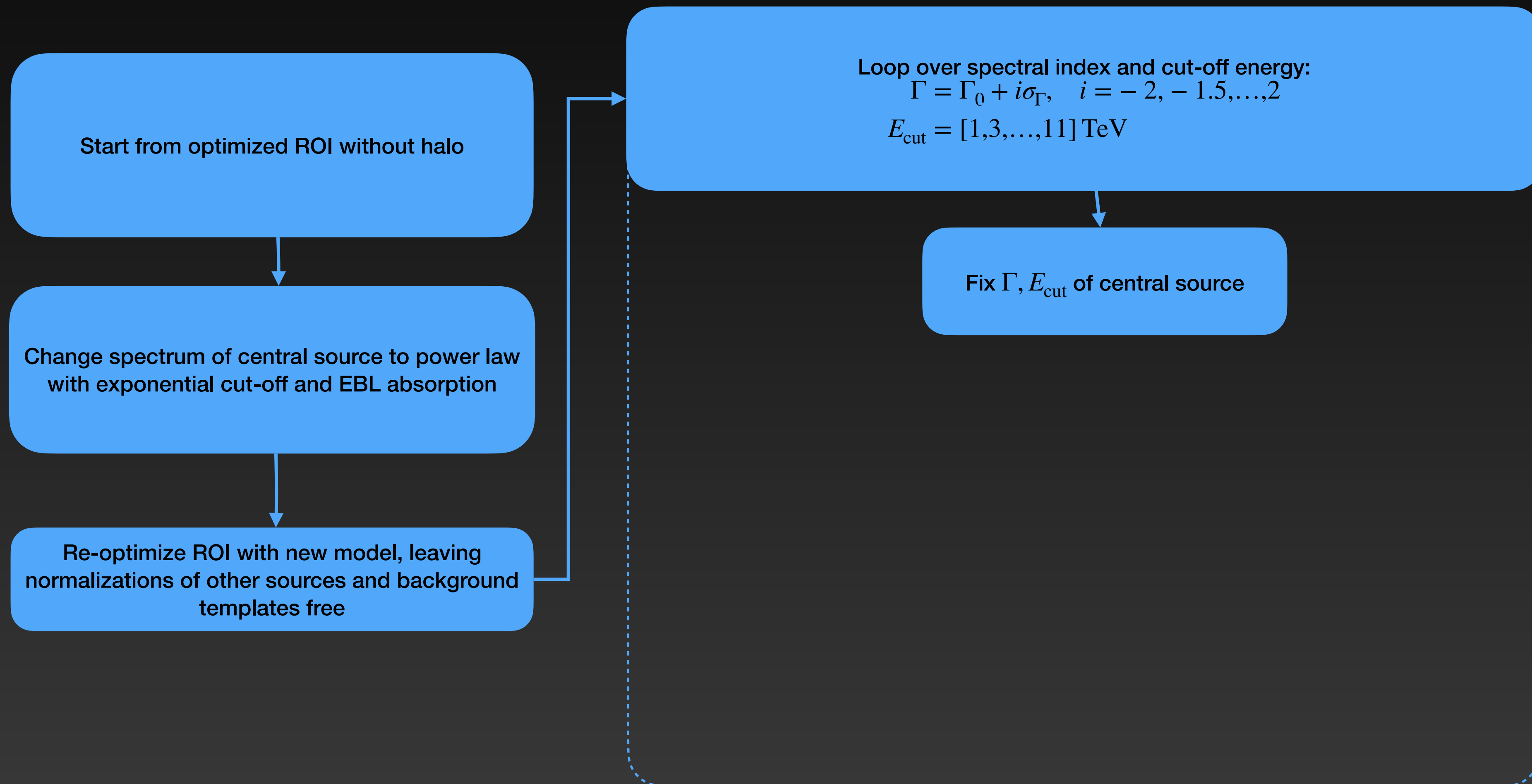
Fermi-LAT analysis with halo component



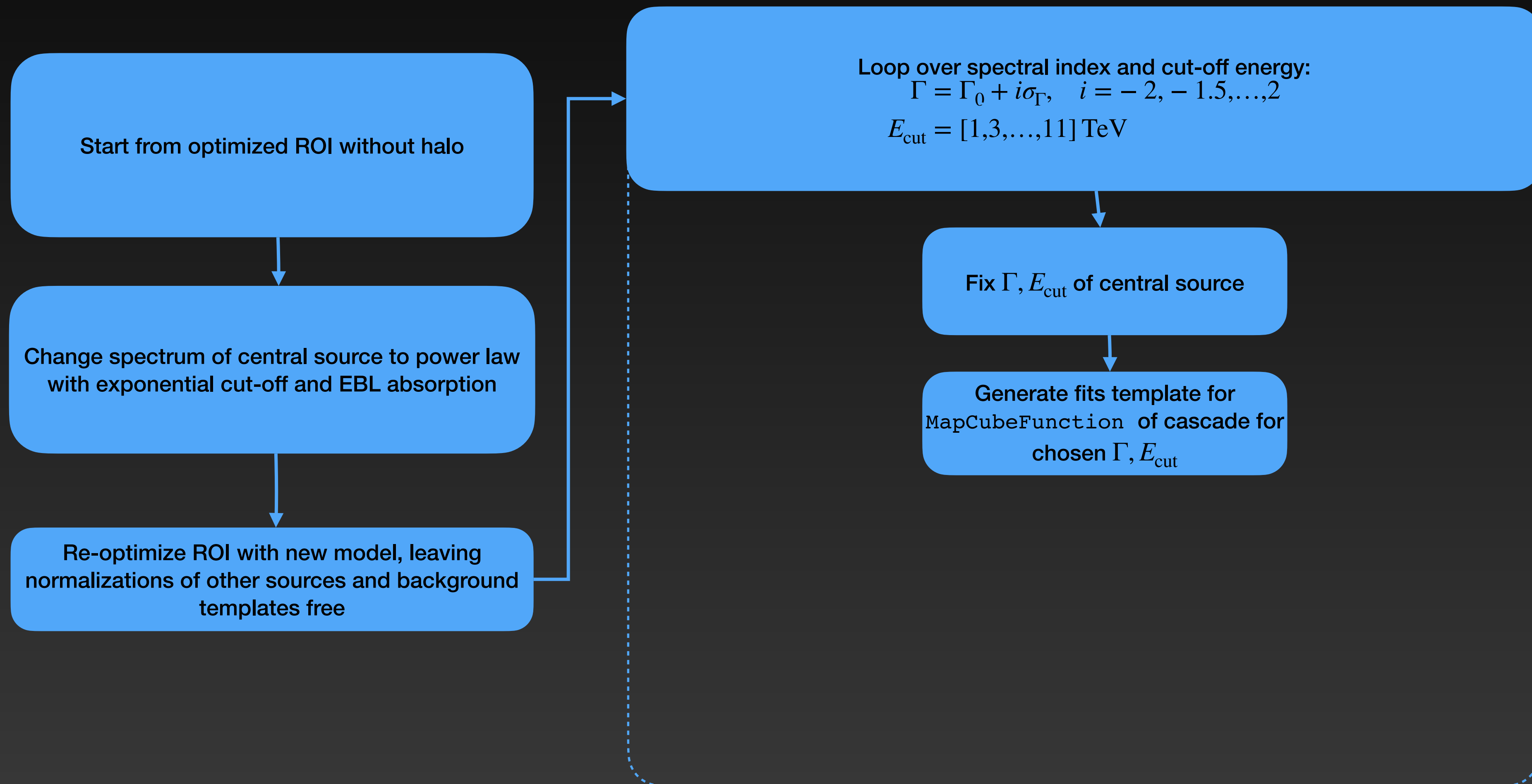
Fermi-LAT analysis with halo component



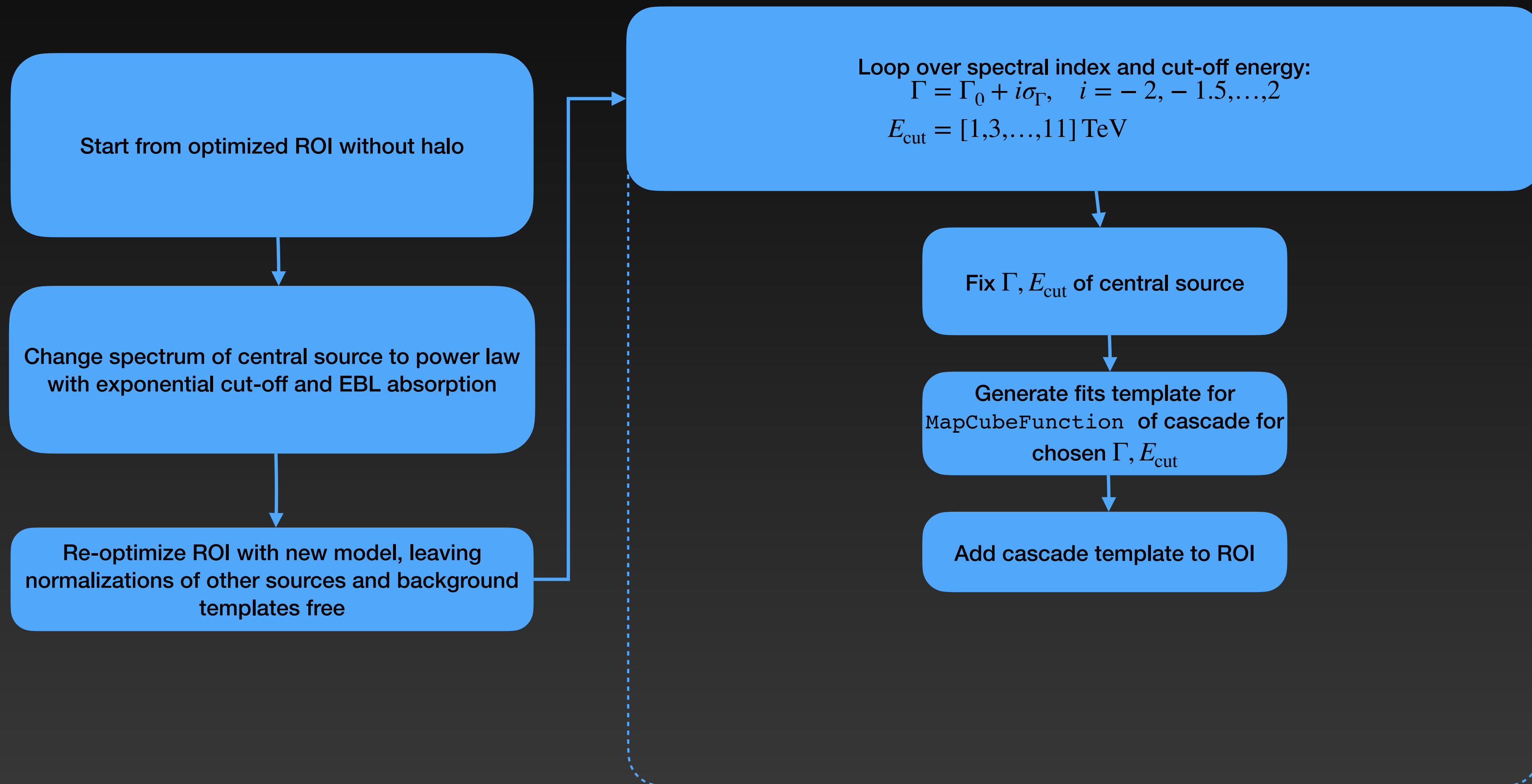
Fermi-LAT analysis with halo component



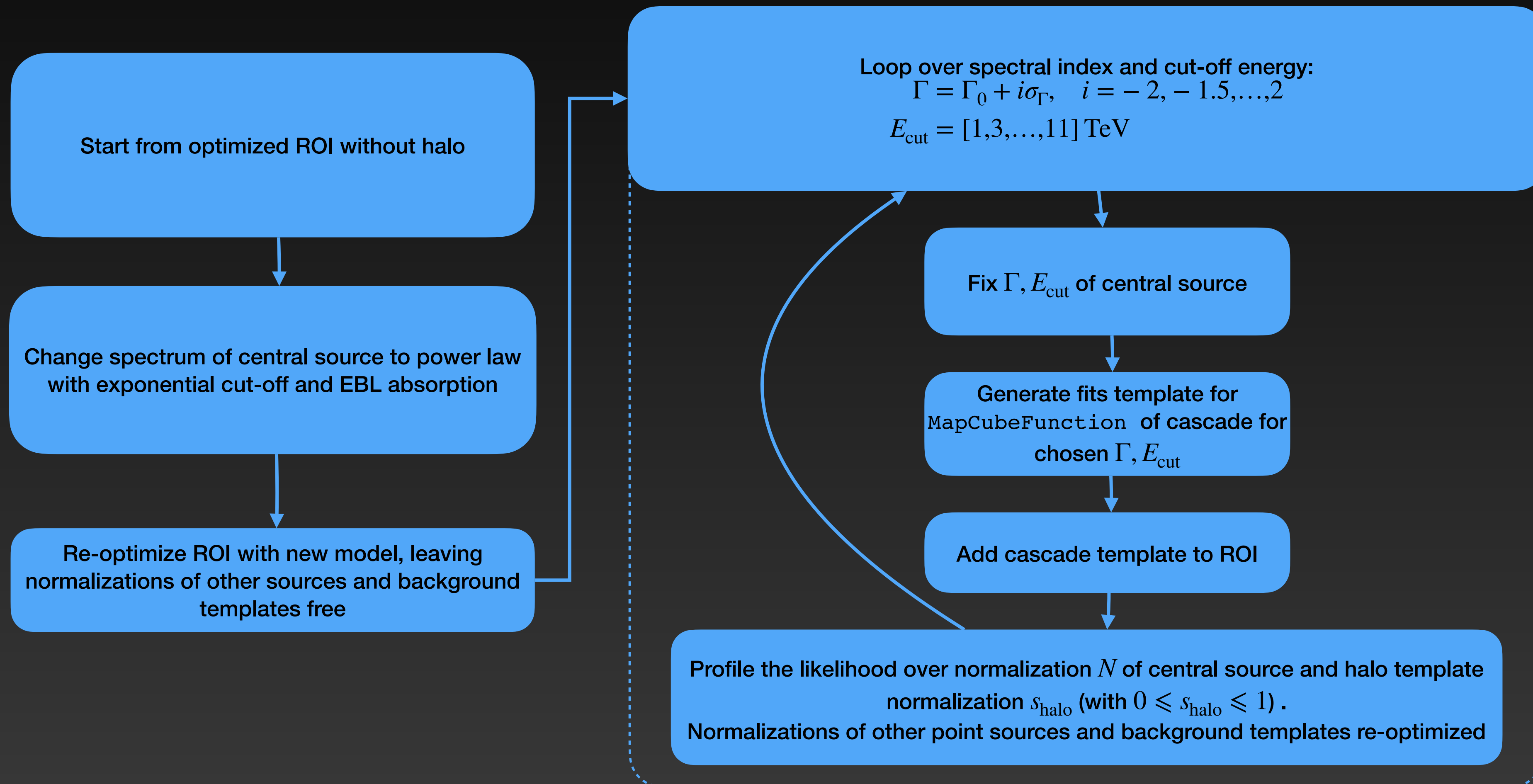
Fermi-LAT analysis with halo component



Fermi-LAT analysis with halo component



Fermi-LAT analysis with halo component



Building cascade templates

Building cascade templates

- From the simulated events we build the intensity as function of injected gamma-ray energy ϵ , observed energy E , solid Ω , and delay time τ :

Building cascade templates

- From the simulated events we build the intensity as function of injected gamma-ray energy ϵ , observed energy E , solid Ω , and delay time τ :

$$\frac{d\mathcal{N}}{d\epsilon dE d\tau d\Omega} = \frac{1}{N_{\text{inj}}(\Delta\epsilon)} \frac{\mathcal{N}}{\Delta E \Delta\epsilon \Delta\tau \Delta\Omega}$$

Building cascade templates

- From the simulated events we build the intensity as function of injected gamma-ray energy ϵ , observed energy E , solid Ω , and delay time τ :

$$\frac{d\mathcal{N}}{d\epsilon dE d\tau d\Omega} = \frac{1}{N_{\text{inj}}(\Delta\epsilon)} \frac{\mathcal{N}}{\Delta E \Delta\epsilon \Delta\tau \Delta\Omega}$$

- Simulation done for discrete injection energies ϵ_i

Building cascade templates

- From the simulated events we build the intensity as function of injected gamma-ray energy ϵ , observed energy E , solid Ω , and delay time τ :

$$\frac{d\mathcal{N}}{d\epsilon dE d\tau d\Omega} = \frac{1}{N_{\text{inj}}(\Delta\epsilon)} \frac{\mathcal{N}}{\Delta E \Delta\epsilon \Delta\tau \Delta\Omega}$$

- Simulation done for discrete injection energies ϵ_i
- From this, we can re-weight the cascade histogram for an arbitrary source spectra $dN/d\epsilon$ (e.g., a power law), by computing weights for bins of injected energy:

Building cascade templates

- From the simulated events we build the intensity as function of injected gamma-ray energy ϵ , observed energy E , solid Ω , and delay time τ :

$$\frac{d\mathcal{N}}{d\epsilon dE d\tau d\Omega} = \frac{1}{N_{\text{inj}}(\Delta\epsilon)} \frac{\mathcal{N}}{\Delta E \Delta\epsilon \Delta\tau \Delta\Omega}$$

- Simulation done for discrete injection energies ϵ_i
- From this, we can re-weight the cascade histogram for an arbitrary source spectra $dN/d\epsilon$ (e.g., a power law), by computing weights for bins of injected energy:

$$w_i = \int_{\Delta\epsilon_i} \frac{dN}{d\epsilon} d\epsilon$$

Building cascade templates

- From the simulated events we build the intensity as function of injected gamma-ray energy ϵ , observed energy E , solid Ω , and delay time τ :

$$\frac{d\mathcal{N}}{d\epsilon dE d\tau d\Omega} = \frac{1}{N_{\text{inj}}(\Delta\epsilon)} \frac{\mathcal{N}}{\Delta E \Delta\epsilon \Delta\tau \Delta\Omega}$$

- Simulation done for discrete injection energies ϵ_i
- From this, we can re-weight the cascade histogram for an arbitrary source spectra $dN/d\epsilon$ (e.g., a power law), by computing weights for bins of injected energy:

$$w_i = \int_{\Delta\epsilon_i} \frac{dN}{d\epsilon} d\epsilon$$

- With the spectral weights, we obtain the expected cascade flux that arrives within some maximum time delay (assuming constant emission with time)

Building cascade templates

- From the simulated events we build the intensity as function of injected gamma-ray energy ϵ , observed energy E , solid Ω , and delay time τ :

$$\frac{d\mathcal{N}}{d\epsilon dE d\tau d\Omega} = \frac{1}{N_{\text{inj}}(\Delta\epsilon)} \frac{\mathcal{N}}{\Delta E \Delta\epsilon \Delta\tau \Delta\Omega}$$

- Simulation done for discrete injection energies ϵ_i
- From this, we can re-weight the cascade histogram for an arbitrary source spectra $dN/d\epsilon$ (e.g., a power law), by computing weights for bins of injected energy:

$$w_i = \int_{\Delta\epsilon_i} \frac{dN}{d\epsilon} d\epsilon$$

- With the spectral weights, we obtain the expected cascade flux that arrives within some maximum time delay (assuming constant emission with time)

$$\frac{d\mathcal{N}}{dE d\Omega} = \int_0^\infty d\epsilon \frac{dN}{d\epsilon} \int_0^{\tau_{\text{max}}} d\tau \frac{d\mathcal{N}}{d\epsilon dE d\tau d\Omega} \approx \sum_i \sum_j \Delta\epsilon_i \Delta\tau_j w_i \left(\frac{d\mathcal{N}}{d\epsilon dE d\tau d\Omega} \right)_{ij}$$

Building cascade templates

- From the simulated events we build the intensity as function of injected gamma-ray energy ϵ , observed energy E , solid Ω , and delay time τ :

$$\frac{d\mathcal{N}}{d\epsilon dE d\tau d\Omega} = \frac{1}{N_{\text{inj}}(\Delta\epsilon)} \frac{\mathcal{N}}{\Delta E \Delta\epsilon \Delta\tau \Delta\Omega}$$

- Simulation done for discrete injection energies ϵ_i
- From this, we can re-weight the cascade histogram for an arbitrary source spectra $dN/d\epsilon$ (e.g., a power law), by computing weights for bins of injected energy:

$$w_i = \int_{\Delta\epsilon_i} \frac{dN}{d\epsilon} d\epsilon$$

- With the spectral weights, we obtain the expected cascade flux that arrives within some maximum time delay (assuming constant emission with time)

$$\frac{d\mathcal{N}}{dE d\Omega} = \int_0^\infty d\epsilon \frac{dN}{d\epsilon} \int_0^{\tau_{\text{max}}} d\tau \frac{d\mathcal{N}}{d\epsilon dE d\tau d\Omega} \approx \sum_i \sum_j \Delta\epsilon_i \Delta\tau_j w_i \left(\frac{d\mathcal{N}}{d\epsilon dE d\tau d\Omega} \right)_{ij}$$

- Cascade flux will depend on IGMF strength B and coherence length λ , injection spectrum, maximum activity time of the source t_{max} , as well as θ_{jet} , θ_{obs} and source redshift z

Cascade templates as function of IGMF strength: sky maps

Smoothed with ASMOOTH

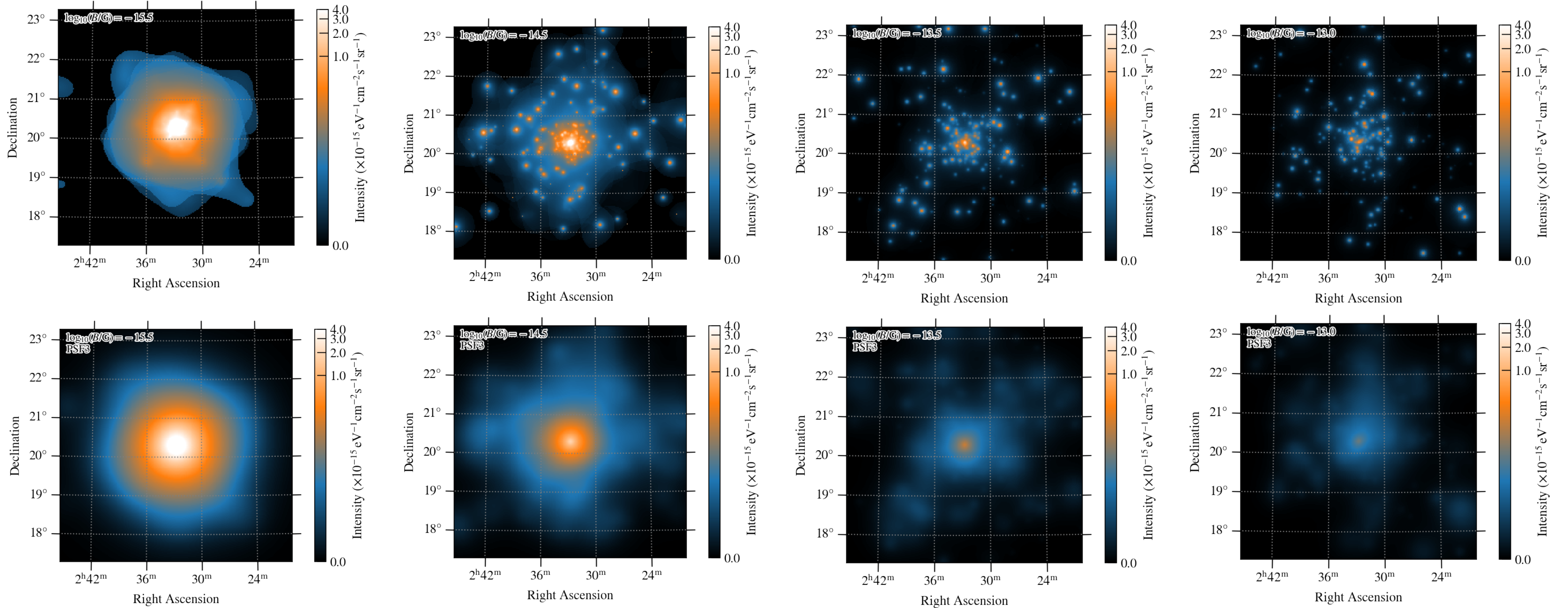
Convolved with Fermi PSF3

$$B = 3.16 \times 10^{-16} \text{ G}$$

$$B = 3.16 \times 10^{-15} \text{ G}$$

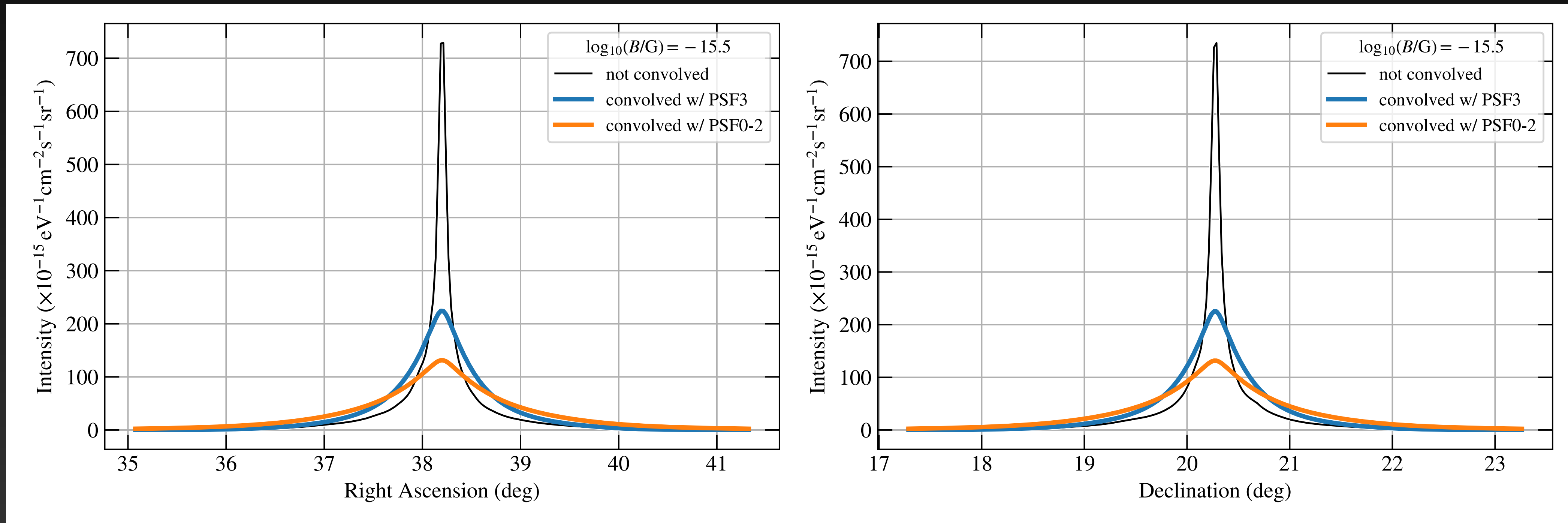
$$B = 3.16 \times 10^{-14} \text{ G}$$

$$B = 10^{-13} \text{ G}$$



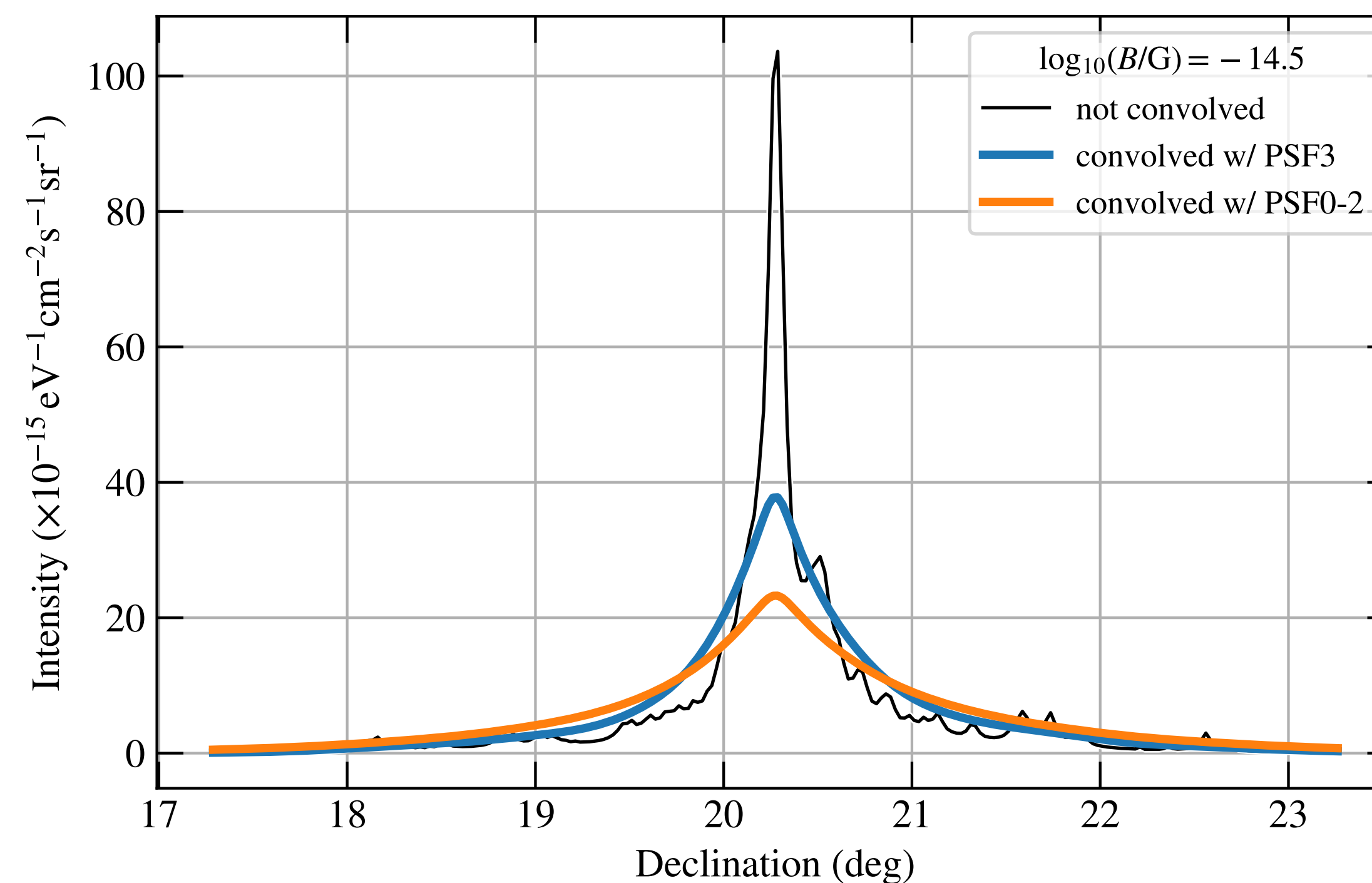
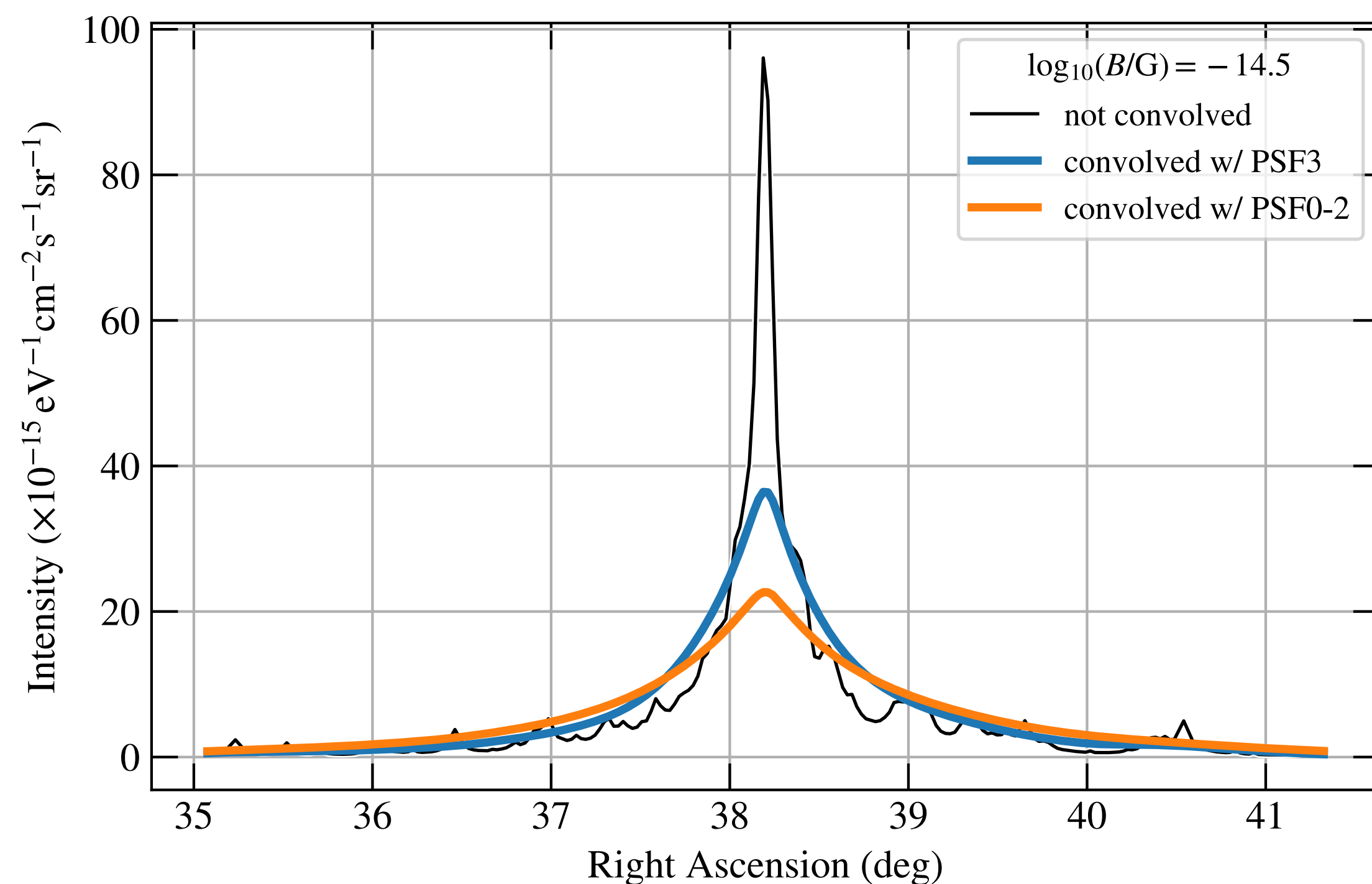
Cascade templates as function of IGMF strength: lon/lat profiles

$B = 3.16 \times 10^{-16}$ G, sky map summed over lon/lat and energy



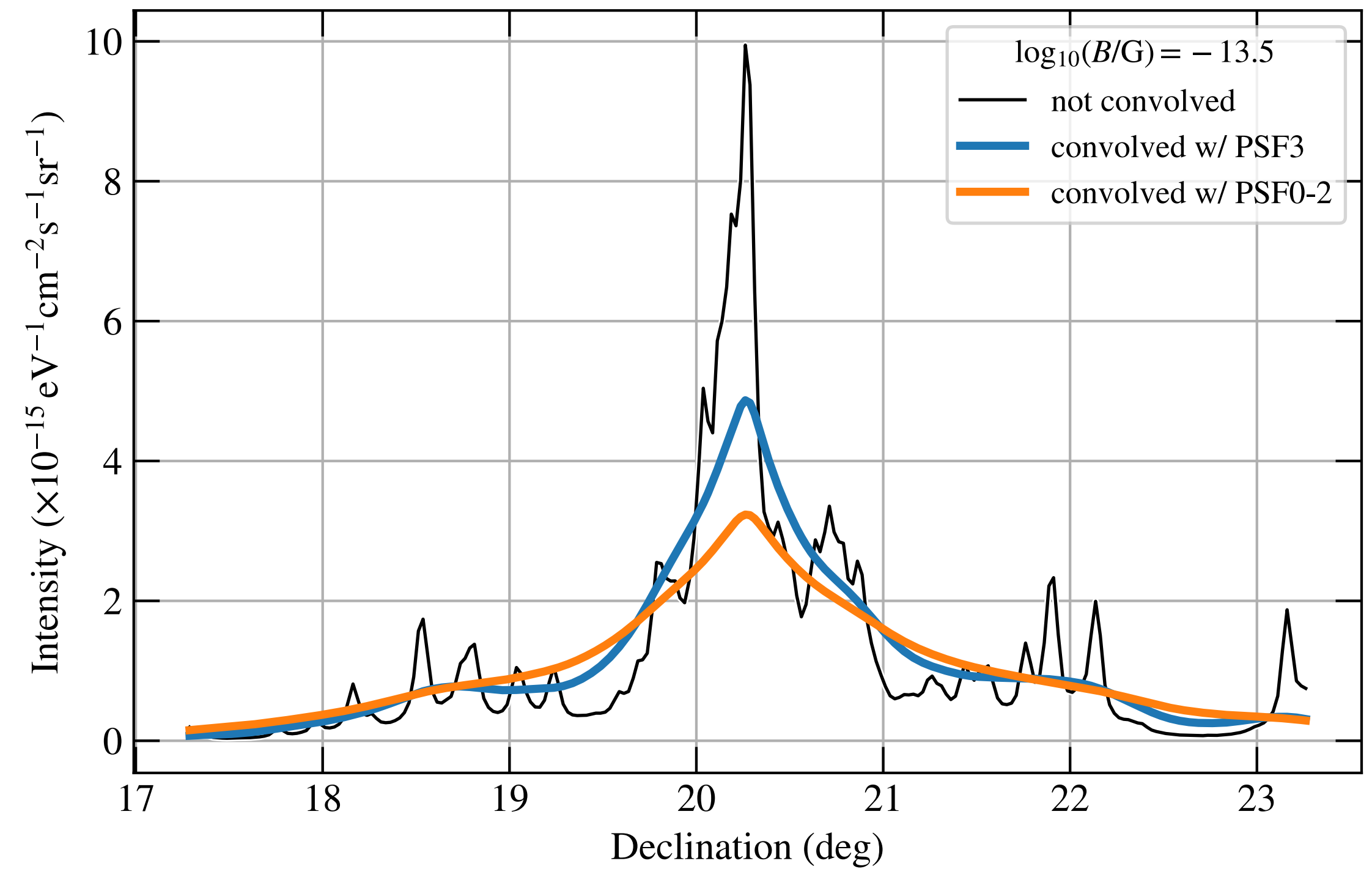
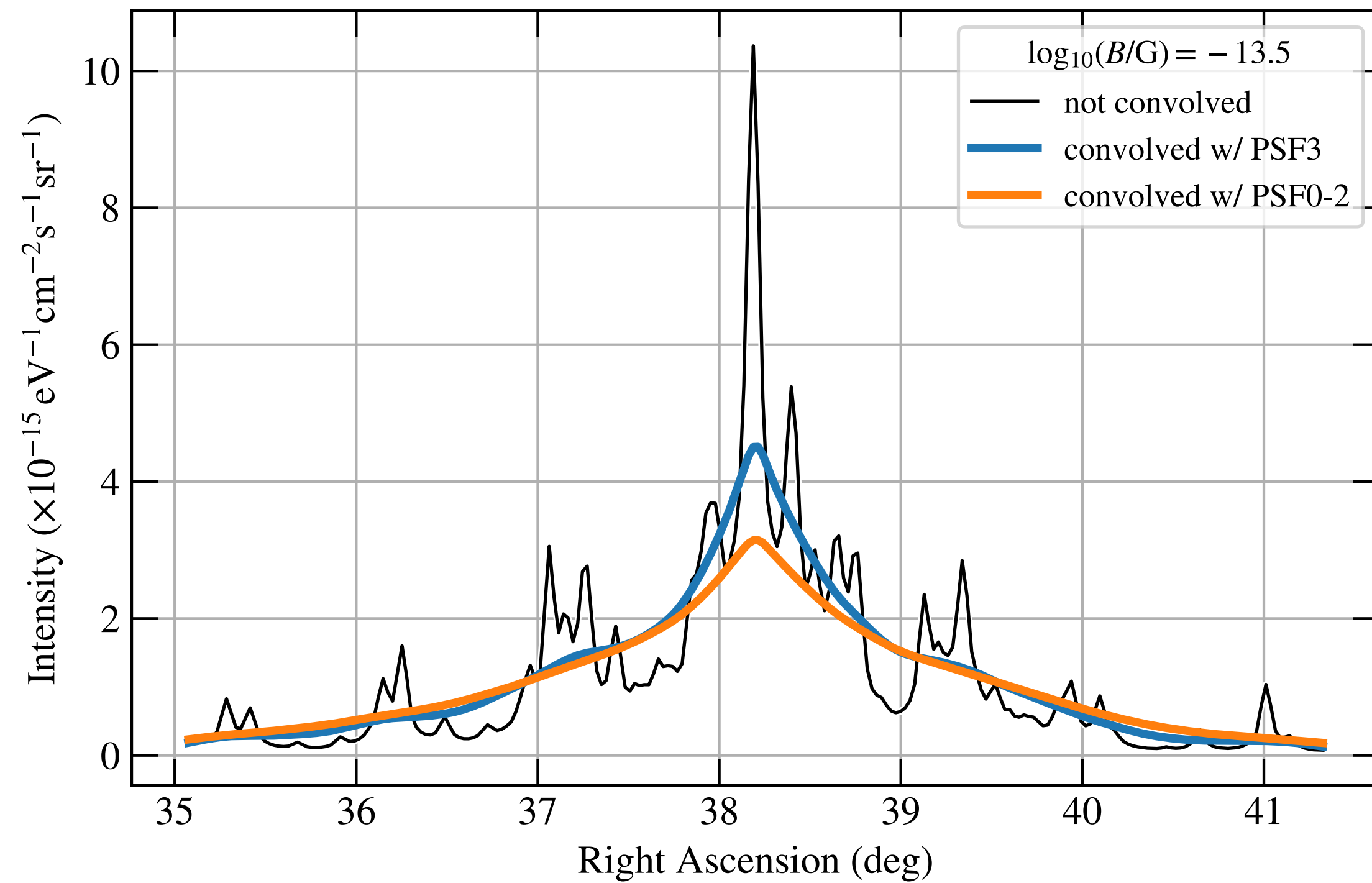
Cascade templates as function of IGMF strength: lon/lat profiles

$B = 3.16 \times 10^{-15}$ G, sky map summed over lon/lat and energy



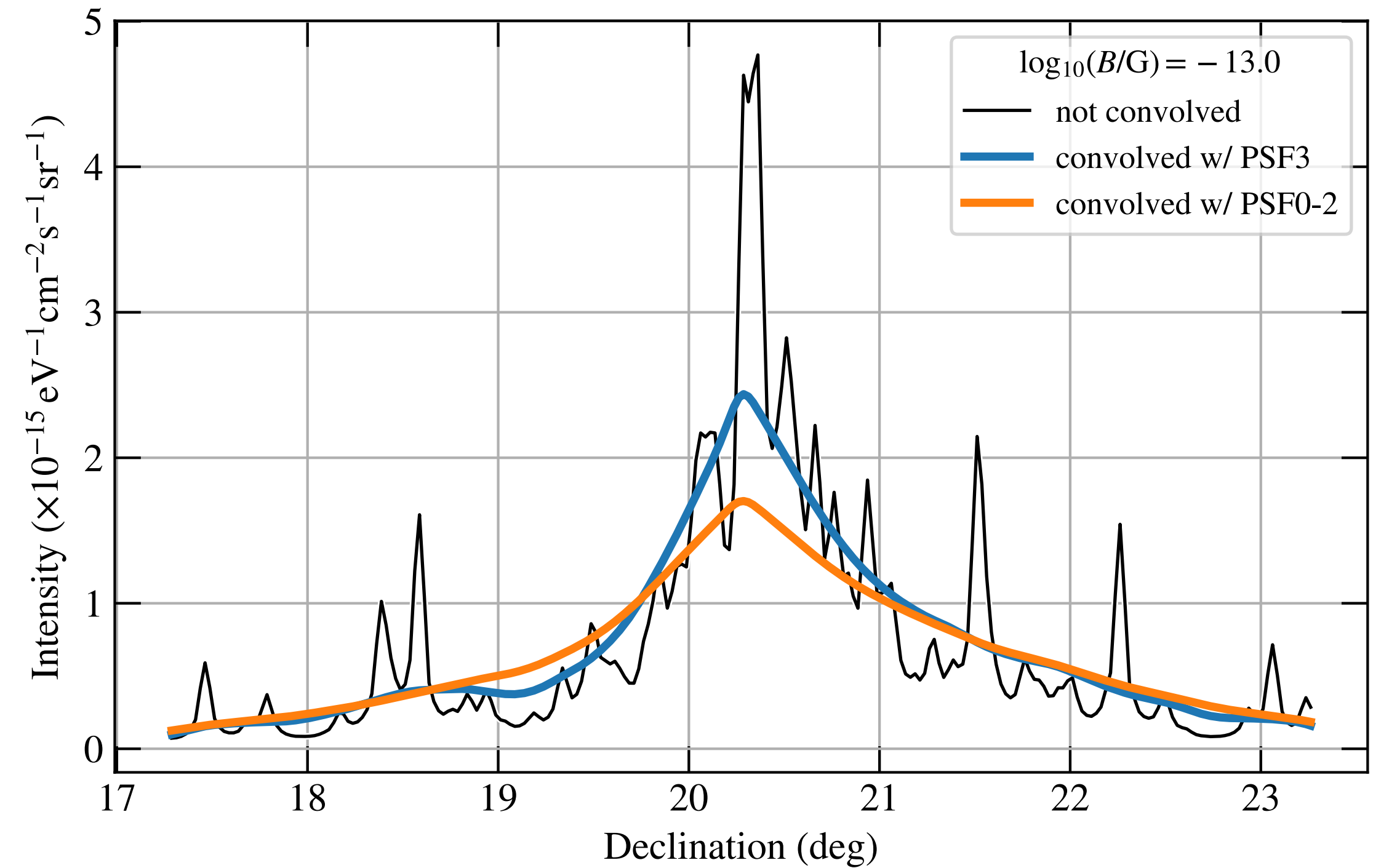
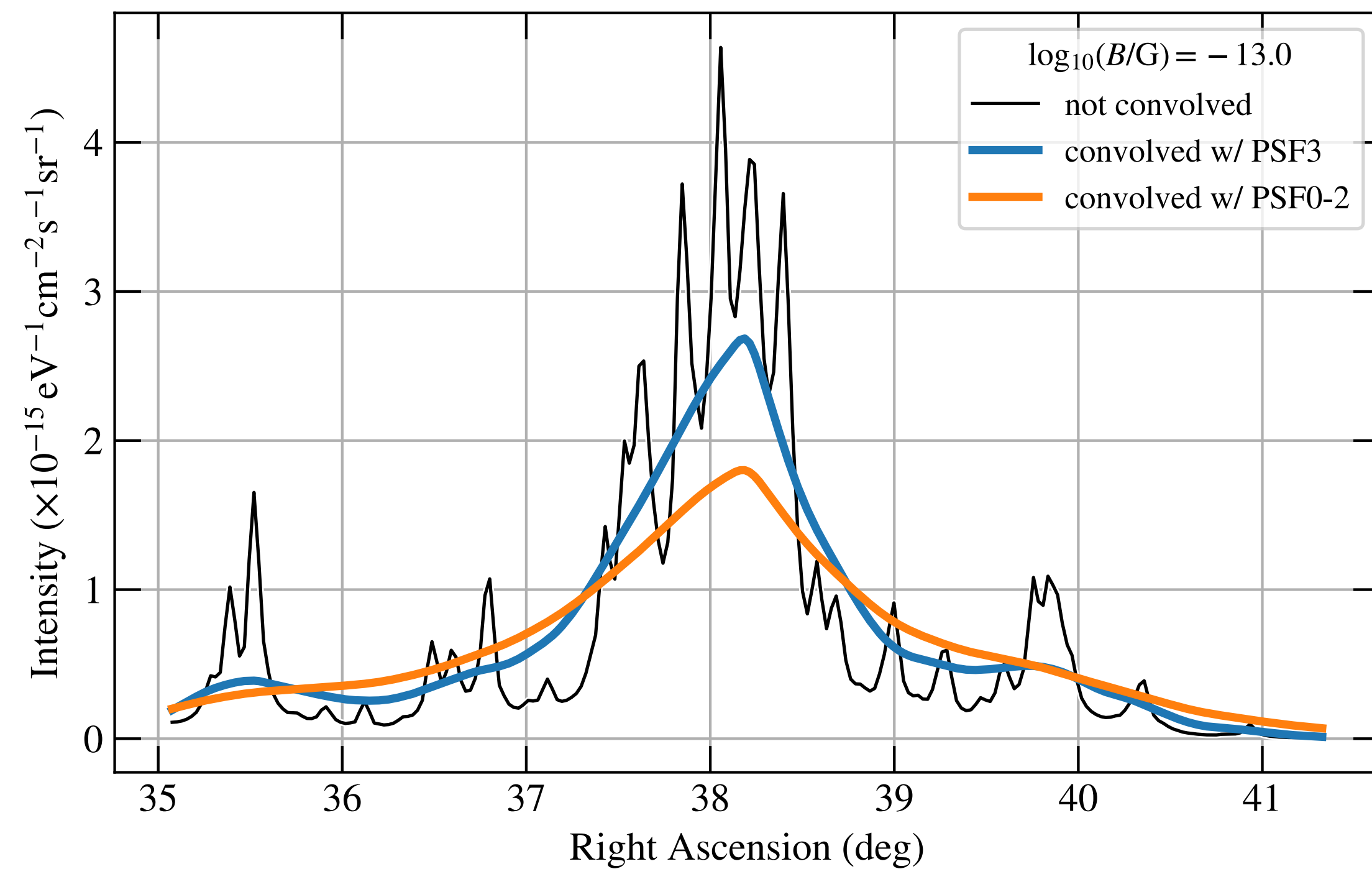
Cascade templates as function of IGMF strength: lon/lat profiles

$B = 3.16 \times 10^{-14}$ G, sky map summed over lon/lat and energy

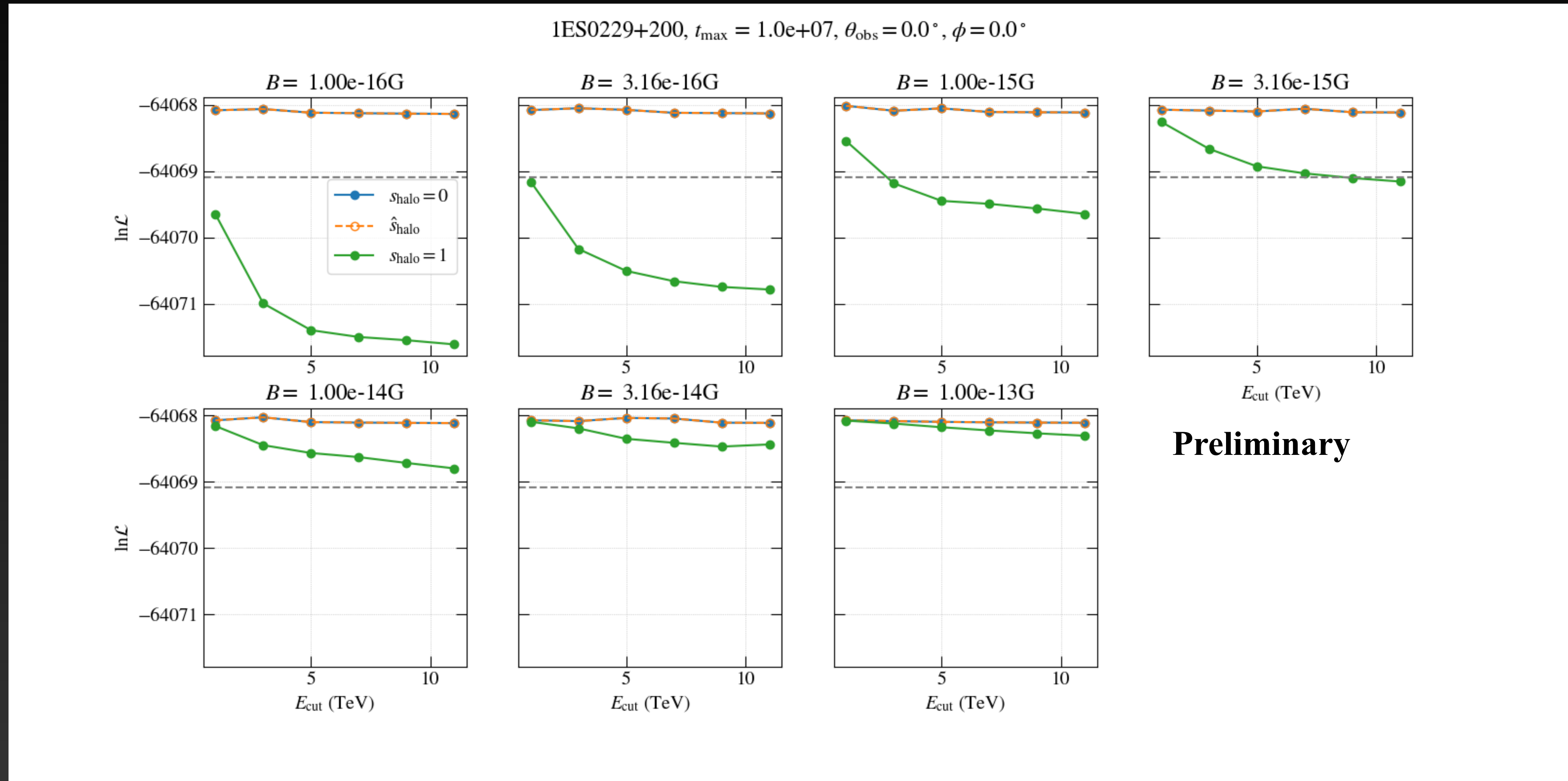


Cascade templates as function of IGMF strength: lon/lat profiles

$B = 10^{-13}$ G, sky map summed over lon/lat and energy



Fermi-LAT Analysis with halo component — Examples of likelihood profile with E_{cut}



Fermi-LAT Analysis with halo component — Examples of likelihood profile with Γ

